

This is to certify that the
dissertation entitled

STUDY OF TYROSINE KINASE LIKE PROTEIN KINASES: I.
A NOVEL ROLE OF MIXED-LINEAGE KINASE 3 IN
MITOCHONDRIA THROUGH ITS INTERACTION PROTEIN,
ADENINE NUCLEOTIDE TRANSLOCASE 2. II.
CHARACTERIZATION OF ROC DOMAIN OF PARKINSON'S
DISEASE-ASSOCIATED KINASE, LEUCINE RICH REPEAT
KINASE 2.

presented by

Geou-Yarh Liou

has been accepted towards fulfillment
of the requirements for the

Doctoral degree in Department of Biochemistry
and Molecular Biology

Kathleen A. Valle

Major Professor's Signature

12/10/2007

Date

LIBRARY
Michigan State
University

PLACE IN RETURN BOX to remove this checkout from your record.
TO AVOID FINES return on or before date due.
MAY BE RECALLED with earlier due date if requested.

DATE DUE	DATE DUE	DATE DUE

STUDY OF TYROSINE KINASE LIKE PROTEIN KINASES:
I. A NOVEL ROLE FOR MIXED-LINEAGE KINASE 3 IN MITOCHONDRIA
THROUGH ITS INTERACTION PROTEIN, ADENINE NUCLEOTIDE
TRANSLOCASE 2.
II. CHARACTERIZATION OF ROC DOMAIN OF PARKINSON'S DISEASE-
ASSOCIATED KINASE, LEUCINE RICH REPEAT KINASE 2.

By

Geou-Yarh Liou

A DISSERTATION

Submitted to
Michigan State University
In partial fulfillment of the requirements
For the degree of

DOCTOR OF PHILOSOPHY

Department of Biochemistry and Molecular Biology

2007

ABSTRACT

STUDY OF TYROSINE KINASE LIKE PROTEIN KINASES:

- I. A NOVEL ROLE FOR MIXED-LINEAGE KINASE 3 IN MITOCHONDRIA THROUGH ITS INTERACTION PROTEIN, ADENINE NUCLEOTIDE TRANSLOCASE 2.**
- II. CHARACTERIZATION OF ROC DOMAIN OF PARKINSON'S DISEASE-ASSOCIATED KINASE, LEUCINE RICH REPEAT KINASE 2.**

By

Geou-Yarh Liou

Mixed Lineage Kinase 3 (MLK3) is a widely expressed mammalian mitogen activated protein kinase kinase kinase (MAPKKK) that activates multiple mitogen-activated protein kinase (MAPK) pathways. Since MLK3 is expressed at high levels in human breast cancer MCF-7 cells, the role of MLK3 in breast cancer was investigated by identifying its interacting proteins. Using immunoaffinity purification coupled with mass spectrometry, adenine nucleotide translocase 2 (ANT2) was identified as one of the components in the MLK3 protein complex.

ANT2 is a mitochondrial ATP/ADP carrier protein and plays an important role in regulating the cellular energetic balance. Co-immunoprecipitation experiments further confirm the presence of expressed ANT2 in MLK3 complexes. The kinase domain of MLK3 was sufficient for MLK3-ANT2 interaction. In addition, ANT2 preferentially interacted with the MLK3 mutants that have enhanced catalytic activity. Results from the biochemical fractionation and confocal microscopy have demonstrated MLK3 partially localized to the mitochondria. Coexpression of MLK3 and ANT2 increased total cellular

ATP level, whereas transiently expressing the kinase inactive MLK3 with ANT2 diminished it. Stable knockdown of MLK3 decreased total cellular ATP content. In contrast, inducible expression of MLK3 enhanced total ATP production. Taken together, these data open up the possibility that in addition to its role in MAPK pathway activation, MLK3 regulation of cellular ATP levels may influence cell proliferation.

Emerging genetic studies have demonstrated that mutations in leucine-rich repeat kinase (LRRK) 2 cause familial Parkinson's disease. LRRK2 contains multiple predicted catalytic and protein-interaction domains. Roc, a putative GTPase, always exists in tandem with COR domain of unknown function. Since of solved GTPase structures, Roc is most similar to the Rab7 GTPase, a molecular homology model of Roc was created using the murine GTP-bound Rab7 crystal structure as a template to predict the functional consequence of PD mutation in the Roc. Roc and its predicted constitutively active mutants, Roc A1396T as well as R1398L, specifically bound GTP, whereas Roc T1348N, the predicted inactive form of Roc GTPase, failed to do so. Consistent with the prediction from the Roc homology model, no apparent deficiency of GTP binding was observed in the PD-associated variant, Roc R1441C. Using an enzymatic coupling assay, weak GTPase activity of a recombinant Roc fusion protein was detected.

A Roc-COR fragment has been demonstrated to complex with the carboxyl terminal region containing the Roc, COR, kinase domains and WD40 repeats of LRRK2. The effect of the PD-associated mutations within the Roc-COR domains on this LRRK2 domain interaction was also studied. Data shown herein suggest that the Roc domain of LRRK2 is a *bona fide* GTPase, and provide evidence that LRRK2 domains interact with one other in ways that are altered by the introduction of PD-associated mutations.

ACKNOWLEDGEMENTS

First and most importantly, I would like to thank my advisor, Dr. Kathleen A. Gallo for her guidance, support and encouragement during my doctoral years at MSU. I do learn lots of lessons from her which will help me both in my science career and my future life.

I would also like to thank the members of my committee, Dr. Jennifer Ekstrom, Dr. Pamela Fraker, Dr. Katheryn Meek and Dr. Shelagh Ferguson-Miller for their precious inputs, comments and suggestions for my search work. Especially, I want to thank Dr. Jennifer Ekstrom for teaching me a lot for recombinant protein expression and purification. In addition, I thank my former two committee members, Dr. Lee McIntosh and Dr. Sara Courtneidge for their good opinions on my projects.

I especially thank the Gallo lab members, including Dr. Hua Zhang, Dr. Karen Schachter, Dr. Yan Du, Dr. Julie Taylor, Eva Miller, Jian Chen and Meghann Devlin-Durante for their friendships, collaborations, and invaluable discussions as well as providing a comfortable working environment. Especial thanks to Michelle Gilmer and Steffany Kekstra for helping not only the lab work but also my communication skills.

I also thank people who work on the 3rd and 4th floor at Biomedical and Physical Science Building and in the Biochemistry and Molecular Biology department for being a continuous source of the reagents, equipments and advice.

Finally, I absolutely thank my family. My father and mother always encourage me and support my decisions. My sister always cheers me up with different kinds of

jokes. Big thanks to my brother and brother in law for their professional help on teaching me the computer programs and dealing with any weird laptop troubles.

TABLE OF CONTENTS

	Page
List of Tables.....	ix
List of Figures.....	x
Key to Abbreviations.....	xiii
I. Literature Review.....	1
1. Protein kinase classification, structure and function.....	1
2. GTPases.....	3
3. Mixed lineage kinases.....	6
3.1 The MLK family members.....	6
3.1.1 MLK.....	6
3.1.2 DLK.....	8
3.1.3 ZAK.....	10
3.1.4 MLK orthologs.....	10
3.2 MLK signaling activities.....	11
3.2.1 Activation of JNK pathway.....	11
3.2.2 Activation of p38 pathway.....	11
3.2.3 Activation of ERK pathway.....	12
3.2.4 Activation of NF- κ B.....	12
3.2.5 Other MLK substrates.....	13
3.3 Regulation of MLK.....	15
3.3.1 Regulation of MLKs by extracellular signals.....	15
3.3.2 Regulation of MLKs by autoinhibition.....	17
3.3.3 Regulation of MLKs by dimerization.....	18
3.3.4 Regulation of MLKs by small GTPases.....	20
3.3.5 Regulation of MLKs by scaffold proteins.....	21
3.3.6 Regulation of MLKs by chaperone proteins.....	24
3.3.7 Regulation of MLKs by phosphorylation.....	24
3.3.8 Regulation of MLKs by subcellular localization.....	26
3.4 The physiological roles of the MLKs.....	27
3.4.1 The <i>Drosophila</i> MLK, <i>slpr</i> and <i>Xenopus</i> MLK.....	27
3.4.2 The mammalian MLKs.....	28
4. Leucine rich repeats kinases.....	30
4.1 LRRK family.....	30
4.2 Physiological roles of LRRKs.....	31
4.3 LRRK signaling activity.....	33
4.3.1 LRRK <i>in vitro</i> kinase activity.....	33
4.3.2 MAP kinases and NF- κ B.....	34
4.4 Regulation of LRRK.....	35

4.4.1	Regulation of LRRK by extracellular signals.....	35
4.4.2	Regulation of LRRK by GTPase.....	37
4.4.3	Regulation of LRRK by chaperones.....	38
4.4.4	Regulation of LRRK by subcellular localization.....	39
5.	Mitochondria.....	40
5.1	Mitochondria and human diseases.....	40
5.2	Mitochondrial signaling.....	41
6.	Objective of the thesis.....	44
7.	References.....	46
II	A Novel Role for MLK3 in Mitochondria through Its Interaction with ANT2.....	59
1.	Abstract.....	59
2.	Introduction.....	61
3.	Materials and Methods.....	69
3.1	Reagents and antibodies.....	69
3.2	Plasmid constructs.....	69
3.3	Cell culture and transfection.....	70
3.4	Construction of MLK3 stable knockdown cell line.....	70
3.5	Cell lysis and immunoprecipitation.....	71
3.6	Gel electrophoresis and Western blot analysis.....	72
3.7	Identification of ANT peptides in the MLK3 immune complex by Mass Spectrometry.....	72
3.8	Immunofluorescence and confocal microscopy.....	72
3.9	Subcellular fractionation.....	73
3.10	Determination of cellular ATP level.....	74
4.	Results.....	75
4.1	ANT was identified in affinity-associated MLK3 complexes.....	75
4.2	Ectopically expressed ANT1 and ANT2 are targeted to the Mitochondria.....	75
4.3	MLK3 interacts with ANT2 through its kinase domain.....	79
4.4	The activation status of MLK3 regulates its association with ANT2.....	84
4.5	A portion of MLK3 is present in mitochondria.....	88
4.6	Mitochondrial MLK3 interacts with ANT2.....	93
4.7	Effect of the MLK3-ANT2 interaction on total cellular ATP level.....	98
5.	Discussion.....	102
6.	References.....	111
III	A Novel GTPase Domain of Parkinson's Disease-Associated Kinase LRRK2.....	115
1.	Abstract.....	115
2.	Introduction.....	117
3.	Materials and Methods.....	124
3.1	Reagents and antibodies.....	124
3.2	Construction of expression vectors and mutagenesis.....	124

3.3	Bacterial expression and purification of GST fusion proteins.....	126
3.4	Cell culture, transfection and cell lysis.....	127
3.5	Immunoprecipitation, gel electrophoresis and western blot analysis.....	128
3.6	GTP-binding assay.....	128
3.7	GTPase activity assay.....	129
4.	Results.....	131
4.1	Recombinant GST-Roc variants, but not GST-Roc-COR are expressed as soluble proteins under condition of auto-induction.....	131
4.2	Roc domain of LRRK2 binds GTP.....	137
4.3	COR region affects the GTP binding of Roc.....	143
4.4	The GTP-binding specificity of Roc.....	145
4.5	Hydrolysis of GTP by the Roc domain of LRRK2.....	145
4.6	Interaction of Roc-COR region with the carboxyl terminal region of LRRK2.....	145
4.7	Effect of PD mutations of Roc-COR on the protein interaction of Roc-COR with RCKWE of LRRK2.....	151
5.	Discussion.....	156
6.	References.....	161
IV	Concluding remarks.....	165

LIST of TABLES

	Page
I. Literature Review	
Table 1.1. Summary of the <i>in vitro</i> kinase activity of LRRK2 pathological Mutations.....	36
II. A Novel Role for MLK3 in Mitochondria through Its Interaction with ANT2	
Table 2.1. Sequences of the ANT peptides identified by mass spectrometry and their correspondence with ANT isoforms.....	78
Table 2.2. Peptide sequences of the oxidative phosphorylation proteins identified by mass spectrometry.....	109
III. A Novel GTPase Domain of Parkinson's Disease-Associated Kinase LRRK2	
Table 3.1. Summary of the protein solubility of bacterial GST-Roc and GST-Roc-COR variant proteins under various induced conditions.....	139

LIST OF FIGURES

	Page
I. Literature Review	
Figure 1.1. Diagram of the GTPases cycle.....	4
Figure 1.2. Block digram structure of human mixed lineage kinases.....	7
Figure 1.3. Schematic of MLK3.....	9
Figure 1.4. Diagram of the activation of MAPK pathways by MLK3.....	14
Figure 1.5. Activation model of MLK3.....	19
II. A Novel Role for MLK3 in Mitochondria through Its Interaction with ANT2	
Figure 2.1. Schematic of mitochondrial ATP synthesis.....	62
Figure 2.2. The architecture of the permeability transition pore complex.....	64
Figure 2.3. ANT was identified in affinity-isolated MLK3 complexes.....	77
Figure 2.4. Ectopically expressed ANTs are mainly present in mitochondria-enriched fraction.....	80
Figure 2.5. Ectopically expressed ANT2 localized to the mitochondria.....	81
Figure 2.6. ANT2, not ANT1, specifically interacts with MLK3.....	83
Figure 2.7. The kinase domain of MLK3 is sufficient for the ANT2 interaction...	86
Figure 2.8. The regulation of MLK3 model and the diagram of the kinase activity of different MLK3 mutations.....	90
Figure 2.9. ANT2 preferentially associates with activated forms of MLK3.....	92
Figure 2.10. A portion of expressed MLK3 is present in mitochondria	94
Figure 2.11. A portion of endogenous MLK3 is present in a mitochondria-enriched fraction.....	96
Figure 2.12. Expressed MLK3 present in the mitochondria-enriched fraction interacts with ANT2.....	97

Figure 2.13. Effect of MLK3 and ANT2 on total cellular ATP level.....	101
Figure 2.14. Alignment of the sequences containing the phosphorylation sites of MLK3 in human MKK4 and MKK7 with human ANT isoforms....	107
Figure 2.15. N-Flag tagged MLK3 partially fractionates with mitochondria.....	108
Figure 2.16. The proposed model of how the interaction of MLK3 with ANT2 in elevation of the total cellular ATP level.....	110
III. A Novel GTPase Domain of Parkinson's Disease Kinase-Associated LRRK2	
Figure 3.1. Diagram of LRRK2 domains with mutations found in Parkinson's disease patients.....	118
Figure 3.2. Molecular model of GTPase domain of LRRK2.....	121
Figure 3.3. Expression and solubility of GST-Roc variants and GST-Roc-COR upon IPTG induction.....	134
Figure 3.4. Expressed GST-Roc variant proteins but not GST-Roc-COR are soluble under the auto-induction condition.....	136
Figure 3.5. Expression and solubility of GST-Roc-COR by IPTG induction with coexpressed chaperones.....	138
Figure 3.6. Purification of recombinant GST-Roc variant proteins induced by auto-induction condition.....	140
Figure 3.7. The GTP-binding ability of Roc variant proteins.....	142
Figure 3.8. The GTP-binding ability of Roc-COR variant proteins.....	144
Figure 3.9. GTP-binding specificity of Roc variant proteins.....	146
Figure 3.10. The GTP hydrolysis ability of Roc.....	147
Figure 3.11. Interaction of Roc-COR with different regions of LRRK2.....	150
Figure 3.12. Association of Roc with Roc-COR-kinase-WD 40 through the end of LRRK2.....	152

Figure 3.13. Effect of PD mutations found in the Roc and COR domains on their interaction with the region of Roc-COR-kinase-WD 40 through the end of LRRK2.....154

KEY TO ABBREVIATIONS

AGC	Protein kinase A, protein kinase G, protein kinase C families
AIF	Apoptosis inducing factor
AKAP	A kinase anchor protein
ANT	Adenine nucleotide translocase
Apaf-1	Apoptotic protease activating factor-1
Bsk	Basket
CAMK	Calcium/calmodulin protein kinase
CDK	Cyclin dependent potein kinase
CMBG	CDK, MAPK, GSK3, CLK families
CNK1/2	Connector enhancer of KSR1/2
COR	C-terminal of Roc
CREB	c-AMP response element binding protein
CRIB	Cdc42/Rac interactive binding
CK1	Casein kinase 1
COXIV	Cytochrome c oxidase IV
DLK	Dual leucine zipper protein kinase
DMEM	Dulbecco's modified eagle's medium
EEA1	Early endosome antigen 1
EGF	Epidermal growth factor
EGFR	Epidermal growth factor receptor
ER	Endoplasmic reticulum
ERK	Extracellular signal regulated kinase

GAP	GTPase activating protein
GEF	Guanine exchange factor
GluR6	Glutamate receptor 6
GSK	Glycogen synthase kinase
GST	Glutathion S transferase
HA	Hemagglutinin
HEK	Human embryonic kidney
Hep	Hemipterous
HPK1	Hematopoietic progenitor kinase 1
Hsp	Heat shock protein
IκB	Inhibitor of NF-κB
IKK	IκB kinase
JIP	JNK interacting protein
JNK	c-Jun N-terminal kinase
KIF	Kinesin superfamily motor protein
KSR	Kinase suppressor of Ras
LC-MS/MS	Liquid chromatography-mass spectrometry/mass spectrometry
LDH	Lactate dehydrogenase
LRR	Leucine rich repeat
LRRK	Leucine rich repeat kinase
LZK	Leucine zipper bearing kinase
MALDI-MS	Matrix-assisted laser desorption/ionization-mass spectrometry
MAPK	Mitogen activated protein kinase

MAPKKK	MAPK kinase kinase
MEF	Mouse embryonic fibroblast
MEK	Mitogen-activated protein/Erk kinase
MESG	2-amino-6-mercapto-7-methyl purine ribose
MKK	MAPK kinase
MLK	Mixed lineage kinase
MMP	Mitochondrial membrane permeabilization
MPTP	1-methyl-4-phenyl-1,2,3,6-tetrahydropyridine
Msn	Misshapen
NGF	Nerve growth factor
OXPHOS	Oxidative phosphorylation
PAS	Phospho-Akt substrate
PAGE	Polyacrylamide gel electrophoresis
PD	Parkinson's disease
PDGF	Platelet derived growth factor
PI3K	Phosphatidylinositol 3 kinase
PKA	protein kinase A
PKC	protein kinase C
PINK-1	PTEN induced kinase-1
PMA	Phorbol myristoyl acetate
PNP	Purine nucleotide phosphorylase
POSH	Plenty of SH3
PSD-95	Post-synaptic density protein 95

PTPC	Permeability transition pore complex
PTPD1	Protein tyrosine phosphatase 1
PTPMT-1	Phosphatase localized to the mitochondria
RCKWE	Roc-COR-kinase-WD40 through the end of LRRK2
RGC	Receptor guanylate cyclase
RIPK	Receptor interacting protein kinase
RNAi	RNA interference
Roc	Ras of complex protein
ROS	Reactive oxygen species
SAM	Sterile alpha motif
SCG	superior cervical ganglion
SH3	Src-homology 3
ShRNA	Short hairpin RNA
SiRNA	Small interference RNA
Smac	Second mitochondria-derived activator of apoptosis
STE	homology of yeast sterile 7, 11, 20 kinases
TAP	Tandem affinity purification
TCR	T cell receptor
TGF	Transforming growth factor
TK	Tyrosine kinase
TKL	Tyrosine kinase like
TNF	Tumor necrosis factor
TOR	Toll like receptor

TPA	Phorbol ester 12-O-tetradecanoylphorbol-13-acetate
TUNEL	Terminal deoxynucleotidyl transferase mediated biotin-dUTP nick end Labeling
VDAC	Voltage dependent anion channel
WE	WD40 through the end of LRRK2
ZAK	Leucine zipper and sterile alpha motif kinase

I. Literature Review

1. Protein kinase classification, structure and function

Among many post-translational modifications, protein phosphorylation is best known because of its broad involvement in cellular processes such as signal transduction, transcription, metabolism, motility, cell cycle progression, proliferation, differentiation and apoptosis. It is also pivotal in regulation of intercellular communication during development and under various physiological conditions.

Protein phosphorylation is achieved by protein kinases which function to catalyze the transfer of the γ phosphate from ATP to protein substrates. Based on information established in public and propriety genomic databases, 518 protein kinases have been identified in the human genome, accounting for about 1.7% of all human genes [1]. The human kinome is categorized into nine groups based on sequence similarity within the catalytic domain. AGC (PKA, PKG and PKC families), CAMK (calcium/calmodulin dependent protein kinases), CMGC (CDK, MAPK, GSK3 and CLK families), TK (tyrosine kinases), STE (homologs of yeast Sterile 7, 11, and 20 kinases), CK1 (casein kinase 1), TKL (tyrosine kinase-like), RGC (receptor guanylate cyclase), and atypical kinases [1]. Most mammalian protein kinases phosphorylate hydroxyl amino acids of the substrate proteins. Therefore, they are also classified as Ser/Thr kinases, Tyr kinases, and dual-specificity kinases which phosphorylate both Ser/Thr and Tyr residues [2, 3]. Mutations and dysregulation of protein kinases are tightly associated with various human diseases including cancers and neurodegenerative diseases. Selective small molecule inhibitors of protein kinases have proven to be valuable therapeutics. For instance,

Gleevec, which inhibits the oncogenic cytosolic tyrosine kinase Bcr-Abl is used to treat chronic myelogenous leukemia; and receptor tyrosine kinase inhibitors such as the EGFR family inhibitor, lapatinib, is approved for treatment of metastatic breast cancer.

Based on solved crystal structures of the catalytic domains, all protein kinases are comprised of a small NH₂ terminal lobe and a large carboxyl terminal lobe [4]. An active-site cleft where magnesium ion (Mg²⁺), ATP and protein substrate bind lies between two lobes. The glycine loop or P loop with the Rossmann motif, GXGXXG, is located at the top of the cleft and modulates the ATP binding through the interaction of phosphates of ATP with backbone [5]. In the absence of ATP, the P-loop is unstructured. A conserved Lys near the P-loop which plays a key role in kinase catalysis by properly orientating the phosphates of ATP is stabilized by an invariant Glu residue through the ionic interactions [6]. This conserved Lys is commonly mutated to create a catalytically defective protein kinase that has been extensively applied in numerous research studies. At the bottom of the cleft are the catalytic loop as well as the activation segment which is a 20-35 residue sequence found between conserved motifs DFG and APE [7, 8]. Upon phosphorylation of residues within the activation segment, the activation segment is stabilized in an open and extended conformation, allowing substrate access to the catalytic site [7, 9].

The substrate specificity of protein kinases is partially determined by the presence of “consensus phosphorylation motif” in substrate proteins [5, 10] This has been widely applied to identify new substrates of various protein kinases based on the results from *in vitro* phosphorylation experiments with the synthetic peptides containing the recognition motif of a given protein kinase. These consensus phosphorylation motifs are considered

as canonical phosphorylation sites. Docking sites and scaffolds are also important for selection of substrates [11].

Besides the catalytic domain, most protein kinases also contain other domains to regulate their functions in several manners, including controlling the subcellular localization, binding activators or releasing inhibitors, associating with other proteins and impacting the protein stability. These regulatory mechanisms are required for protein kinase specificity in response to various extracellular stimuli.

2. GTPases

Small G proteins, also called GTPases are enzymes which hydrolyze GTP. GTP hydrolysis allows the GTPase to function as a binary molecular switch to play crucial roles in signal transduction and various cellular processes. In physiological settings, GTPases are cycled between a GTP-bound (conformationally active) state and a GDP-bound (conformationally inactive) state (Figure 1.1) with a conformational change. Enzymatically active GTPases hydrolyze GTP with a weak intrinsic catalytic activity. Only the GTP-bound conformation of GTPases which is conformationally active, bind effector proteins, resulting in signal transduction processes. The GTPases are regulated by guanine exchange factors (GEFs) and GTPase activating proteins (GAPs). GEFs catalyze the release of GDP, allowing GTP to bind since the GTP concentration in cells is higher than GDP. GAPs potentiate GTP hydrolysis to GDP, rendering GTPase inactive.

The Ras family of small GTPases is categorized into 5 subgroups, including Ras, Rho, Ran, Rab and Arf subfamilies. Each subfamily is involved in different cellular

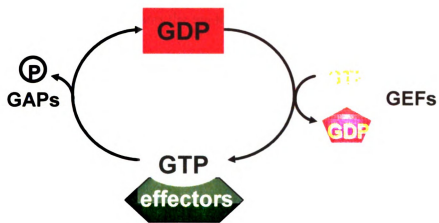


Figure 1.1. Diagram of the GTPase cycle. GTPases cycling between a GDP-bound state and a GTP-bound state is accomplished by a conformational change. Cycling of GTPase is regulated by guanine exchange factors (GEFs) and GTPase activating proteins (GAPs). GTP-bound (conformationally active) GTPases are competent to bind their effector proteins.

processes. The Ras subfamily primarily participates in cell proliferation through signaling to the Raf-MEK-ERK pathway. Ras is an oncogene and point mutations that render Ras conformationally active including G12V, A59T and Q61L have been found in the different types of human tumors [12]. It is estimated that 1/3 of solid human tumors contain oncogenic Ras. Ran modulates the nucleo-cytoplasmic transport, spindle assembly and post-mitotic nuclear envelope assembly [13]. The Rab and Arf subfamily members are primarily involved in vesicular trafficking and cellular transports. Finally, the Rho subfamily containing Cdc42, Rac and Rho mainly affects protein kinase signaling and cytoskeletal remodeling [14].

A large body of work aimed at understanding the biological functions of GTPase in different cellular processes as well as identifying their GEFs and GAPs is based largely on overexpression of conformationally active and inactive mutants of GTPases. In the paradigm GTPase, Ras, a substitution of Ser17 to Asn [15, 16] at the catalytic site renders Ras GDP-bound and conformationally inactive. However, Gly12 to Val oncogenic variant is conformationally active due to GTP binding but a failure of GTP hydrolysis because of an inappropriately positioned magnesium ion [17, 18]. The conformationally active Ras variants, Gln61 to Leu and Ala59 to Thr, function in a mechanistically analogous manner [17, 19]. Most small GTPases undergo post-translational prenylation, with a farnesyl or geranylgeranyl group [20, 21]. These modifications render the conformationally active GTPases hydrophobic and allow them to be targeted to cellular membranes [22].

3. Mixed Lineage Kinases

Mixed lineage kinases (MLKs) belong to the serine/threonine kinase family and are categorized in the tyrosine kinase like (TKL) branch of the human kinome. The kinase domain of TKL family members share sequence similarity of the kinase domain with both tyrosine kinases and serine/threonine kinases. Mixed lineage kinases are known to function as MAPKKKs to activate MAPK signaling pathways. A large body of work has demonstrated that MLKs induce apoptosis through the persistent activation of JNK pathway in the neuronal system [23, 24]. Administration of CEP-1347, an MLK inhibitor [25], in cultured cells and animal models rescued this apoptotic effect. Indeed, CEP-1347 was tested in clinical trial for neuroprotection in Parkinson's disease but ultimately failed. Other biological functions of MLKs still need to be intensively studied.

3.1 The MLK family members

The mixed lineage kinases can be divided into three subgroups, including the MLKs, the dual leucine zipper bearing kinases (DLKs) and the zipper sterile- α motif kinases (ZAK) based on the sequence homology of the kinase domain and in the domain arrangements (Figure 1.2)[26].

3.1.1 MLK

The MLK subfamily consists of MLK1 [27], MLK2 [28, 29], MLK3 [30-32] and MLK4. MLK4 has two splicing forms, MLK4 α and MLK4 β . MLK1-4 have a NH₂

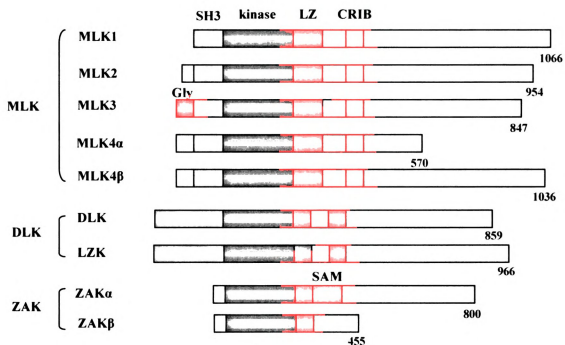


Figure 1.2. Block diagram structure of human mixed lineage kinases. The relative position of the SH3 domain, leucine zipper (LZ), CRIB motif and sterile α motif (SAM) is indicated (adapted from Gallo & Johnson, 2002)). Abbreviation, SH3: *Src* homology 3, CRIB: Cdc42/Rac interactive binding.

terminal Src homology 3 (SH3) domain followed by a catalytic domain, a centrally located leucine zipper region, a Cdc42/Rac1 interactive binding (CRIB) motif and a proline rich carboxyl terminal region (Figure 1.3). MLK1-4 share a high sequence identity, over 75% identity within the kinase domain and 60% identity from the SH3 domain through the CRIB motif.

The expression patterns of each MLK vary among MLK family members. Messenger RNA of MLK1 is expressed in neuronal cells as well as epithelial cancer cell lines of breast, colonic and esophageal origin [27]. Additionally, MLK1 protein is detected in an immature β cell line, RIN-5AH cells, but not in PIN-A12 cells, a more mature β cell line, suggesting that MLK1 play a role in regulation of β cell development [27]. MLK2 mRNA is primarily expressed in brain, testis, skeletal muscle and at lower levels in pancreas [28, 29]. MLK3 mRNA is ubiquitously expressed in human tissues, but with a lower level in brain and heart [30-32]. To date, no expression pattern of MLK4 has been reported.

3.1.2 DLK

The DLK subfamily contains DLK [33] and leucine-zipper kinase (LZK) [34]. As compared to MLK subfamily, DLKs contain only a kinase domain, two small leucine zipper motifs interrupted by 31 amino acids and a proline-rich carboxyl terminal region with the undefined function. The kinase domain of DLK and LZK is 87% identical, but shares only 35% sequence identity with MLK subfamily. DLK mRNA is predominantly expressed in the adult mouse brain especially the hippocampus, cerebral cortex and the



Figure 1.3. Schematic of MLK3. The numbers in the diagram represent amino acid number. SH3: Src homology 3 domain, CRIB: Cdc42/Rac Interactive Binding motif.

Purkinje cells of the cerebellum [33]. Messenger RNA of LZK is widely expressed, with the highest level in the pancreas [34].

3.1.3 ZAK

The ZAK subfamily only comprises ZAK (also known as MLTK) which has two splicing isoforms as ZAK α and ZAK β [35]. In addition to the kinase domain and a leucine zipper region, a sterile- α motif (SAM) is also present in ZAK α isoform. In contrast, ZAK β does not possess the SAM structure due to the splicing process. It has been demonstrated that SAM of the MAPKKK Ste11 mediates homo-oligomerization in yeast [36]. ZAK mRNA is ubiquitously expressed in human tissues, with a highest level in heart and skeletal muscle [35, 37].

3.1.4 MLK orthologs

MLKs are absent in yeast, but MLK orthologs are present in *C. elegans*, *Drosophila* and *Xenopus*. The single ortholog of MLK subfamily in *Drosophila* is called Slipper (Slpr). Disruption of Slpr which blocks cell movement during the process of dorsal closure in the fly embryo is lethal [38]. The *Xenopus* MLK ortholog, which is most similar to MLK2 with a 62% sequence identity, is mainly expressed in cement gland, brain and pronephros [39]. Based on studies of antisense inactivation and introduction of dominant negative constructs, the requirement of *Xenopus* MLK in normal cement gland development and pronephros tubule formation has been demonstrated [39]. Analysis of the amino acid sequences within kinase domain and zipper regions of DLK suggests there is a DLK ortholog in *Drosophila* and *C. elegans*.

In addition, *C. elegans* also contains a ZAK ortholog and a distantly related SH3 containing MLK without other recognized structural domains.

3.2 MLK signaling activities

3.2.1 Activation of JNK pathway

All MLK family members, except MLK1 and MLK4, have been demonstrated to activate JNK pathway upon their overexpression in mammalian cells [35, 40-42]. Both MLK2 and MLK3 phosphorylate MKK4 and MKK7 in the *in vitro* kinase assays [43], whereas DLK only phosphorylates MKK7 under the same conditions [44], suggesting that DLK may activate JNK specifically through activation of MKK7 *in vivo*.

Ectopically expressed ZAK promotes the catalytic activity of MKK7 as well as MKK4 *in vitro* [35]. However, only dominant negative MKK7 but not MKK4 is able to suppress ZAK mediated JNK activation [45], suggesting that MKK7 might be the physiological substrate of ZAK.

3.2.2 Activation of p38 pathway

Activation of the p38 pathway through phosphorylation of MKK3 and MKK6 is also observed upon ectopic mammalian expression of MLK2 [40, 46], MLK3 [47], DLK [41] and ZAK α [35, 37]. Upon TGF- β treatment, p38 is activated by endogenous MLK3 in hepatoma cells probably through an indirect mechanism since this activation occurs in a very late stage after stimulation [48]. Knockdown MLK3 by RNAi attenuates TNF α -induced p38 activation in human CCD-18Co colorectal fibroblasts and Jurkat T lymphocytes [49]. In addition, treatment of MLK3 depleted mouse embryonic fibroblasts

with TNF- α partially reduces p38 activation [50], suggesting a role for MLK3 in p38 activation. .

3.2.3 Activation of ERK pathway

Whether ERK can be activated by all MLK family members is still an ongoing debate. It has been reported that ERK is activated upon overexpression of MLK2 [46, 51] and ZAK [35]. Overexpression of MLK3 results in ERK activation in MCF-7 breast cancer cells as well as HEK 293T cells (Gallo KA, unpublished data and [48]). On the contrary, it has been demonstrated that ectopically expressed MLK3 impedes Phorbol Myristoyl Acetate (PMA) and Platelet-Derived Growth Factor (PDGF)-induced ERK activation in mesangial cells [52, 53]. Despite of the ability of MLK3 to phosphorylate MEK1 *in vitro* and *in vivo* under certain circumstances, it has been proposed that overexpressed MLK3 suppresses ERK activation because of the persistent activation of JNK induced by MLK3 [54], suggesting negative cross-talk between the ERK and JNK pathways when MLK3 is overexpressed.

A novel role for MLK3 in activation of ERK pathway has been proposed based on the results of knockdown MLK3 by small interference RNA (siRNA) in human and murine cells (Figure 1.4). It has been demonstrated that knockdown of MLK3 impairs ERK activation resulting in loss of cell proliferation in response to serum stimulation [49]. Furthermore, MLK3 was demonstrated to complex with B-Raf and Raf-1 and introduction of the kinase defective MLK3 rescued the cell proliferation defect induced by MLK3 siRNA, suggesting that MLK3 functions as a scaffold protein that is required for efficient signaling to ERK.

3.2.4 Activation of NF- κ B

NF- κ B is a transcription factor that participates in immune, inflammatory and anti-apoptotic responses. Under normal condition, NF- κ B is sequestered in the cytosol through its interaction with the scaffold protein, I κ B. Phosphorylation of I κ B by serine/threonine I κ B kinases (IKKs) results in polyubiquitylation of I κ B, targeting it to the 26S proteasome for degradation thereby releasing NF- κ B [55]. Free NF- κ B translocates to the nucleus where it activates transcription. In Jurkat lymphocytes, T cell receptor signaling can be induced by receptor cross linking with CD3/CD28 antibodies. Expressed MLK3 induces phosphorylation and activation of IKK α and IKK β in Jurkat T cells [56]. Expressed catalytically deficient MLK3 suppresses NF- κ B-dependent transcription upon CD3/CD28 costimulation. Similar to MLK3, LZK also activates and phosphorylates IKK β through the interaction of its kinase domain with IKK β [57]. Both LZK and ZAK have been demonstrated to activate NF- κ B as judged by luciferase reporter gene assays [42, 57].

3.2.5 Other MLK substrates

Most MLK substrates are protein kinases whose activation loops are phosphorylated by MLKs, although MLK3 has been shown to phosphorylate golgin-160 *in vitro* [58]. Golgin-160 is a peripheral membrane protein at the cytoplasmic face of the Golgi complex [59]. In response to apoptotic stresses, cleavage of golgin-160 by caspases results in the disassembly of the Golgi complex during apoptosis [60]. Coexpression of MLK3 with golgin-160 reduces the gel mobility of golgin-160, supporting the idea that MLK3 enhances golgin-160 phosphorylation *in vivo* [58].

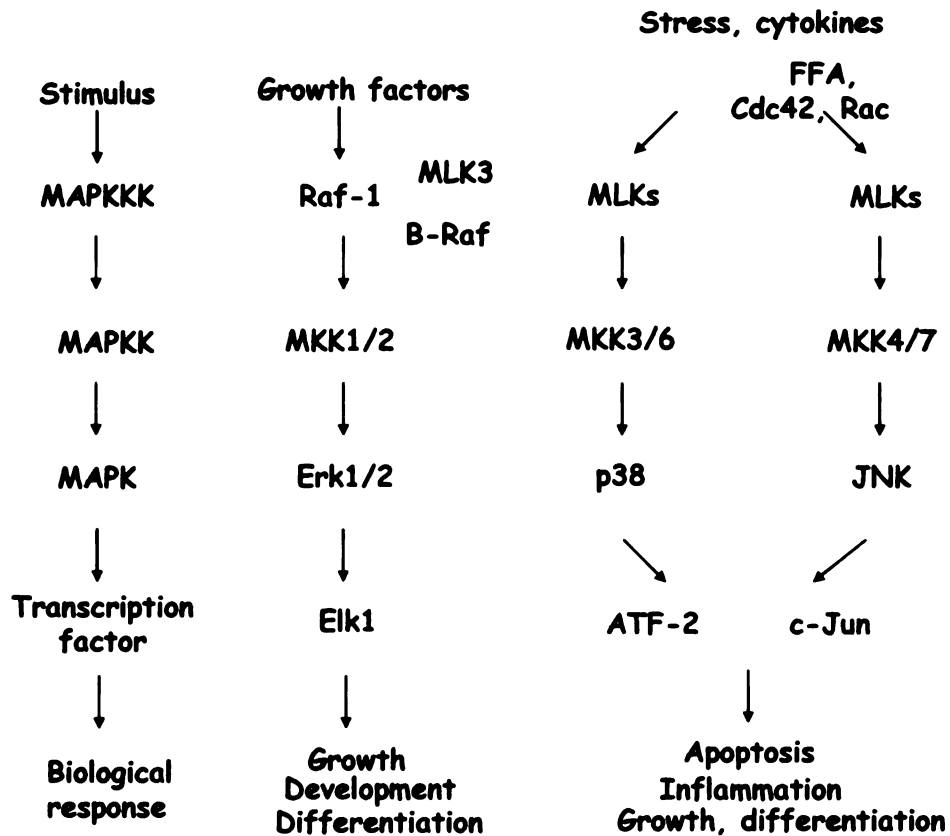


Figure 1.4. Diagram of the activation of MAPK pathways by MLK3. The best characterized mammalian MAPK pathways are the ERK, JNK and p38 pathways. Activation of MAPK is tightly regulated through a cascade which a MAPKKK phosphorylates and activates a MAPKK which in turns phosphorylates and activates a MAPK. Activation of different MAPK pathways in response to diverse stimuli leads to different biological response. The diagram shows the activation of MAPK pathways by MLK3 in response to different extracellular stimuli and the known biological effects of MLK3-mediated MAPK activation. MLK3 is proposed to act catalytically as a MAPKKK to activate the JNK and p38 pathways, and as a scaffold in B-Raf-mediated ERK activation. Abbreviation, FFA: free fatty acid.

NeuroD is a transcription factor that belongs to the basic helix-loop-helix family and plays a crucial role in neuronal development and survival in vertebrates [61]. NeuroD was identified as an MLK2-associating protein in a yeast two hybrid screen. NeuroD and MLK2 can be coimmunoprecipitated from transfected neuroblastoma N2A cells [62]. Purified recombinant MLK2 phosphorylates cellular NeuroD *in vitro*. However, results from *in vitro* kinase assay indicate that NeuroD is a poor substrate for MLK2. It has been suggested that other cofactors or modifications of NeuroD in cells are essential for its phosphorylation by MLK2. Coinjection of NeuroD and MLK2 into *Xenopus* embryos potentiates expressed NeuroD-mediated neurogenesis [62].

3.3 Regulation of MLK

3.3.1 Regulation of MLKs by extracellular signals

Although ectopically expressed MLKs have relatively high catalytic activities *in vitro*, the extracellular signals that activate endogenous MLKs largely remain unknown. The majority of MLK work has focused on MLK3, probably due to its broad tissue expression as well as the availability of antibodies.

Early studies of the impact of extracellular signals on MLK3 rely on the alteration of electrophoretic mobility in SDS-PAGE gels as a readout for MLK3 phosphorylation. In Jurkat T lymphocytes, PMA treatment and co-stimulation with CD3/CD28 antibodies induced an electrophoretic mobility shift of MLK3 [56], implying that PMA and CD3/CD28 activate MLK3 in Jurkat T lymphocytes. Treatment of HeLa cells with sorbitol induces hyperosmotic stress and significantly alters the mobility of MLK3 in SDS-PAGE (Karen Schachter, unpublished data). A phospho-specific antibody directed

against the phosphopeptide containing phospho-Thr at 277 and phospho-Ser at 281 within the activation loop of MLK3 has recently become commercially available. Using this antibody, the activation loop phosphorylation of endogenous MLK3 has been detected in A431 human epidermoid carcinoma cells treated with sorbitol [63]. In addition, camptothecin, a topoisomerase inhibitor, induced activation loop phosphorylation of endogenous MLK3 in HeLa cells as well as in PC12 neuronal cells [63]. These data indicate that MLK3 plays a role in cellular responses in response to stress stimuli.

TNF- α stimulation has been shown to increase endogenous MLK3 catalytic activity as judged by *in vitro* kinase assay in Jurkat T lymphocytes [64] as well as in MCF-7 breast cancer cells [65]. However, there is no significant change in the electrophoretic mobility of MLK3 upon TNF- α treatment, suggesting that TNF- α induced MLK3 phosphorylation does not result in alteration of the electrophoretic mobility of MLK3. Lipid C6-ceramide treatment is reported to augment the endogenous MLK3 *in vitro* kinase activity in Jurkat T lymphocytes [64]. Ceramide is generated in response to TNF- α because activation of sphingomyelinases converts sphingomyelin to ceramide and phosphocholine. Ceramide potentiates apoptosis resulting from the permeabilization of mitochondrial membranes [66]. The MLK inhibitor, CEP-11004, decreases TNF- α -induced and ceramide-induced JNK activation [64]. Taken together, these data suggest in response to TNF- α , MLK3 induces apoptosis.

Endogenous MLK3 is activated by TGF- β in rat hepatoma FatO cells and human hepatoma Hep3B cells as judged by the reactivity with the phospho-MLK3 antibody [48]. However, MLK3 is activated by TGF- β after long time incubation, suggesting that MLK3 is not directly activated through TGF- β receptor signaling. Expressed kinase

inactive MLK1, MLK2 or MLK3 abolishes TGF- β induced apoptosis in these cells [48], suggesting that the activation of MLKs is required for TGF- β mediated cell death.

Recent work has investigated the effect of growth factors on the MLK3 activation. EGF increases the MLK3 catalytic activity *in vitro* as judged by the phosphorylation of recombinant MEK1 as the substrate in an *in vitro* kinase assay in immortal human colon CCD-18Co cells [49]. Knockdown of MLK3 by small interference RNA eliminates EGF-induced activation of ERK, JNK and P38 pathways, suggesting that MLK3 is required for EGF induced signaling transduction.

Very recent work has linked MLKs to metabolic stress signaling pathways in response to saturated fatty acids. Palmitic acid (16:0) but not oleic acid (18:1) results in activation of endogenous MLK3 and JNK as judged by the reactivity of phospho-MLK3 and phosphor-JNK antibodies in mouse embryonic fibroblasts and this activation is abrogated in *mlk3* knockout MEFs or upon treatment with PKC inhibitor[67]. These data suggest that MLK3 participates in saturated fatty acid induced signaling pathways.

The mechanisms by which extracellular signals regulate the activation of different MLKs are still not completely understood.

3.3.2 Regulation of MLKs by autoinhibition

SH3 domains are independently folding domains of about 60 amino acids. The structural domain of SH3 binds to the proline rich sequence, PXXP, flanked by basic amino acids [68]. The MLK subfamily members possess an SH3 domain at their amino terminus. Hematopoietic progenitor kinase 1 (HPK1) phosphorylates kinase defective MLK3 *in vitro* through the interaction of its proline-rich region with the SH3 domain of

MLK3 [69]. However, no alteration in MLK3 activity was observed upon coexpression of HPK1 and MLK3 (Gallo KA, unpublished data).

The most famous mechanism for the SH3 domain to control the activity of protein kinases is the autoinhibitory regulation of Src tyrosine kinase [70]. In addition, the SH3 domain of the Src tyrosine kinase can also be modulated by inter-protein interactions. Work from our lab suggests that MLK3 is kept in an inactive state by an interaction of its SH3 domain with a single proline-containing sequence located between the leucine zipper region and the CRIB motif (Figure 1.5)[71]. Disruption of this interaction by mutation of either a conserved tyrosine within the SH3 or of the single proline results in an increase of MLK3 catalytic activity both *in vitro* and *in vivo*. The single proline containing sequence of MLK3 is well conserved in all MLK subfamily and MLK orthologs in fruit flies and African clawed frogs, suggesting that this SH3 domain mediated autoinhibition applies to all MLK subfamily proteins.

3.3.3 Regulation of MLKs by dimerization

All MLKs contain a leucine zipper region which is a structural motif that creates attractive forces in parallel α helices. The hydrophobic coiled coil is primarily stabilized by placing leucine residues that repeat every 7 amino acids. Leucine zippers commonly mediate protein dimerization or oligomerization [72, 73]. It has been demonstrated that the leucine zipper region of MLK3 mediates oligomerization [74]. Even though MLK3 can coimmunoprecipitate with DLK from the total cellular lysates, the isolated DLK

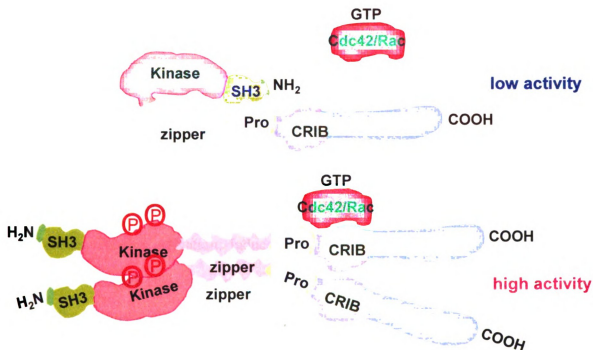


Figure 1.5. Activation model of MLK3. The proposed regulation model of MLK3. *Top*, MLK3 is autoinhibited through a protein interaction mediated by the SH3 domain and a proline located between the zipper region and Cdc42/Rac interactive binding (CRIB) motif. *Bottom*, GTP-bound Cdc42/Rac binds to the CRIB motif of MLK3 and disrupts the MLK3 autoinhibition, allowing the dimerization of MLK3 through the zipper region. Dimerization of MLK3 brings two kinase domains of MLK3 close to each other, resulting in the transphosphorylation of the activation loops of MLK3 and the fully active form of MLK3.

leucine zipper region does not dimerize with other MLKs efficiently [75], suggesting that heterodimerization of MLKs is unlikely mediated by this region.

The leucine zipper region of MLK3 is necessary for MLK3 oligomerization [76]. Elimination of the entire leucine zipper region in MLK3 renders MLK3 catalytically inactive and fails to activate JNK pathway [74]. Destabilization of the leucine zipper region of MLK3 by introducing the mutation, L410P, impedes MLK3 dimerization and its downstream signaling to JNK due to its inability to dually phosphorylate MKK4 [77]. Similar to MLK3, the leucine zipper mediation of DLK is necessary for DLK activation and subsequent JNK activation. Induced dimerization of DLK by an artificial FK-binding protein (FKBP) system potentiates DLK autophosphorylation and JNK activation [78]. Ectopically expressed leucine zipper region of DLK, which competes for the binding of the leucine zipper region between the full length DLKs, results in suppression of DLK activation [78]. LZK has also been demonstrated to form oligomers. LZK with a deleted leucine zipper region fails to activate JNK pathway [79].

In conclusion, leucine zipper region mediated dimerization is commonly used in MLKs to regulate their activity and downstream pathways possibly by controlling their autophosphorylation.

3.3.4 Regulation of MLKs by small GTPases

Small GTPases, also called G proteins, function as molecular switches in the regulation of various cellular processes such as cell proliferation, cell movement, cytoskeletal rearrangement and vesicular trafficking [80]. Under physiological conditions, their cycling between GTP-bound and GDP-bound states is controlled by

guanine exchange factors (GEFs) and GTPase activating proteins (GAPs). Only GTP-bound GTPases which are conformationally active bind to their effectors, resulting in signal transduction. It has been demonstrated that conformationally active Rac and Cdc42 activate the JNK and p38 pathways [81, 82].

Among MLKs, only MLK1-4 contain a CRIB GTPase binding motif. The CRIB motif is composed of 14-16 amino acids containing eight conserved residues within the motif which are critical for binding with activated Cdc42 and Rac [83]. It has been shown that MLK3 binds to activated Rac and Cdc42 [76, 83, 84]. Knockdown of MLK3 by small interference RNA blocks ectopically expressed Cdc42 mediated JNK activation in HEK 293T cells[85], further strengthening the notion that Cdc42 is an upstream activator of MLK3. Coexpression of MLK3 with activated Cdc42 enhances MLK3 oligomerization, increases its catalytic activity, potentiates MLK3-mediated JNK activation and increases the *in vivo* phosphorylation of MLK3, as judged by the retarded motility of MLK3 and *in vivo* labeling [74, 76, 78, 86]. Additionally, activated prenylated Cdc42 translocates MLK3 to cellular membrane compartments resulting in full activation of MLK3 [85].

Coexpression of MLK3 with a constitutively active form of Rac1 increases MLK3 catalytic activity *in vitro* [87]. Overexpression of dominant negative MLK3 or DLK diminishes activated Rac1 mediated neuronal apoptosis[24], suggesting that Rac1 induces neuronal apoptosis through activation of MLK family protein kinases.

3.3.5 Regulation of MLKs by scaffold proteins

JNK interacting proteins (JIPs) 1-4 are a group of scaffold proteins encoded from four genes. JIPs are classified in 2 subgroups based on their sequence similarity. All JIPs have common biochemical properties including a cargo function for kinesin motor proteins and a scaffold function for JNK and P38 [88]. Other important signaling molecules including the guanine nucleotide exchange factor (GEF), Tiam, protein kinases, Akt and Src, as well as MAPK phosphatase 7 (MKP7) have also been revealed to associate with JIPs [88-90].

JIP1 and JIP2 are structurally similar. JIP1 mainly participates in JNK signaling and complexes with JNKs, MKK7 and several MLKs including MLK2, MLK3, DLK and LZK. Coexpression of JIP1 with MLK3 promotes JNK activation, suggesting that scaffolds facilitate signaling by assembling the cascade module and ensuring the signaling specificity. However, a different model of JIP1-mediated DLK and JNK activation has also been suggested. DLK is sequestered in the monomeric, inactive state by binding to JIP1 [78, 91]. Upon stimulation with extracellular signals, JNK is recruited to JIP1 and phosphorylates JIP1, allowing for DLK dissociation from JIP1. Released DLK dimerizes and subsequently becomes catalytically active resulting in phosphorylation and activation of MKK7 and JNK in the JIP1 complex [78, 91]. The binding specificity of JIP1 and JIP2 with other proteins is primarily controlled by the binding affinity. JIP2 is mainly involved in p38 signaling. JIP2 associates with MLK3, MKK3 and p38 isoforms [92, 93]. JIP2 also complexes with Tiam1 and Ras-GRF, which are the GEFs of Rac GTPase. Expression of either of these GEFs increases the association of JIP2 with MLK3, MKK3 and p38 [92].

The other subgroup of JIPs is composed of JIP3 and JIP4. JIP3 interacts with JNK, MKK7 and MLK family members. JIP3 also complexes with MEKK1, MKK4 and ASK1 [94, 95]. JIP4 associates with MEKK3 and MKK4 [96]. Since all JIPs associate with kinesin motor complexes, it is conceivable that JIP proteins may be involved in kinesin-mediated axonal transport and regulate the subcellular localization of the JNK signalsome.

In addition to JIPs, plenty of SH3 (POSH) has been demonstrated to function as a scaffold protein in JNK-induced neuronal apoptosis [97]. POSH interacts directly with activated Rac1, MLKs including MLK1-3 and DLK, and indirectly with MKK4/7 and JNKs [23]. The neuronal apoptosis induced by overexpressed POSH can be rescued by either dominant negative protein kinases in the POSH complex or MLK inhibitor, CEP-1347 [23]. Binding of Akt2 to POSH disrupts the POSH-MLK-MKK-JNK complex and impairs activation of JNK pathway [98]. Very recent data has demonstrated that POSH interacts directly with JIP proteins, forming a signalsome [99].

Post-synaptic density protein 95 (PSD-95) is a neuronal scaffold protein comprised of three PDZ domains, a SH3 domain and a catalytically inactive guanylate kinase domain [100]. PSD-95 forms a complex with glutamate receptor 6 (GluR6) and MLK2 and/or MLK3 upon the interaction of its PDZ domain with GluR6 and of the SH3 domain with MLK2 and/or MLK3. Expressed kinase dead MLK2 or MLK3 abolishes GluR6 mediated JNK activation and subsequent neuronal toxicity. Taken together, PSD-95 functions as a scaffold protein to mediate signaling from ion channels to JNK pathway by anchoring MLK family members to the GluR6 receptor complex [101].

Connector enhancer of KSR (CNK) was originally identified in a genetic screen for genes which enhance the phenotype of flies with the overexpressed kinase domain of kinase suppressor of Ras (KSR) [102]. There are three isoforms of CNK: CNK1, CNK2 and CNK3. CNK1 interacts with Raf-1 and c-Src, resulting in potentiation of Raf-1 activation [103]. Upon activation of the GTPase Rho, CNK1 interacts with members of the JNK pathway, including MLK2, MLK3 and MKK7, leading to c-Jun phosphorylation [104]. Taken together, these data have suggested that CNK1 functions as a scaffold protein and may mediate cross talk among signaling pathways.

3.3.6 Regulation of MLKs by chaperone proteins

The function of chaperones is to maintain proteins in an appropriate folded conformation, preventing aggregation. Hsp90 is one of the most abundant and highly conserved proteins in eukaryotes. The co-chaperone Cdc37 is essential for the interaction of Hsp90 with its client protein kinases, which occurs through their kinase domains. The client proteins of Hsp90 include steroid hormone receptors and various protein kinases including Src, Raf and CDK4 [105]. MLK3 associates with Hsp90/Cdc37 through its kinase domain but this interaction is independent to the activation status of MLK3 [65]. Ablation of the ATPase activity of Hsp90 which is required for its chaperone function reduces endogenous MLK3 protein levels [65], suggesting that MLK3 is stabilized with a proper folded conformation which is maintained by Hsp90/Cdc37.

3.3.7 Regulation of MLKs by phosphorylation

Phosphorylation is the most common posttranslational modification that regulates protein kinase activities. Phosphorylation of the activation loop which is flanked by the conserved trinucleotide motifs, DFG and APE, is prerequisite for activation of most protein kinases. Based on site-directed mutagenesis studies, Thr 277 and Ser 281 are the phosphorylation sites within the MLK3 activation loop [106]. The commercially available phospho-MLK3 antibody has been raised to recognize the phospho-Thr 277 and phospho-Ser 281 of MLK3 and widely used to study MLK3 activity under various physiological conditions.

Insulin stimulation activates phosphatidylinositol 3-kinase (PI3K), which in turns activates protein kinase B, known as Akt, resulting in cell proliferation and survival. It has been demonstrated that Akt is activated upon treatment of insulin in HepG2 liver tumor cells. However, the catalytic activities of MLK3, MKK7 and JNK are reduced. It has been suggested that Akt phosphorylates Ser 674 of MLK3, negatively regulating MLK3 activity and JNK activation to block MLK3-mediated apoptotic effect [107].

Eleven serines located in the proline-rich carboxyl terminal region of MLK3 have been identified as Cdc42 activated *in vivo* phosphorylation sites of MLK3 by mass spectrometry coupled with phosphopeptide mapping analysis [86]. Seven of them are proline directed kinase sites, which appear to be phosphorylated by JNK through a positive feedback loop mechanism. Ablation of MLK3 phosphorylation mediated by JNK reduces MLK3 activity, as judged by activation loop phosphorylation, and redistributes MLK3 to a Triton-insoluble fraction. These data have suggested that phosphorylation of the proline-rich carboxyl terminus of MLK3 by JNK maintains

MLK3 in the Triton soluble compartments where MLK3 signaling pathway is constitutively activated through positive feedback regulation [108].

3.3.8 Regulation of MLKs by subcellular localization

Signaling specificity can also be achieved by regulation of the subcellular localization, allowing the modulation of the substrate accessibility. Studies of immunohistochemical staining indicate that endogenous DLK localizes to the Golgi apparatus. Upon biochemical fractionation, DLK is present in a crude membrane-enriched fraction and can only be solubilized with Triton-X114, indicating that DLK is associated with the cytosolic face of the Golgi membranes [109]. Similar to DLK, MLK3 has been shown to be located at the perinuclear region [85] and colocalized with the Golgi marker [58]. Introduction of catalytic inactive MLK3 does not change its localization upon the biochemical fractionation [85], suggesting that the presence of MLK3 in the perinuclear region/Golgi is not regulated by MLK3 activity. Expressed MLK3 is targeted to cellular membranes by prenylated, activated Cdc42, resulting in full activation of MLK3 [85]. MLK3 has been reported to locate at the centrosome with the retarded gel motility during G2/M phase [110], suggesting that MLK3 is phosphorylated at that stage. As mentioned previously, inhibition of JNK-mediated MLK3 phosphorylation within its proline-rich carboxyl terminus redistributes MLK3 to a Triton insoluble fraction and attenuates MLK3 activity [108].

Expressed MLK2 localizes along microtubular structures with a punctate staining pattern [51]. Furthermore, kinesin superfamily proteins (KIFs) have been identified as MLK2-interacting proteins by yeast two hybrid assays [51]. KIFs are motor proteins

mainly involving in vesicular trafficking. MLK2 and MLK3 interact with KIF3 and the putative cargo recognition protein, KAP3 [51]. Taken together, these data have suggested that MLK2 and MLK3 might participate in regulation of vesicular trafficking.

3.4 The physiological roles of the MLKs

The function of MLKs is tightly associated with their upstream activators and downstream effector pathways under different physiological conditions. A large body of research work has demonstrated MLKs in development, cancer cell proliferation and neuronal apoptosis

3.4.1 The *Drosophila* MLK, *slpr* and *Xenopus* MLK

The *Drosophila* MLK ortholog, *slpr*, is required for JNK mediated dorsal closure during embryogenesis. During dorsal closure, the dorsal ectoderm moves from a lateral position to the dorsal midline to cover the embryo in a continuous protective epidermis [111]. GTPase dRac1, a MAP4K named Misshapen (Msn), *Slpr*, the MKK7 ortholog Hemipterous (Hep), the JNK ortholog Basket (Bsk) and the AP-1 transcription factors containing dJun and dFos comprise the JNK pathway in *Drosophila* in guidance of dorsal closure process [112]. *Slpr* mutant embryos have a dorsal open cuticle phenotype and fail to maintain the stretched morphology [112].

The *Xenopus* MLK ortholog, most similar to MLK2 with a 62% sequence identity, is expressed in the cement gland which is a mucus-secreting epithelium that forms from the extreme anterior ectoderm during the early development [39]. The expression of xMLK2 is associated with cell elongation and the apoptotic phase. at later stage,

expressed xMLK2 in the pronephros correlates with differentiation and opening of the nephric tubules [39]. These data suggest that MLKs function to regulate the differentiation of the epithelial layers.

3.4.2 The mammalian MLKs

Using RNAi-mediated MLK3 silencing, MLK3 has been connected to cell proliferation in tumor cells [49]. Recent reports suggest that MLK3 complexes with B-Raf and Raf-1 and is required for B-Raf- resulting in activation of ERK and promotion of cell proliferation. Furthermore, the catalytic activity of MLK3 is not required for EGF-induced ERK activation [113]. These data, suggest a scaffolding role, rather than catalytic role for MLK3 in growth factor mediated cell proliferation. The *mlk3* knockout mice are viable without any obvious defects [50]. TNF- α induced JNK activation was reduced two fold in *mlk3* knockout mouse embryonic fibroblasts (MEFs) [50], suggesting that MLK3 is essential for TNF- α mediated JNK activation and other MLKs may particularly compensate for the lack of MLK3. The *mlk3*^{-/-} MEFs retain intact MAPK activation pathways in response to various growth factor stimulations [50], whereas knockdown MLK3 by small interference RNA abolishes mitogen-induced and cytokines-induced MAPK activations [49]. It is possible that the deficiencies in MAPK activation are compensated by other MLKs during development. With transient knockdown by RNAi, the cellular phenotype observed will reflect effects of acute MLK3 depletion. Recently, the mutations of MLK4 have been found in clinical samples of gastric cancers, hepatocellular carcinomas, and colorectal cancers in Asian population [114-116]. The MLK4 gene mutation is present in 6.8% colorectal cancers and 50% mutations occur

within the kinase domain [114]. It has been proposed that MLK4 is a tumor suppressor gene.

Recent work has placed MLKs in metabolic stress signaling pathway which is important in insulin resistance and the development of type 2 diabetes. The saturated fatty acid, palmitic acid has been demonstrated to activate endogenous MLK3 in MEFs which in turns activates MKK7, MKK4 and JNK, resulting in phosphorylation of insulin receptor adaptor protein, IRS1, which causes the insulin resistance [67]. These demonstrated effects are abolished in *mlk3^{-/-}*, *mkk4^{-/-}* and *mkk7^{-/-}* MEFs. Additionally, treatment of MEFs with TPA, an inhibitor of all PKC isoforms, blocks MLK3 activation induced by palmitate, suggesting that PKC is the upstream activator of MLK3 [67]. Taken together, these data suggest that MLK3 activation in response to saturated fatty acids could contribute to insulin resistance and diabetes.

Some studies have implicated the MLKs in JNK-mediated neuronal apoptosis relying primarily on ectopic expression. It has been demonstrated that nerve growth factor (NGF) deprivation induces apoptosis through the substantial activation of JNK [117]. Expressed MLK2, MLK3 or DLK induces neuronal apoptosis in neuronal-like PC12 cells [24]. Overexpression of MLK3 in superior cervical ganglion (SCG) sympathetic neurons activates JNK and induces apoptosis, whereas expressed catalytically inactive MLK3 abrogates apoptosis in response to NGF deprivation [118]. Treatment with the MLK inhibitor CEP-1347 protects the cultured rat motoneurons and mice from neuronal apoptosis in response to various neurotoxins and neuronal stresses [25, 119]. Taken together, these data suggest that MLKs are activated by various neuronal stresses, resulting in potentiation of neuronal apoptosis through the persistent

activation of JNK. However, CEP-1347 failed to show efficacy in treating PD in a phase II/III clinical trial [120].

4. Leucine rich repeat kinases

Leucine rich repeat kinases (LRRKs) are members of the tyrosine kinase like (TKL) subfamily. These sequences of the kinase domain of TKL family members are similar to both tyrosine kinases and serine/threonine kinases. LRRKs are most similar to MLKs and receptor interacting protein kinases (RIPKs) which are crucial sensors of cellular stress connecting the extracellular stimuli to intracellular signal pathways. To date, LRRK2 mutations have been tightly associated with familial Parkinson's disease. No biological functions of wild type LRRKs have been reported.

4.1 LRRK family

The human genome encodes two LRRKs, LRRK1 and LRRK2. LRRKs are extremely large proteins. LRRK1 contains 2014 amino acids, giving a calculated molecular weight around 225 kDa. LRRK2 has 2527 amino acids, resulting in a predicted protein size of nearly 286 kDa. Based on amino acid sequence prediction, LRRK1 and LRRK2 share the same domain arrangements which are an amino terminal ankyrin (Ank) domain, a leucine rich repeat (LRR) domain, a putative Roc GTPase domain followed by a C-terminal of Roc (COR) region, a protein kinase domain and a carboxyl terminal WD-40 repeat domain [121]. The sequence identity within each structural domain between LRRK1 and LRRK2 is: 36% in the ankyrin repeat domain,

62% in the LRR domain, 47% in the Roc domain, 46% in the COR domain, 50% in the kinase domain and 59% in the WD40 repeat domain [121].

In human tissues, LRRK1 mRNA is primarily expressed in testis, with lower levels found in brain, prostate, lymph node, placenta and pancreas [122]. LRRK2 mRNA is highly expressed in lung, heart and putamen, at a lower level in substantial nigra [123, 124]. In mouse, both LRRKs are widely expressed in all brain regions. Murine LRRK1 mRNA is predominantly expressed in olfactory bulb and murine LRRK2 mRNA is mainly expressed in striatum, cortex, cerebellum and brainstem, at a lower level in hippocampus, midbrain and olfactory bulb [121]. In addition, mRNA of murine LRRK2 is also highly expressed in lung, spleen, and kidney tissues [125, 126]. However, murine LRRK2 protein is only detected in kidney and brain perhaps due to the low sensitivity of the used antibody [125].

4.2 Physiological roles of LRRKs

Mutations of LRRK2 have been segregated with familial Parkinson's disease (PD). PD is the most common neurodegenerative motor disorder in the western countries affecting 1-2% of the population aged 65 and older. The clinical symptoms of PD include resting tremor, bradykinesia (slowness of movement), muscle rigidity and impaired balance. The loss of the dopaminergic neurons in the *substantia nigra* and the presence of protein aggregates named Lewy bodies in the surviving neurons of the brainstem are the pathological hallmarks of PD [127]. To date, all available treatments are to ameliorate the clinical symptoms but do not cure the disease. Many environmental or genetic factors have been demonstrated to increase the risk of PD. To date, the

etiology of PD is ambiguous. It has been generally thought to correlate with the mitochondrial dysfunction, abnormal protein aggregation/degradation and defects in vesicular trafficking [128].

LRRK2 mutations cause autosomal dominant late-onset Parkinsonism, and are estimated to be responsible for about in 7% of familial PD and 0.4-1.6% in idiopathic PD cases [123, 124]. At present, more than 20 LRRK2 mutations have been reported from clinical genetic studies and these mutations are found in multiple LRRK2 structural domains (review in [129]), suggesting that each domain of LRRK2 which has a different predicted function which is somehow involved in the etiology of PD. Pathological examination of postmortem PD human brains that harbor LRRK2 mutations has revealed the loss of dopaminergic neurons in the substantia nigra, as expected, but other uncommon heterogeneous pathological features are sometimes present. While some cases retain α -synuclein positive Lewy body intracytoplasmic aggregates, other cases either do not have Lewy body aggregates, instead displaying widespread Lewy body pathology in the cerebral cortex or the presence of tau-positive axonal inclusions.

Interestingly, LRRK2 mutations within certain structural segments are prevalent in populations with different ethnic backgrounds. G2019, the most prevalent LRRK2 mutation within the kinase domain, is predominantly responsible for familial and sporadic PD in Arabs from North Africa; R1441C/G/H within the Roc domain accounts for LRRK2-associated familial PD in Spanish population and G2385R of the WD40 repeats is the major familial PD mutation found in Asian populations.

Although LRRK2 is widely expressed in various tissues, very little is known about LRRK2 function. Because LRRK2 mutations increase the risk of getting PD,

recent studies have intensively focused on the impact of pathological mutations of LRRK2 on neuronal toxicity, as judged by the aberrant neuronal morphology, viability, terminal deoxynucleotidyl transferase mediated biotin-dUTP nick end labeling (TUNEL) positive staining and caspase3 activation. Overexpression of kinase-defective LRRK2 in rat primary cortical neurons was demonstrated to prolong the neurite length and branching [130], suggesting a role of normal LRRK2 in controlling of neurite process. All expressed LRRK2 pathological mutants diminish the neurite length and complexity, with a most severe impairment in G2019S and I2020T-transfected neurons and a minor defect in R1441G and Y1699C expressed neurons [130]. Knockdown of LRRK2 by short hairpin RNA rescues this axonal deterioration mediated by LRRK2 mutations. Furthermore, expressed LRRK2 pathological mutants including G2019S, R1441C, Y1699C and G2358R enhanced caspase 3 activation, nuclear DNA fragmentation and TUNEL positive stained cells [130-132], resulting in neuronal apoptosis. Overexpression of the kinase-defective LRRK2 or mutants that disrupt GTP binding site of Roc significantly increases neuronal viability [130-132], suggesting that activation of LRRK2 or Roc results in neuronal apoptosis.

4.3 LRRK signaling activity

4.3.1 LRRK *in vitro* kinase activity

Recent emerging biochemical studies have demonstrated that both LRRK1 and LRRK2 possess *in vitro* kinase activity as judged by autophosphorylation [122, 126, 131-137]. In addition, LRRK2 has been shown to phosphorylate myelin basic protein (MBP), myosin light chain, moesin, creatine kinase and collapsing response mediator protein

(CRMP) 2 *in vitro* [126, 130, 135-137]. Interestingly, overexpressed LRRK1 failed to phosphorylate histone H1, casein and MBP which are commonly used as the exogenous kinase substrates *in vitro*, suggesting that the overexpressed LRRK1 is not very active [122]. Recently, LRRK2 purified from transgenic mouse brain has a higher *in vitro* catalytic activity than that from lung and transfected cultured cells [126].

Various amino acid substitutions in LRRK2 segregate with familial Parkinson's disease. These pathological mutations fall through all LRRK2 structural domains. G2019S, the most prevalent mutation which is located in the kinase domain, slightly increases LRRK2 catalytic activity *in vitro* [130-135, 137]. The impact of other LRRK2 pathological mutations on the *in vitro* kinase activity is still controversial (Table 1.1).

The conformationally active (GTP-bound) GTPases including Ras, Cdc42 and Rac ([76, 83, 84] and data not shown) have been demonstrated to bind their effector protein kinases, resulting in phosphorylation and activation of the protein kinases. Similarly, incubation of non-hydrolysable GTP, GTP γ S, enhances LRRK1 and LRRK2 *in vitro* autophosphorylation levels [122, 131, 132], suggesting that conformationally active GTPases increase LRRK1 and LRRK2 *in vitro* kinase activities.

4.3.2 MAP kinases and NF- κ B

Mitogen activated protein (MAP) kinases basically include ERK, JNK and p38 protein kinases that participate in the regulation of cell growth, differentiation, immune responses and apoptosis. The kinase sequence of LRRK2 is most closely related to that of MLKs and of RIP kinases in the TKL subfamily of protein kinases. MLKs function as MAPKKKs to activate MAP kinases and overexpressed MLKs also activate NF- κ B in

response to immune stimulation. RIP kinases mediate extracellular immune stresses through tumor necrosis factor α (TNF α) receptor, toll-like receptor (TOR) and T cell receptor (TCR) to cellular signaling pathways, MAP kinase pathways and NF- κ B (review in [138]). In spite of the high sequence similarity of the LRRK2 kinase domain with MLKs and RIP kinases, none of MAP kinase pathways including ERK, JNK, p38 and ERK5 is directly activated by overexpressed LRRK2 in human embryonic kidney 293T and human neuroblastoma SH-SY5Y cells (data not shown and [132]). Furthermore, upon overexpression of LRRK2, no NF- κ B activation was detected as judged by the luciferase reporter gene assay (data not shown).

4.4 Regulation of LRRK

Several recent biochemical studies have mainly focused on the impacts of LRRK2 pathological mutations for regulation of the LRRK2 kinase activity and neuronal apoptosis.

4.4.1 Regulation of LRRK by extracellular signals

Reactive oxygen species (ROS) are largely produced from the mitochondrial respiratory chain in cells. In animal experiments, administration of 1-methyl-4-phenyl-1,2,3,6-tetrahydropyridine (MPTP), a neurotoxin that inhibits the electron transport chain complex I of mitochondria which increases ROS level, induces symptoms similar to these in human PD. Moreover, 25-30% inhibition of complex I is observed in the postmortem samples of substantia nigra from PD patients. These data have revealed a key role of

Table 1.1. Summary of the *in vitro* kinase activity of LRRK2 pathological mutations.

amino acid substitution	location (domain)	kinase substrate ^a	kinase activity ^b	references
I1122V	LRR	LRRK2	+/-	[132]
I1371V	Roc	LRRK2	+/-	[132]
R1441C	Roc	LRRK2, MBP	+	[132, 137]
		LRRK2	-	[136]
		LRRK2, MBP	+/-	[136]
		LRRK2*	+	[135]
R1441G	Roc	LRRK2	+	[132, 137]
		MBP, myosin light chain	+	[130]
		LRRK2*	+/-	[135]
R1514Q	COR	LRRK2	+	[132]
Y1699C	COR	LRRK2	++	[132]
		LRRK2	-	[136]
		LRRK2*	+	[135]
I2012T	kinase	LRRK2	-	[132]
		LRRK2*	--	[135]
G2019S	kinase	LRRK2	+	[131, 132, 134, 135]
		LRRK2*	+	[135]
		MBP, myosin light chain	+	[130]
		MBP	+	[137]
I2020T	kinase	LRRK2	++	[132, 133]
		LRRK2*	+/-	[135]
T2356I	kinase	LRRK2*	+/-	[135]
G2358R	WD-40	LRRK2	+/-	[132]
		LRRK2*	-	[135]

a, the exogenous substrate used in the *in vitro* kinase assay.

b, *in vitro* kinase activity of LRRK2.

LRRK2*: truncated LRRK2 with AA1326-2527.

Abbreviations: LRR, leucine rich repeat; COR, C-terminal of Roc; MBP, myelin basic protein.

+: increased *in vitro* kinase activity, -: decreased *in vitro* kinase activity, +/-: no difference in *in vitro* kinase activity as compared to wild type LRRK2

ROS in PD. Treatment of the LRRK2-overexpressed mouse primary cortical neurons with hydrogen peroxide significantly induced neuronal death as judged by propidium-iodide positive nuclei and formation of nuclear fragmentation [132]. Whereas kinase defective LRRK2, D1994A, abolished hydrogen peroxide induced neuronal death, implicating that activation of LRRK2 induced by hydrogen peroxide results in neuronal death [132]. However, whether hydrogen peroxide modulates LRRK2 catalytic activity has not been tested.

4.4.2 Regulation of LRRK by GTPase

GTPases are molecular switches that regulate numerous cellular processes including activation of protein kinases in signal transduction. Roc, a putative GTPase evolutionally distinct from Ras GTPase superfamily, is always found in tandem with COR of unknown function in the ROCO proteins. ROCO proteins widely exist in prokaryotes, *Dictyostelium*, plants and metazoa but little is known about their functions.

LRRK1 and LRRK2 are ROCO proteins. Both have been shown to be competent to bind GTP [122, 126, 131, 132, 136, 139]. Disruption of the nucleotide binding pocket of Roc domain in full length LRRKs abolished the GTP binding ability *in vitro*, suggesting that GTP binds to the Roc domain of LRRKs [122, 126, 131, 132, 136, 139]. Purified murine LRRK2 from transgenic brain tissues has a 2-fold higher GTPase activity than that from lung and transfected HEK 293T cells [126]. It is possible that the interaction of LRRK2 with specific proteins within brain cells results in this higher GTPase activity of LRRK2. Moreover, expression of Roc domain alone is capable to bind and hydrolyze GTP, suggesting that Roc domain functions as a GTPase [126].

Addition of GTP γ S, the non-hydrolysable GTP, in the LRRK kinase assays potentiates the *in vitro* catalytic activity of LRRK about 2.5 fold [122, 131, 132]. These data suggest that Roc domain of LRRKs functions as a GTPase to regulate LRRK kinase activity *in vitro*.

Recent biochemical studies have mainly concentrated on the relationship of the pathological LRRK2 mutations and its *in vitro* kinase activity mediated by Roc domain. R1441C/G, the PD mutation within Roc domain, resides on the Roc surface which is far away from the nucleotide catalytic pocket based on the Roc structural model and is predicted to influence its protein interaction rather than the catalytic activity [129]. Recent results from other groups have demonstrated that this mutation decreases the GTP hydrolysis efficiency of both Roc and LRRK2, but does not affect their GTP-binding ability (unpublished data, [126, 136]). However, another contradictory report has demonstrated the bacterially expressed Roc domain containing R1441C has a similar GTPase activity as wild type [140]. Notably, there is a discrepancy from the published studies of R1441C/G and R1699C, which are the PD-associated mutations within the Roc and COR segments, in activation of LRRK2 *in vitro* (Table 1.1).

4.4.3 Regulation of LRRK by chaperones

Recently, the tandem affinity purification (TAP) procedure coupled with MALDI mass spectrometry analysis was used to identify proteins interacting with the LRRK2 kinase domain and full length LRRK2 in transient transfected HEK 293T cells. Hsp90 and its co-chaperone, Cdc37, were found to complex with LRRK2 kinase domain and full length LRRK2 under this condition [133]. Hsp90, one of the most abundant proteins in

eukaryotes, functions to assist protein folding and maintain the conformation of the client proteins. Many protein kinases including Raf-1 [141], MLK3 [65] and Src [141] have been demonstrated to interact with Hsp90 and Cdc37 through the catalytic domains of protein kinases. In these cases, the catalytic activity of protein kinases is not required for their interactions, suggesting that Hsp90 and Cdc37 are not substrates of protein kinases but serve as molecular chaperones. It is conceivable that Hsp90 and Cdc37 are required as chaperones function for LRRK2 because of its tremendously large size.

4.4.4 Regulation of LRRK by subcellular localization

In general, LRRK2 seems to be present in the cytosol and also associated with the membrane surface of various organelles. Upon biochemical fractionations, expressed LRRK2 in HEK 293T cells appears in an organelle-enriched fraction which includes mitochondria, peroxisomes and endoplasmic reticulum (ER) and the microsomal membrane-enriched fraction [133]. Upon treatment of the microsomal membrane fraction with basic carbonate buffer which releases most peripheral proteins from membranes, expressed LRRK2 is recovered in the supernatant portion [133], suggesting that LRRK2 associates with membranes rather than is integrated into membranes. Meanwhile, in addition to the membranous organelles, mitochondria, Golgi and ER, endogenous LRRK2 is also detected in the synaptic vesicle-enriched and synpatosomal cytosolic fractions from rodent brain tissues [125]. Submitochondrial fractionation experiments using purified mitochondria isolated from rodent brain have demonstrated that endogenous LRRK2 primarily locates on the outer membrane and matrix of mitochondria at a similar level [125]. It has been proposed that LRRK2 possibly binds

phospholipids through the LRR and WD40 domains due to their positive charge surfaces [129].

From analysis of immunofluorescent staining, expressed LRRK2 displays a diffuse cytoplasmic distribution and partially colocalizes with mitochondria, ER, Golgi and β -tubulin in HEK 293T cells [133]. In rat primary cortical neurons, endogenous LRRK2 colocalizes with mitochondria, lysosomes, at a less level with microtubular β -tubulin and with a negligible amount associated with synaptic vesicles[125]. Furthermore, in human and rat brain tissues, endogenous LRRK2 is ubiquitously distributed to cerebral cortex, substantial nigra, caudate putamen, olfactory bulb and brainstem. It also localizes at dopaminergic neurons with a punctate staining pattern around the cell body, at a lower content in dendrites and axons [125]. Same distribution of LRRK2 in the central nerve system has also been reported in LRRK2 transgenic mouse brain specimen [126]. However, whether the catalytic activity of LRRK2 is involved in regulation of its subcellular localizations and whether pathological mutations of LRRK2 are associated with the alteration of subcellular localization are still unknown.

5. Mitochondria

5.1 Mitochondria and human diseases

Mitochondria are the major sites to produce ATP through oxidative phosphorylation, and also serve as pivotal centers in determining programmed cell death. Aberrant mitochondrial function is tightly associated with various human diseases including cancer, cardiac disorders, diabetes and neurodegenerative disease [142-144].

Several lines of evidence have tightly linked the dysfunctional mitochondria to neurodegenerative diseases such as Parkinson's disease, Alzheimer disease, and Huntington disease. Biochemical studies demonstrated that defects in enzymes of the electron transport chain in postmortem human brain tissues of patients. The ganglia and substantia nigra are vulnerable to the accumulation of age dependent mitochondrial DNA deletions. Administration of MPTP, a neurotoxin which inhibits mitochondrial complex I of the electron transport chain, in animals, the subsequent symptoms resemble those observed in PD patients. In addition, the electron transport chain complex II inhibitor, 3-nitropropionic acid reconstitutes the clinical hallmarks of Huntington disease in animal models.

Under aerobic condition, the majority of cellular ATP is from the oxidative phosphorylation (OXPHOS) of mitochondria, with a slight level from glycolysis. In cancers, especially the solid tumor tissues which are under hypoxia environment, tumor cells primarily rely on glycolysis for ATP production rather than through OXPHOS, as known as the "Warburg effect" [145]. In this regard, suppression of glycolysis pathway should arrest tumor progression. Consequently, drugs that inhibit glycolysis have been applied in clinical cancer therapy to abate the growth of several carcinomas. For instance, 2-deoxy-D-glucose is in phase I clinical trial for lung, breast, pancreatic, gastric and head and neck cancers (Clinical study, 2007).

5.2 Mitochondrial signaling

Recently, mitochondrial signaling has been attracted intensive attentions. Upon development of the phospho-specific and phosphor-motif antibodies, many mitochondrial

proteins have been demonstrated as the phosphor-proteins. In addition to the metabolic labeling with radioisopes, an invention of the pro-Q diamond dye for detecting the steady-state phosphorylated proteins in SDS-PAGE allows more than 60 mitochondrial proteins from all mitochondrial compartments were identified (review in [146]). Enormous emerging evidence has been reported that more than 40 well known kinases and phosphatases which are involved in various signaling pathways and their downstream transcription factors were found to impact the mitochondrial functions.

Many well known protein kinases that play crucial roles in cell survival and tumorigenesis are also found in mitochondria, manipulating cellular energetics to potentiate cell proliferation and protecting cells against stress-induced cell death. Ectopically expressed, catalytic active Raf-1 is located at the outer membrane of mitochondria through its direct interaction with the BH4 domain of Bcl-2 which is a mitochondrial protein [147]. Mitochondrial Raf-1 phosphorylates Bad and cooperates with Bcl-2 to prevent staurosporine-induced apoptosis. Src tyrosine kinase is targeted to the mitochondria upon forming a protein complex with c-AMP dependent protein kinase (PKA), A-kinase anchor proteins (AKAP) 121 and protein tyrosine phosphatase 1 (PTPD1) [148]. AKAP121 increases Src-dependent phosphorylation of mitochondrial substrates, activity of oxidative respiratory chain and ATP production, resulting in an elevation of mitochondrial potential and the protective effect from apoptosis [148]. In response to epidermal growth factor (EGF) stimulation, tyrosine 845 of the expressed EGFR is phosphorylated by overexpressed Src kinase, allowing to be translocated to mitochondria where its associates with cytochrome c oxidase subunit II (COXII) [149]. Substitution of tyrosine 845 to phenylalanine sensitizes casapse-3 activation induced by

adriamycin, an anticancer drug commonly used in chemotherapy, in highly invasive human MDA-MB-231 breast cancer cells under EGF stimulation. These data suggest that translocation of EGFR to mitochondria interacting with COXII may positively control cell survival pathways and enhance oncogenesis.

A large body of work has also demonstrated that numerous protein kinases regulate mitochondrial proteins including Bcl-2 family proteins and components in electron transport chain reaction as well as metabolism, resulting in promotion of cellular apoptosis. JNK retranslocates to the mitochondria and phosphorylates Bcl-X_L at Thr 47 and 115 upon ionizing radiation [150]. Mutating these two phosphorylation sites in Bcl-X_L reduces ionizing radiation-induced apoptosis. These data suggest that the translocation of JNK to mitochondria regulates Bcl-X_L, the antiapoptotic protein, through its kinase activity, resulting in genotoxic induced apoptosis. Similarly, with phorbol ester 12-O-tetradecanoylphorbol-13-acetate (TPA) treatment, protein kinase C (PKC) δ is translocated to the mitochondria and induces apoptosis by releasing cytochrome c [151]. Expressed kinase inactive PKC δ fails to target to the mitochondria, suggesting that the kinase activity of PKC δ is required for TPA-mediated PKC mitochondrial redistribution to the mitochondria.

6. Objective of the thesis

Protein kinases are pivotal regulators in numerous cellular processes and the aberrant regulation of protein kinases results in human diseases. My thesis work has primarily concentrated on understanding the role of MLK3 protein kinase in human MCF-7 breast cancer cell line through its interacting protein, ANT2. The other part of my thesis is to characterize the Roc domain of LRRK2 whose mutations are segregated with familial Parkinson's disease.

As mentioned previously, MLK3 is widely expressed in most human tissues. Survey of various human epithelial cell lines has revealed the highest expression of MLK3 in breast cancer cell lines. To decipher the role of MLK3 in human breast cancers, an inducible Flag-MLK3 human breast cancer MCF-7 cell line and the immunoaffinity purification coupled with mass spectrometry were used to identify MLK3 interacting proteins. Data in Chapter II demonstrates the role of MLK3 interaction with the mitochondrial adenine nucleotide translocase 2 (ANT2) in regulation of cellular energetics in a breast cancer cell line. This study also unveils the mechanism of MLK3 associating with ANT2.

Various LRRK2 mutations cause the autosomal dominant late-onset familial Parkinson's disease with diverse pathological phenotypes. The pathological mechanisms resulted from these mutations are obscure. In addition to the kinase domain, LRRK2 also contains a putative GTPase domain, Roc, a COR region which is always in tandem with Roc and several protein-interaction domains including ankyrin, LRR and WD40. LRR2 mutations are found in all structural segments, suggesting that each domain is crucial in PD etiology. Data in Chapter III reveals the Roc domain of LRRK2 is a *bona fide*

GTPase. Introduction of R1441C/G, the PD-associated mutation within the Roc domain, has no effect on the GTP binding of the Roc domain. We have previously hypothesized that the PD-associated mutation, R1441C/G disrupts protein interaction rather impacts the GTP binding and hydrolysis of the Roc domain. Another part of Chapter III has also described studies of the Roc-COR domain-mediated protein interactions of LRRK2. In addition, the effect of the PD-associated mutations within the Roc-COR region on the Roc-COR mediated LRRK2 protein interaction has been assessed. In Chapter IV, the results presented in this work are summarized and final remarks as well as future directions are also included.

7. References

1. Manning, G., et al., *The protein kinase complement of the human genome*. Science, 2002. 298(5600): p. 1912-34.
2. Dhanasekaran, N. and E. Premkumar Reddy, *Signaling by dual specificity kinases*. Oncogene, 1998. 17(11 Reviews): p. 1447-55.
3. Lindberg, R.A., A.M. Quinn, and T. Hunter, *Dual-specificity protein kinases: will any hydroxyl do?* Trends Biochem Sci, 1992. 17(3): p. 114-9.
4. Knighton, D.R., et al., *Crystal structure of the catalytic subunit of cyclic adenosine monophosphate-dependent protein kinase*. Science, 1991. 253(5018): p. 407-14.
5. Kemp, B.E. and R.B. Pearson, *Protein kinase recognition sequence motifs*. Trends Biochem Sci, 1990. 15(9): p. 342-6.
6. Hanks, S.K., A.M. Quinn, and T. Hunter, *The protein kinase family: conserved features and deduced phylogeny of the catalytic domains*. Science, 1988. 241(4861): p. 42-52.
7. Huse, M. and J. Kuriyan, *The conformational plasticity of protein kinases*. Cell, 2002. 109(3): p. 275-82.
8. Morgan, D.O. and H.L. De Bondt, *Protein kinase regulation: insights from crystal structure analysis*. Curr Opin Cell Biol, 1994. 6(2): p. 239-46.
9. Johnson, L.N., M.E. Noble, and D.J. Owen, *Active and inactive protein kinases: structural basis for regulation*. Cell, 1996. 85(2): p. 149-58.
10. Pearson, R.B. and B.E. Kemp, *Protein kinase phosphorylation site sequences and consensus specificity motifs: tabulations*. Methods Enzymol, 1991. 200: p. 62-81.
11. Biondi, R.M. and A.R. Nebreda, *Signalling specificity of Ser/Thr protein kinases through docking-site-mediated interactions*. Biochem J, 2003. 372(Pt 1): p. 1-13.
12. Bos, J.L., *ras oncogenes in human cancer: a review*. Cancer Res, 1989. 49(17): p. 4682-9.
13. Joseph, J., *Ran at a glance*. J Cell Sci, 2006. 119(Pt 17): p. 3481-4.

14. Raftopoulou, M. and A. Hall, *Cell migration: Rho GTPases lead the way*. Dev Biol, 2004. 265(1): p. 23-32.
15. Farnsworth, C.L. and L.A. Feig, *Dominant inhibitory mutations in the Mg(2+)-binding site of RasH prevent its activation by GTP*. Mol Cell Biol, 1991. 11(10): p. 4822-9.
16. Feig, L.A. and G.M. Cooper, *Inhibition of NIH 3T3 cell proliferation by a mutant ras protein with preferential affinity for GDP*. Mol Cell Biol, 1988. 8(8): p. 3235-43.
17. Gibbs, J.B., et al., *Intrinsic GTPase activity distinguishes normal and oncogenic ras p21 molecules*. Proc Natl Acad Sci U S A, 1984. 81(18): p. 5704-8.
18. Manne, V., E. Bekesi, and H.F. Kung, *Ha-ras proteins exhibit GTPase activity: point mutations that activate Ha-ras gene products result in decreased GTPase activity*. Proc Natl Acad Sci U S A, 1985. 82(2): p. 376-80.
19. Der, C.J., T. Finkel, and G.M. Cooper, *Biological and biochemical properties of human rasH genes mutated at codon 61*. Cell, 1986. 44(1): p. 167-76.
20. Seabra, M.C., *Membrane association and targeting of prenylated Ras-like GTPases*. Cell Signal, 1998. 10(3): p. 167-72.
21. Silvius, J.R., *Mechanisms of Ras protein targeting in mammalian cells*. J Membr Biol, 2002. 190(2): p. 83-92.
22. Leung, K.F., R. Baron, and M.C. Seabra, *Thematic review series: lipid posttranslational modifications. geranylgeranylation of Rab GTPases*. J Lipid Res, 2006. 47(3): p. 467-75.
23. Xu, Z., N.V. Kukekov, and L.A. Greene, *POSH acts as a scaffold for a multiprotein complex that mediates JNK activation in apoptosis*. Embo J, 2003. 22(2): p. 252-61.
24. Xu, Z., et al., *The MLK family mediates c-Jun N-terminal kinase activation in neuronal apoptosis*. Mol Cell Biol, 2001. 21(14): p. 4713-24.
25. Maroney, A.C., et al., *Motoneuron apoptosis is blocked by CEP-1347 (KT 7515), a novel inhibitor of the JNK signaling pathway*. J Neurosci, 1998. 18(1): p. 104-11.
26. Gallo, K.A. and G.L. Johnson, *Mixed-lineage kinase control of JNK and p38 MAPK pathways*. Nat Rev Mol Cell Biol, 2002. 3(9): p. 663-72.

27. Dorow, D.S., et al., *Identification of a new family of human epithelial protein kinases containing two leucine/isoleucine-zipper domains*. Eur J Biochem, 1993. 213(2): p. 701-10.
28. Dorow, D.S., et al., *Complete nucleotide sequence, expression, and chromosomal localisation of human mixed-lineage kinase 2*. Eur J Biochem, 1995. 234(2): p. 492-500.
29. Katoh, M., et al., *Cloning and characterization of MST, a novel (putative) serine/threonine kinase with SH3 domain*. Oncogene, 1995. 10(7): p. 1447-51.
30. Ezoe, K., et al., *PTK1, a novel protein kinase required for proliferation of human melanocytes*. Oncogene, 1994. 9(3): p. 935-8.
31. Gallo, K.A., et al., *Identification and characterization of SPRK, a novel src-homology 3 domain-containing proline-rich kinase with serine/threonine kinase activity*. J Biol Chem, 1994. 269(21): p. 15092-100.
32. Ing, Y.L., et al., *MLK-3: identification of a widely-expressed protein kinase bearing an SH3 domain and a leucine zipper-basic region domain*. Oncogene, 1994. 9(6): p. 1745-50.
33. Holzman, L.B., S.E. Merritt, and G. Fan, *Identification, molecular cloning, and characterization of dual leucine zipper bearing kinase. A novel serine/threonine protein kinase that defines a second subfamily of mixed lineage kinases*. J Biol Chem, 1994. 269(49): p. 30808-17.
34. Sakuma, H., et al., *Molecular cloning and functional expression of a cDNA encoding a new member of mixed lineage protein kinase from human brain*. J Biol Chem, 1997. 272(45): p. 28622-9.
35. Gotoh, I., M. Adachi, and E. Nishida, *Identification and characterization of a novel MAP kinase kinase kinase, MLTK*. J Biol Chem, 2001. 276(6): p. 4276-86.
36. Bhattacharjya, S., et al., *Polymerization of the SAM domain of MAPKKK Ste11 from the budding yeast: implications for efficient signaling through the MAPK cascades*. Protein Sci, 2005. 14(3): p. 828-35.
37. Gross, E.A., et al., *MRK, a mixed lineage kinase-related molecule that plays a role in gamma-radiation-induced cell cycle arrest*. J Biol Chem, 2002. 277(16): p. 13873-82.

38. Stronach, B. and N. Perrimon, *Activation of the JNK pathway during dorsal closure in Drosophila requires the mixed lineage kinase, slipper*. *Genes Dev*, 2002. 16(3): p. 377-87.
39. Poitras, L., et al., *A tissue restricted role for the Xenopus Jun N-terminal kinase kinase kinase MLK2 in cement gland and pronephric tubule differentiation*. *Dev Biol*, 2003. 254(2): p. 200-14.
40. Cuenda, A. and D.S. Dorow, *Differential activation of stress-activated protein kinase kinases SKK4/MKK7 and SKK1/MKK4 by the mixed-lineage kinase-2 and mitogen-activated protein kinase kinase (MKK) kinase-1*. *Biochem J*, 1998. 333 (Pt 1): p. 11-5.
41. Fan, G., et al., *Dual leucine zipper-bearing kinase (DLK) activates p46SAPK and p38mapk but not ERK2*. *J Biol Chem*, 1996. 271(40): p. 24788-93.
42. Liu, T.C., et al., *Cloning and expression of ZAK, a mixed lineage kinase-like protein containing a leucine-zipper and a sterile-alpha motif*. *Biochem Biophys Res Commun*, 2000. 274(3): p. 811-6.
43. Rana, A., et al., *The mixed lineage kinase SPRK phosphorylates and activates the stress-activated protein kinase activator, SEK-1*. *J Biol Chem*, 1996. 271(32): p. 19025-8.
44. Merritt, S.E., et al., *The mixed lineage kinase DLK utilizes MKK7 and not MKK4 as substrate*. *J Biol Chem*, 1999. 274(15): p. 10195-202.
45. Yang, J.J., *Mixed lineage kinase ZAK utilizing MKK7 and not MKK4 to activate the c-Jun N-terminal kinase and playing a role in the cell arrest*. *Biochem Biophys Res Commun*, 2002. 297(1): p. 105-10.
46. Hirai, S., et al., *MST/MLK2, a member of the mixed lineage kinase family, directly phosphorylates and activates SEK1, an activator of c-Jun N-terminal kinase/stress-activated protein kinase*. *J Biol Chem*, 1997. 272(24): p. 15167-73.
47. Tibbles, L.A., et al., *MLK-3 activates the SAPK/JNK and p38/RK pathways via SEK1 and MKK3/6*. *Embo J*, 1996. 15(24): p. 7026-35.
48. Kim, K.Y., et al., *Mixed lineage kinase 3 (MLK3)-activated p38 MAP kinase mediates transforming growth factor-beta-induced apoptosis in hepatoma cells*. *J Biol Chem*, 2004. 279(28): p. 29478-84.

49. Chadee, D.N. and J.M. Kyriakis, *MLK3 is required for mitogen activation of B-Raf, ERK and cell proliferation*. Nat Cell Biol, 2004. 6(8): p. 770-6.
50. Brancho, D., et al., *Role of MLK3 in the regulation of mitogen-activated protein kinase signaling cascades*. Mol Cell Biol, 2005. 25(9): p. 3670-81.
51. Nagata, K., et al., *Activation of G1 progression, JNK mitogen-activated protein kinase, and actin filament assembly by the exchange factor FGD1*. J Biol Chem, 1998. 273(25): p. 15453-7.
52. Parameswaran, N., et al., *Mixed lineage kinase 3 inhibits phorbol myristoyl acetate-induced DNA synthesis but not osteopontin expression in rat mesangial cells*. Mol Cell Biochem, 2002. 241(1-2): p. 37-43.
53. Parameswaran, N., et al., *Mixed lineage kinase 3 inhibits platelet-derived growth factor-stimulated DNA synthesis and matrix mRNA expression in mesangial cells*. Cell Physiol Biochem, 2002. 12(5-6): p. 325-34.
54. Shen, Y.H., et al., *Cross-talk between JNK/SAPK and ERK/MAPK pathways: sustained activation of JNK blocks ERK activation by mitogenic factors*. J Biol Chem, 2003. 278(29): p. 26715-21.
55. Israel, A., *The IKK complex: an integrator of all signals that activate NF-kappaB?* Trends Cell Biol, 2000. 10(4): p. 129-33.
56. Hehner, S.P., et al., *Mixed-lineage kinase 3 delivers CD3/CD28-derived signals into the IkappaB kinase complex*. Mol Cell Biol, 2000. 20(7): p. 2556-68.
57. Masaki, M., et al., *Mixed lineage kinase LZK and antioxidant protein-1 activate NF-kappaB synergistically*. Eur J Biochem, 2003. 270(1): p. 76-83.
58. Cha, H., et al., *Phosphorylation of golgin-160 by mixed lineage kinase 3*. J Cell Sci, 2004. 117(Pt 5): p. 751-60.
59. Hicks, S.W. and C.E. Machamer, *Isoform-specific interaction of golgin-160 with the Golgi-associated protein PIST*. J Biol Chem, 2005. 280(32): p. 28944-51.
60. Mancini, M., et al., *Caspase-2 is localized at the Golgi complex and cleaves golgin-160 during apoptosis*. J Cell Biol, 2000. 149(3): p. 603-12.
61. Lee, J.E., et al., *Conversion of Xenopus ectoderm into neurons by NeuroD, a basic helix-loop-helix protein*. Science, 1995. 268(5212): p. 836-44.

62. Marcora, E., K. Gowan, and J.E. Lee, *Stimulation of NeuroD activity by huntingtin and huntingtin-associated proteins HAP1 and MLK2*. Proc Natl Acad Sci U S A, 2003. 100(16): p. 9578-83.
63. Xu, Z., N.V. Kukekov, and L.A. Greene, *Regulation of apoptotic c-Jun N-terminal kinase signaling by a stabilization-based feed-forward loop*. Mol Cell Biol, 2005. 25(22): p. 9949-59.
64. Sathyanarayana, P., et al., *Activation of the Drosophila MLK by ceramide reveals TNF-alpha and ceramide as agonists of mammalian MLK3*. Mol Cell, 2002. 10(6): p. 1527-33.
65. Zhang, H., et al., *Hsp90/p50cdc37 is required for mixed-lineage kinase (MLK) 3 signaling*. J Biol Chem, 2004. 279(19): p. 19457-63.
66. Ding, W.X. and X.M. Yin, *Dissection of the multiple mechanisms of TNF-alpha-induced apoptosis in liver injury*. J Cell Mol Med, 2004. 8(4): p. 445-54.
67. Jaeschke, A. and R.J. Davis, *Metabolic stress signaling mediated by mixed-lineage kinases*. Mol Cell, 2007. 27(3): p. 498-508.
68. Yu, H., et al., *Structural basis for the binding of proline-rich peptides to SH3 domains*. Cell, 1994. 76(5): p. 933-45.
69. Kiefer, F., et al., *HPK1, a hematopoietic protein kinase activating the SAPK/JNK pathway*. Embo J, 1996. 15(24): p. 7013-25.
70. Hubbard, S.R., M. Mohammadi, and J. Schlessinger, *Autoregulatory mechanisms in protein-tyrosine kinases*. J Biol Chem, 1998. 273(20): p. 11987-90.
71. Zhang, H. and K.A. Gallo, *Autoinhibition of mixed lineage kinase 3 through its Src homology 3 domain*. J Biol Chem, 2001. 276(49): p. 45598-603.
72. Hu, J.C., et al., *Sequence requirements for coiled-coils: analysis with lambda repressor-GCN4 leucine zipper fusions*. Science, 1990. 250(4986): p. 1400-3.
73. O'Shea, E.K., et al., *X-ray structure of the GCN4 leucine zipper, a two-stranded, parallel coiled coil*. Science, 1991. 254(5031): p. 539-44.
74. Leung, I.W. and N. Lassam, *Dimerization via tandem leucine zippers is essential for the activation of the mitogen-activated protein kinase kinase kinase, MLK-3*. J Biol Chem, 1998. 273(49): p. 32408-15.

75. Nihalani, D., S. Merritt, and L.B. Holzman, *Identification of structural and functional domains in mixed lineage kinase dual leucine zipper-bearing kinase required for complex formation and stress-activated protein kinase activation*. J Biol Chem, 2000. 275(10): p. 7273-9.
76. Bock, B.C., et al., *Cdc42-induced activation of the mixed-lineage kinase SPRK in vivo. Requirement of the Cdc42/Rac interactive binding motif and changes in phosphorylation*. J Biol Chem, 2000. 275(19): p. 14231-41.
77. Vacratsis, P.O. and K.A. Gallo, *Zipper-mediated oligomerization of the mixed lineage kinase SPRK/MLK-3 is not required for its activation by the GTPase cdc 42 but is necessary for its activation of the JNK pathway. Monomeric SPRK L410P does not catalyze the activating phosphorylation of Thr258 of murine MITOGEN-ACTIVATED protein kinase kinase 4*. J Biol Chem, 2000. 275(36): p. 27893-900.
78. Nihalani, D., et al., *Mixed lineage kinase-dependent JNK activation is governed by interactions of scaffold protein JIP with MAPK module components*. Embo J, 2001. 20(13): p. 3447-58.
79. Ikeda, A., et al., *Identification and characterization of functional domains in a mixed lineage kinase LZK*. FEBS Lett, 2001. 488(3): p. 190-5.
80. Bar-Sagi, D. and A. Hall, *Ras and Rho GTPases: a family reunion*. Cell, 2000. 103(2): p. 227-38.
81. Coso, O.A., et al., *The small GTP-binding proteins Rac1 and Cdc42 regulate the activity of the JNK/SAPK signaling pathway*. Cell, 1995. 81(7): p. 1137-46.
82. Minden, A., et al., *Selective activation of the JNK signaling cascade and c-Jun transcriptional activity by the small GTPases Rac and Cdc42Hs*. Cell, 1995. 81(7): p. 1147-57.
83. Burbelo, P.D., D. Drechsel, and A. Hall, *A conserved binding motif defines numerous candidate target proteins for both Cdc42 and Rac GTPases*. J Biol Chem, 1995. 270(49): p. 29071-4.
84. Teramoto, H., et al., *Signaling from the small GTP-binding proteins Rac1 and Cdc42 to the c-Jun N-terminal kinase/stress-activated protein kinase pathway. A role for mixed lineage kinase 3/protein-tyrosine kinase 1, a novel member of the mixed lineage kinase family*. J Biol Chem, 1996. 271(44): p. 27225-8.
85. Du, Y., et al., *Cdc42 induces activation loop phosphorylation and membrane targeting of mixed lineage kinase 3*. J Biol Chem, 2005. 280(52): p. 42984-93.

86. Vacratsis, P.O., et al., *Identification of in vivo phosphorylation sites of MLK3 by mass spectrometry and phosphopeptide mapping*. *Biochemistry*, 2002. 41(17): p. 5613-24.
87. Lambert, J.M., et al., *Role of MLK3-mediated activation of p70 S6 kinase in Rac1 transformation*. *J Biol Chem*, 2002. 277(7): p. 4770-7.
88. Morrison, D.K. and R.J. Davis, *Regulation of MAP kinase signaling modules by scaffold proteins in mammals*. *Annu Rev Cell Dev Biol*, 2003. 19: p. 91-118.
89. Whitmarsh, A.J., et al., *A mammalian scaffold complex that selectively mediates MAP kinase activation*. *Science*, 1998. 281(5383): p. 1671-4.
90. Yasuda, J., et al., *The JIP group of mitogen-activated protein kinase scaffold proteins*. *Mol Cell Biol*, 1999. 19(10): p. 7245-54.
91. Nihalani, D., H.N. Wong, and L.B. Holzman, *Recruitment of JNK to JIP1 and JNK-dependent JIP1 phosphorylation regulates JNK module dynamics and activation*. *J Biol Chem*, 2003. 278(31): p. 28694-702.
92. Buchsbaum, R.J., B.A. Connolly, and L.A. Feig, *Interaction of Rac exchange factors Tiam1 and Ras-GRF1 with a scaffold for the p38 mitogen-activated protein kinase cascade*. *Mol Cell Biol*, 2002. 22(12): p. 4073-85.
93. Schoorlemmer, J. and M. Goldfarb, *Fibroblast growth factor homologous factors are intracellular signaling proteins*. *Curr Biol*, 2001. 11(10): p. 793-7.
94. Kelkar, N., et al., *Interaction of a mitogen-activated protein kinase signaling module with the neuronal protein JIP3*. *Mol Cell Biol*, 2000. 20(3): p. 1030-43.
95. Matsuura, H., et al., *Phosphorylation-dependent scaffolding role of JSAP1/JIP3 in the ASK1-JNK signaling pathway. A new mode of regulation of the MAP kinase cascade*. *J Biol Chem*, 2002. 277(43): p. 40703-9.
96. Lee, C.M., et al., *JLP: A scaffolding protein that tethers JNK/p38MAPK signaling modules and transcription factors*. *Proc Natl Acad Sci U S A*, 2002. 99(22): p. 14189-94.
97. Tapon, N., et al., *A new rac target POSH is an SH3-containing scaffold protein involved in the JNK and NF-kappaB signalling pathways*. *Embo J*, 1998. 17(5): p. 1395-404.

98. Figueroa, C., et al., *Akt2 negatively regulates assembly of the POSH-MLK-JNK signaling complex*. J Biol Chem, 2003. 278(48): p. 47922-7.
99. Kukekov, N.V., Z. Xu, and L.A. Greene, *Direct interaction of the molecular scaffolds POSH and JIP is required for apoptotic activation of JNKs*. J Biol Chem, 2006. 281(22): p. 15517-24.
100. Garcia, E.P., et al., *SAP90 binds and clusters kainate receptors causing incomplete desensitization*. Neuron, 1998. 21(4): p. 727-39.
101. Savinainen, A., et al., *Kainate receptor activation induces mixed lineage kinase-mediated cellular signaling cascades via post-synaptic density protein 95*. J Biol Chem, 2001. 276(14): p. 11382-6.
102. Kolch, W., *Coordinating ERK/MAPK signalling through scaffolds and inhibitors*. Nat Rev Mol Cell Biol, 2005. 6(11): p. 827-37.
103. Ziogas, A., K. Moelling, and G. Radziwill, *CNK1 is a scaffold protein that regulates Src-mediated Raf-1 activation*. J Biol Chem, 2005. 280(25): p. 24205-11.
104. Jaffe, A.B., A. Hall, and A. Schmidt, *Association of CNK1 with Rho guanine nucleotide exchange factors controls signaling specificity downstream of Rho*. Curr Biol, 2005. 15(5): p. 405-12.
105. Pearl, L.H., *Hsp90 and Cdc37 -- a chaperone cancer conspiracy*. Curr Opin Genet Dev, 2005. 15(1): p. 55-61.
106. Leung, I.W. and N. Lassam, *The kinase activation loop is the key to mixed lineage kinase-3 activation via both autophosphorylation and hematopoietic progenitor kinase 1 phosphorylation*. J Biol Chem, 2001. 276(3): p. 1961-7.
107. Barthwal, M.K., et al., *Negative regulation of mixed lineage kinase 3 by protein kinase B/AKT leads to cell survival*. J Biol Chem, 2003. 278(6): p. 3897-902.
108. Schachter, K.A., et al., *Dynamic positive feedback phosphorylation of mixed lineage kinase 3 by JNK reversibly regulates its distribution to Triton-soluble domains*. J Biol Chem, 2006. 281(28): p. 19134-44.
109. Douziech, M., et al., *Localization of the mixed-lineage kinase DLK/MUK/ZPK to the Golgi apparatus in NIH 3T3 cells*. J Histochem Cytochem, 1999. 47(10): p. 1287-96.

110. Swenson, K.I., K.E. Winkler, and A.R. Means, *A new identity for MLK3 as an NIMA-related, cell cycle-regulated kinase that is localized near centrosomes and influences microtubule organization*. Mol Biol Cell, 2003. 14(1): p. 156-72.
111. Noselli, S., *JNK signaling and morphogenesis in Drosophila*. Trends Genet, 1998. 14(1): p. 33-8.
112. Stronach, B., *Dissecting JNK signaling, one KKKinase at a time*. Dev Dyn, 2005. 232(3): p. 575-84.
113. Chadee, D.N., et al., *Mixed-lineage kinase 3 regulates B-Raf through maintenance of the B-Raf/Raf-1 complex and inhibition by the NF2 tumor suppressor protein*. Proc Natl Acad Sci U S A, 2006. 103(12): p. 4463-8.
114. Bardelli, A., et al., *Mutational analysis of the tyrosine kinome in colorectal cancers*. Science, 2003. 300(5621): p. 949.
115. Lin, W., et al., *Tyrosine kinases and gastric cancer*. Oncogene, 2000. 19(49): p. 5680-9.
116. Shao, R.X., et al., *Absence of tyrosine kinase mutations in Japanese colorectal cancer patients*. Oncogene, 2007. 26(14): p. 2133-5.
117. Mielke, K. and T. Herdegen, *JNK and p38 stresskinases--degenerative effectors of signal-transduction-cascades in the nervous system*. Prog Neurobiol, 2000. 61(1): p. 45-60.
118. Mota, M., et al., *Evidence for a role of mixed lineage kinases in neuronal apoptosis*. J Neurosci, 2001. 21(14): p. 4949-57.
119. Saporito, M.S., et al., *CEP-1347/KT-7515, an inhibitor of c-jun N-terminal kinase activation, attenuates the 1-methyl-4-phenyl tetrahydropyridine-mediated loss of nigrostriatal dopaminergic neurons In vivo*. J Pharmacol Exp Ther, 1999. 288(2): p. 421-7.
120. Waldmeier, P., et al., *Recent clinical failures in Parkinson's disease with apoptosis inhibitors underline the need for a paradigm shift in drug discovery for neurodegenerative diseases*. Biochem Pharmacol, 2006. 72(10): p. 1197-206.
121. Taylor, J.P., et al., *Leucine-rich repeat kinase 1: a paralog of LRRK2 and a candidate gene for Parkinson's disease*. Neurogenetics, 2007. 8(2): p. 95-102.

122. Korr, D., et al., *LRRK1 protein kinase activity is stimulated upon binding of GTP to its Roc domain*. Cell Signal, 2006. 18(6): p. 910-20.
123. Paisan-Ruiz, C., et al., *Cloning of the gene containing mutations that cause PARK8-linked Parkinson's disease*. Neuron, 2004. 44(4): p. 595-600.
124. Zimprich, A., et al., *Mutations in LRRK2 cause autosomal-dominant parkinsonism with pleomorphic pathology*. Neuron, 2004. 44(4): p. 601-7.
125. Biskup, S., et al., *Localization of LRRK2 to membranous and vesicular structures in mammalian brain*. Ann Neurol, 2006. 60(5): p. 557-69.
126. Li, X., et al., *Leucine-rich repeat kinase 2 (LRRK2)/PARK8 possesses GTPase activity that is altered in familial Parkinson's disease R1441C/G mutants*. J Neurochem, 2007. 103(1): p. 238-47.
127. Fahn, S., *Description of Parkinson's disease as a clinical syndrome*. Ann N Y Acad Sci, 2003. 991: p. 1-14.
128. Cookson, M.R., *The biochemistry of Parkinson's disease*. Annu Rev Biochem, 2005. 74: p. 29-52.
129. Mata, I.F., et al., *LRRK2 in Parkinson's disease: protein domains and functional insights*. Trends Neurosci, 2006. 29(5): p. 286-93.
130. MacLeod, D., et al., *The familial Parkinsonism gene LRRK2 regulates neurite process morphology*. Neuron, 2006. 52(4): p. 587-93.
131. Smith, W.W., et al., *Kinase activity of mutant LRRK2 mediates neuronal toxicity*. Nat Neurosci, 2006. 9(10): p. 1231-3.
132. West, A.B., et al., *Parkinson's disease-associated mutations in LRRK2 link enhanced GTP-binding and kinase activities to neuronal toxicity*. Hum Mol Genet, 2007. 16(2): p. 223-32.
133. Gloeckner, C.J., et al., *The Parkinson disease causing LRRK2 mutation I2020T is associated with increased kinase activity*. Hum Mol Genet, 2006. 15(2): p. 223-32.
134. Greggio, E., et al., *Kinase activity is required for the toxic effects of mutant LRRK2/dardarin*. Neurobiol Dis, 2006. 23(2): p. 329-41.

135. Jaleel, M., et al., *LRRK2 phosphorylates moesin at threonine-558: characterization of how Parkinson's disease mutants affect kinase activity*. *Biochem J*, 2007. 405(2): p. 307-17.
136. Lewis, P.A., et al., *The R1441C mutation of LRRK2 disrupts GTP hydrolysis*. *Biochem Biophys Res Commun*, 2007. 357(3): p. 668-71.
137. West, A.B., et al., *Parkinson's disease-associated mutations in leucine-rich repeat kinase 2 augment kinase activity*. *Proc Natl Acad Sci U S A*, 2005. 102(46): p. 16842-7.
138. Meylan, E. and J. Tschopp, *The RIP kinases: crucial integrators of cellular stress*. *Trends Biochem Sci*, 2005. 30(3): p. 151-9.
139. Ito, G., et al., *GTP binding is essential to the protein kinase activity of LRRK2, a causative gene product for familial Parkinson's disease*. *Biochemistry*, 2007. 46(5): p. 1380-8.
140. Guo, L., et al., *The Parkinson's disease-associated protein, leucine-rich repeat kinase 2 (LRRK2), is an authentic GTPase that stimulates kinase activity*. *Exp Cell Res*, 2007. 313(16): p. 3658-70.
141. Helmbrecht, K., E. Zeise, and L. Rensing, *Chaperones in cell cycle regulation and mitogenic signal transduction: a review*. *Cell Prolif*, 2000. 33(6): p. 341-65.
142. Carew, J.S. and P. Huang, *Mitochondrial defects in cancer*. *Mol Cancer*, 2002. 1: p. 9.
143. DiMauro, S. and E.A. Schon, *Mitochondrial respiratory-chain diseases*. *N Engl J Med*, 2003. 348(26): p. 2656-68.
144. MacKenzie, J.A. and R.M. Payne, *Mitochondrial protein import and human health and disease*. *Biochim Biophys Acta*, 2007. 1772(5): p. 509-23.
145. Kim, J.W. and C.V. Dang, *Cancer's molecular sweet tooth and the Warburg effect*. *Cancer Res*, 2006. 66(18): p. 8927-30.
146. Pagliarini, D.J. and J.E. Dixon, *Mitochondrial modulation: reversible phosphorylation takes center stage?* *Trends Biochem Sci*, 2006. 31(1): p. 26-34.
147. Wang, H.G., U.R. Rapp, and J.C. Reed, *Bcl-2 targets the protein kinase Raf-1 to mitochondria*. *Cell*, 1996. 87(4): p. 629-38.

148. Livigni, A., et al., *Mitochondrial AKAP121 links cAMP and src signaling to oxidative metabolism*. Mol Biol Cell, 2006. 17(1): p. 263-71.
149. Boerner, J.L., et al., *Phosphorylation of Y845 on the epidermal growth factor receptor mediates binding to the mitochondrial protein cytochrome c oxidase subunit II*. Mol Cell Biol, 2004. 24(16): p. 7059-71.
150. Kharbanda, S., et al., *Translocation of SAPK/JNK to mitochondria and interaction with Bcl-x(L) in response to DNA damage*. J Biol Chem, 2000. 275(1): p. 322-7.
151. Majumder, P.K., et al., *Mitochondrial translocation of protein kinase C delta in phorbol ester-induced cytochrome c release and apoptosis*. J Biol Chem, 2000. 275(29): p. 21793-6.

II. A Novel Role for MLK3 in Mitochondria through Its Interaction with ANT2

1. Abstract

Mixed Lineage Kinase 3 (MLK3) is a widely expressed mammalian mitogen activated protein kinase kinase kinase (MAPKKK) that activates multiple mitogen-activated protein kinase (MAPK) pathways. In addition to its catalytic domain, MLK3 also contains multiple protein binding domains that participate in the regulation of MLK3 activity and signaling. Immunoblotting of cellular lysates from a variety of human epithelial cell lines revealed that MLK3 is expressed at high levels in breast cancer cell lines. To identify MLK3-interacting proteins in breast cancer cells, human breast cancer MCF-7 cells were engineered to inducibly express Flag-tagged MLK3. Using immunoaffinity purification coupled with mass spectrometry, adenine nucleotide translocase 2 (ANT2) was identified as one of the components of the Flag-MLK3 complex.

ANT2 functions as an ATP/ADP translocase in the mitochondria and plays an important role in regulating the energetic balance of cells. Co-immunoprecipitation experiments further confirmed the association of ectopically expressed ANT2 and MLK3. The kinase domain of MLK3 was sufficient for its interaction with ANT2. In addition, ANT2 preferentially bound to mutant forms of MLK3 that have enhanced catalytic activity. A portion of MLK3 biochemically fractionated with mitochondria. Confocal microscopy results demonstrated that MLK3 partially localized to the mitochondria. Ectopic coexpression of MLK3 and ANT2 resulted in elevation of the total cellular ATP level. In contrast, cellular ATP content was diminished upon transient expression of

catalytically inactive MLK3 with ANT2. Stable knockdown of MLK3 by short hairpin RNA decreased the total cellular ATP content whereas stable expression of MLK3 enhanced total ATP production. Taken together, these data open up the possibility that in addition to its role in MAPK pathway activation, MLK3 regulation of cellular ATP levels may influence cell proliferation.

2. Introduction

Mitochondria are cellular organelles with double membrane structures, giving rise to the different compartments including the outer membrane, intermembrane space, inner membrane and matrix (Figure 2.1). Mitochondria, a major site of oxidative metabolism in the cell, contain pyruvate dehydrogenase, the Krebs cycle enzymes, lipid-oxidizing enzymes as well as redox proteins involved in electron transport and oxidative phosphorylation (Figure 2.1). Aberrant mitochondrial function is associated with numerous human diseases including cancer, diabetes, cardiac disorders and neurodegenerative diseases [1-3]. Under aerobic conditions, the majority of cellular ATP is produced through oxidative phosphorylation mediated by electron chain transport complexes in the inner membrane of the mitochondria.

Mitochondria are also the decisive centers in apoptosis. Apoptosis, the name for energy-dependent programmed cell death, is critical in development. However, dysregulation of apoptosis is involved in pathologies, including cancer and neurodegenerative diseases. Apoptosis is accomplished through release of proapoptogenic factors, including cytochrome c, apoptosis inducing factor (AIF), second mitochondria-derived activator of apoptosis (Smac) and endo G nuclease, from the mitochondria. Released cytochrome c interacts with the apoptotic protease activating factor 1 (Apaf-1) and dATP to form the apoptosome, leading to the activation of caspase cascade. Caspases are proteases responsible for cleavage and inactivation of various proteins involved in DNA repair, cytoskeleton and chromosome integrity during apoptosis. In addition, released AIF [4, 5] and endo G nuclease [6] cause DNA fragmentation.

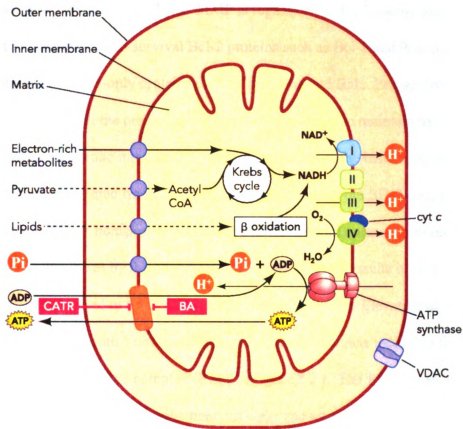


Figure 2.1. Schematic of mitochondrial ATP synthesis. Substrates, from pyruvates, electron-rich metabolites and the degradation of lipids through the β oxidation, are oxidized to produce NADH used by complex I, II, III and IV of the respiratory chain, generating a proton gradient across the inner mitochondrial membrane. ATP synthase uses the proton gradient to produce ATP from phosphate and ADP. The mitochondrial ATP is exported by ANT. ANT: adenine nucleotide translocase, VDAC: voltage dependent anion channel, BA: bongkreikic acid, CATR: carboxyatractyloside. Figure used is from Dahout-Gonzalez C. et al. Physiology, 2006, 21:242-249 with permission.

The release of proapoptogenic factors is accomplished by mitochondrial membrane permeabilization (MMP). MMP is regulated by Bcl-2 family proteins. The Bcl family includes the pro-survival Bcl-2 proteins such as Bcl-2 and Bcl-x_L as well as the pro-apoptotic BH-3-only proteins such as Bax, Bad and Bak. Pro-survival Bcl-2 proteins complex with the pro-apoptotic BH-3-only proteins to maintain the mitochondrial membrane integrity [7]. In response to apoptotic insults, pro-survival Bcl-2 proteins are sequestered from the heterocomplex, allowing the BH-3-only proteins to oligomerize and form nonspecific pores in the mitochondrial outer membrane. Formation of the nonspecific pores by the oligomeric BH3-only proteins results in an increase of MMP [8, 9], considered to be the irreversible step of apoptosis. Elevation of MMP is believed to partially result from the opening of different channels including the permeability transition pore complex (PTPC) (Figure 2.2.). The PTPC is an assembled protein complex built up at the mitochondrial outer and inner membranes and consists of three central components: the outer membrane voltage dependent anion channel (VDAC), the inner membrane adenine nucleotide translocase (ANT) and the matrix cyclophilin D [10].

In addition to its role as a major component of the PTPC, ANT also functions to exchange ADP and ATP across the mitochondrial membrane. Two conformational states of ANT have been described which exist in equilibrium in the mitochondrial membrane. In the *c* conformation, ANT faces the intermembrane space and in the *m* conformation, ANT faces the matrix. Based on studies from structure, functional characterization, and native gel electrophoresis, the current transport model of ANT has been proposed in

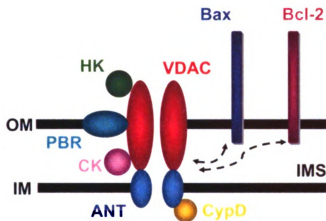


Figure 2.2. The architecture of the permeability transition pore complex. The precise components of the permeability transition pore complex (PTPC) are not completely known yet. The PTPC is primarily composed of the VDAC in the outer mitochondrial membrane and the ANT in the inner mitochondrial membrane. In addition, other proteins, including HK (interacting with VDAC from the cytosol), PBR (interacting within PTPC from the outer membrane), CK (interacting with PTPC from the intermembrane space) and CypD (interacting with ANT from the mitochondrial matrix), interact to bridge the outer and inner mitochondrial membranes of the PTPC. Both Bcl-2 and Bax proteins can directly interact and regulate the PTPC. Abbreviations, HK: hexokinase, VDAC: voltage dependent anion channel, PBR: peripheral-type benzodiazepine receptor, CK: creatine kinase, CypD: cyclophilin D, OM: outer membrane, IM: inner membrane, IMS: intermembrane space. Figure used is from Kroemer G et al. *Physiological review*, 2007, 87:99-163 with permission.

which two nucleotides bind the ANT monomer at the same time, one binding a nucleotide coming from the intermembrane space and the other one from the matrix. Cyclophilin D cooperates with the two monomers of ANT for synchronous exchange of ADP and ATP [11].

ANT isoforms are found in all organisms containing mitochondria but the number of ANT isoforms varies among different organisms. Yeast has three ANT isoforms from different genes but only ANT3 is required for cell growth under anaerobic condition [12]. Mouse and rat contain three ANT isoforms. In human, four isoforms of ANT are encoded by four different genes. ANT1, ANT2 and ANT3 share 88% sequence identity whereas ANT4 is less related, with about 70% sequence identity. The expression patterns of ANT isoforms seem to be determined by tissue type. The highest levels ANT1 mRNA are found in terminally differentiated tissues that do not undergo mitotic division such as heart, skeletal muscles and brain [13, 14]. ANT2 mRNA is mainly expressed in tissues capable of proliferation and regeneration including liver, kidney and spleen. Furthermore, it is also highly expressed in transformed and tumor cell lines and is down-regulated in quiescent cells [15]. ANT3 mRNA is ubiquitously expressed in various tissues [13, 14]. The transcripts of ANT4 are predominantly present in brain, liver and testis [14]. The expression of different ANT isoforms is also associated with developmental stage. Studies of muscle cell differentiation have demonstrated an increase in ANT1 mRNA and a decrease in ANT2 mRNA through the process of muscle cell differentiation [16]. The level of ANT3 mRNA is relatively low and stable during differentiation.

Alterations of levels of ANT isoforms lead to different biological outcomes in some experimental settings. For instance, transient overexpression of ANT1 or ANT3 in HEK 293T and HeLa cells induces a rapid apoptotic response through activation of caspase 9 and 3 [17], whereas overexpression of ANT2 has no effect on apoptosis [17]. A cumulative body of work has demonstrated that purified ANT (probably ANT1 since ANT is isolated from rat heart or brain tissues and ANT1 is the predominant isoform of ANT in these tissues) in the reconstituted liposomes forms nonspecific pores in response to diverse proapoptotic stimuli including pro-oxidants, calcium, nitric oxide and the ceramide derivative ganglioside GD3 [18]. Knockdown of ANT2 by small interference RNA (siRNA) in HeLa cells resulted in an elevation of mitochondrial membrane potential, increased ROS content and the decrease of total cellular ATP level, but had no effect on glycolysis and cell cycle [19]. Moreover, ANT2 knockdown sensitized HeLa cancer cells to Lonidamine, a clinical antitumor compound targeting mitochondrial ANT, leading to the induction of MMP [19]. Since ANT is involved in cellular energetics through ATP exchange as well as MMP regulation by forming the PTPC, ANT^{-/-} mice have been created to further assess these functions. ANT1 knockout mice are viable, fertile and have normal growth characteristics [20]. However, ANT1^{-/-} mice exhibit exercise intolerance and collapse during the incremental exercise stress test. Notably, the numbers of mitochondria present in the skeletal muscle of ANT1 knockout mice are increased and the respiration rate of complex III is also decreased. To date, ANT2 has been conditionally depleted in the murine liver tissue but no ANT2^{-/-} mice have been reported yet.

Until recently most research in signal transduction has focused on cytosolic and nuclear processes. However, recent results from several labs are giving rise to the idea that the mitochondrion and its constituent proteins are regulated by phosphorylation and other signaling events. Several labs have used phospho-specific and phospho-motif [21] antibodies such as the phospho-Akt substrate (PAS) antibody to identify the mitochondrial phosphoproteins under physiological conditions. In addition, pro-Q diamond staining[22] of phosphoproteins has been used in conjunction with SDS-PAGE to demonstrate steady state phosphorylation of mitochondrial proteins. Based on published reports, along metabolic labeling experiments using inorganic phosphate, more than 60 mitochondrial proteins from different mitochondrial compartments were identified as phosphoproteins [23] so far.

Since it is now known that mitochondrial phosphoproteins exist, it is reasonable that protein kinases may exist in association with or within the mitochondrion. Indeed, several signaling proteins have been discovered that are constitutively found in the mitochondria, including the protein kinase PINK-1 [24] and the protein phosphatase PTPMT1 [25]. One challenge has been to determine how these signaling proteins can be translocated to the mitochondria. Most mitochondrial proteins are synthesized in the nucleus and transported to the mitochondria through the canonical N-terminal mitochondrial targeting sequence. However, some resident mitochondrial proteins, including ANT and VDAC, lack canonical mitochondrial targeting sequences. The precise mechanism of translocation for these proteins precisely to the mitochondria is still a mystery.

Several signaling proteins lacking the canonical mitochondrial targeting sequence have been shown to be translocated to mitochondria through interaction with the mitochondrial (adaptor) proteins. For instance, in response to ionizing irradiation, JNK is translocated to mitochondria through its interaction with Bcl-XL [26]. Expressed Src tyrosine kinase is targeted to mitochondria through its protein interaction with A-kinase anchor proteins (AKAP) 121, which contains the canonical mitochondria targeting sequence [27]. However, the mechanisms of how these signaling molecules regulate resident mitochondrial proteins and their specific mitochondrial substrates remain unclear.

In the present study, using immunoaffinity purification coupled with mass spectrometry to identify MLK3 interacting proteins in breast cancer cells, ANT2 was discovered as one of the components in the MLK3 complexes. The data presented in this chapter show that the interaction of MLK3 with ANT2 is ANT isoform-specific and regulated by MLK3 activation status. Results from biochemical fractionation and confocal microscopy demonstrate that expressed MLK3 partially colocalizes with mitochondrial cytochrome c oxidase IV (COXIV). Coexpression of MLK3 and ANT2 in HEK 293T cells resulted in an elevation of the total cellular ATP level. Depletion of MLK3 by short hairpin RNA in MCF-7 breast cancer cells decreased the total cellular ATP content whereas induced expression of active MLK3 in MCF-7 cells enhanced it. Taken together, these data presented here suggest an upregulation of cellular energetics by MLK3 in a human breast cancer cell line and sheds light on the development of possible therapeutic targets for breast cancer.

3. Materials and Methods

3.1 Reagents and antibodies

TRIzol and SuperScript one-step RT-PCR for long templates were obtained from Invitrogen. The antibodies against phospho-JNK (G9), phospho-MLK3 and cleaved PARP were from Cell Signaling Biotechnology Inc. The sodium/potassium ATPase α 1 (N15) antibody was purchased from Santa Cruz Biotechnology Inc. The antibodies against cytochrome c oxidase subunit IV (COXIV), Flag-FITC and Alexa Fluor 488- or Alexa Fluor 546-conjugated secondary antibody were from Molecular Probes. The platelet derived growth factor receptor (PDGFR) β antiserum was obtained from BD PharMingen Biotechnology Inc. The Flag M2 and actin monoclonal antibodies were from Sigma-Aldrich. Other antibodies used were the MLK3 antibody, hemagglutinin (HA) antibody (BAbCO), and horseradish peroxidase-conjugated secondary antibodies (Bio-Rad).

3.2 Plasmid constructs

Mammalian expression constructs of wild type MLK3 and its mutations as well as truncation variants have been described previously [28-30]. The cDNAs encoding ANT1 or ANT2 were obtained by RT-PCR using total RNA isolated from HeLa cells or human MCF-7 breast cancer cells and the following oligonucleotides:

ANT1: 5'-CTTCTAGAATGGGTGATCACGCTTGGAGC-3',

5'-TAACTAGTGACATATTTTTTGATCTCATC-3';

ANT2: 5'-TGACCTTCTAGAATGACAGATGCCGCTGTGTCC-3',

5'-TAACTAGTTGTGTA CTTCTTGATTTCATC-3'.

The amplified ANT1 and ANT2 cDNAs were individually subcloned into the pCF1 mammalian expression vector (a gift from Dr. Joan Brugge, Harvard Medical School) using XbaI and SpeI restriction sites with the HA tag at the C-terminus. All constructs were subsequently verified by DNA sequencing.

3.3 Cell culture and transfection

Human embryonic kidney (HEK) 293T cells were cultured in Ham's F12/ low glucose DMEM media (1:1) supplemented with 8% fetal bovine serum, 2 mM glutamine and 100 U/ml penicillin/streptomycin and transfected using either Lipofectamine 2000 reagent (Invitrogen) following the manufacturer's instructions, or using the calcium phosphate method. Human breast cancer MCF-7 cells, human neuroblastoma SH-SY5Y cells and HeLa cells were cultured in high glucose Dulbecco's modified Eagle's medium supplemented with 10% fetal bovine serum, 2 mM glutamine, and 100 U/ml penicillin/streptomycin. All cell lines were maintained at 37 °C in a humidified incubator containing 5% CO₂ in air. MCF-7/iFlag-MLK3 cells inducibly expressing Flag-MLK3 have been described elsewhere [31].

3.4 Construction of MLK3 stable knockdown cell line

The oligonucleotides for short hairpin RNAs predicted to target human MLK3, 5'-GATCCCCGCAGTGACGTCTCCAGTTTTTCAAGAGAAAACCTCCAGACGT CACTGCTTTTTA-3' and 5'-AGCTTAAAAAGCAGTGACGTCTGGAGTTTTCT CTTGAAAAACTCCAGACGTCCTGCGGG-3' were designed using OligoEngine 2.0 program, synthesized, annealed and then ligated into the pSuper-retro-puro vector

(OligoEngine) with HindIII and Bgl II sites. 293-GPG packaging cells were transfected with pSuper-shMLK3 plasmid using Lipofectamine 2000. Viral supernatant was collected on days 4, 5, 6 and 7 post transfection, pooled virus was filtered and added to MCF-7 cells for 24 h. After removal of the retrovirus-containing media, infected MCF-7 cells were selected with 2 $\mu\text{g}/\text{ml}$ puromycin for 1 week. The MCF-7 cell line stably expressing the short hairpin RNA for MLK3 was maintained in DMEM growth media containing 1 $\mu\text{g}/\text{ml}$ puromycin for further experiments. This cell line was established by Eva Miller in the Gallo lab.

3.5 Cell lysis and immunoprecipitation

After transfection, cells were rinsed with ice-cold PBS and lysed in lysis buffer (50 mM HEPES (pH 7.5), 150 mM NaCl, 1.5 mM MgCl_2 , 2 mM EGTA, 1% Triton X-100, 10% glycerol, 1 mM Na_4PPi , 100 μM β -glycerophosphate, 1 mM Na_3VO_4 and 1X protease inhibitor cocktail (Sigma Aldrich)) on ice.

Antibodies against the proteins of interest were prebound to protein A agarose beads for 30 min at room temperature: MLK3 antiserum (0.25 $\mu\text{g}/\mu\text{l}$ slurry), M2 monoclonal Flag antibody (0.45 $\mu\text{g}/\mu\text{l}$ slurry), HA antibody (0.45 $\mu\text{g}/\mu\text{l}$ slurry). Clarified cellular lysates were incubated with 20 μl of antibody-bound protein A agarose for 90 min at 4°C. Immunoprecipitates were washed twice with HNTG buffer (20 mM HEPES (pH 7.5), 150 mM NaCl, 0.1% Triton X-100, and 10% glycerol).

3.6 Gel electrophoresis and Western blot analysis

Clarified cellular lysates and immunoprecipitates were resolved by SDS-PAGE. Proteins were transferred to nitrocellulose membranes and immunoblotted using appropriate antibodies. Immunoblots were developed by the chemiluminescence method.

3.7 Identification of ANT peptides in the MLK3 immune complex by Mass Spectrometry

Flag-MLK3 expression was induced by the addition of 50 nM AP21967 for 20 h to MCF-7/iFlag-MLK3 cells. Flag-MLK3 protein complexes were isolated as described previously [31] and further subjected to an in-gel digestion with trypsin. Nano-electrospray liquid chromatography/tandem mass spectrometry (LC/MS/MS) was performed to identify the proteins co-purified with MLK3 [31]. The identification of MLK3 interacting proteins by mass spectrometry was performed by Hua Zhang and Yan Du in the Gallo lab in conjunction with the MSU Proteomics facility.

3.8 Immunofluorescence and confocal microscopy

Transfected HeLa cells grown on cover slips were incubated with 0.1 μ M MitoTracker Red for 30 min, rinsed twice with PBS and fixed in 2% formaldehyde (Polyscience, Inc.) for 10 min at room temperature. Cells were permeabilized in PBS containing 0.15% Triton X-100 for 10 min. For COXIV staining, transfected HeLa cells were directly fixed and permeabilized with cold methanol for 15 min at -20°C. Samples were blocked with 2% bovine serum albumin in PBS for 1 h at room temperature. After

incubation with primary antibody (Flag M2 monoclonal antibody, FITC-Flag antibody and COXIV mouse monoclonal antibody) in PBS containing 2% bovine serum albumin for 1 h at room temperature, cells were washed three times with PBS and incubated with the appropriate Alexa Fluor 488- or/and Alexa Fluor 546-conjugated secondary antibodies (Molecular Probes) for 1 h at room temperature. After extensive washing with PBS, cover slips were mounted onto glass slides. The fluorescently labeled cells were examined with a Zeiss LSM Pascal confocal laser scanning microscope. Three separate tracks were used for capturing fluorescence and phase contrast images; excitation was done using 488 nm- and 543 nm-lasers with BP 500-530 nm, BP 560-615 nm and phase 3, respectively, as emission filters.

3.9 Subcellular fractionation

Cells were washed with phosphate-buffered saline (PBS) after trypsinization and resuspended in ice-cold Buffer A (10 mM Tris-HCl (pH7.6), 0.15 mM MgCl₂, 10 mM KCl) supplemented with protease inhibitor cocktail (Sigma), Na₄PPi and Na₃VO₄. Cells were incubated on ice for 1 h and homogenized with a Dounce homogenizer. Nuclei and unbroken cells were eliminated after centrifugation at 900 x g for 3 min at 4°C. Subsequent centrifugation of the supernatant at 6800 x g for 10 min at 4°C generates a soluble fraction (S6.8) and a mitochondrial-enriched pellet fraction (P6.8). The pellet fraction was resuspended with Buffer A. Equal cellular equivalents from the S6.8 and P6.8 fractions were resolved by SDS-PAGE and analyzed by immunoblotting.

3.10 Determination of cellular ATP level

Twenty four hours post-transfection, HEK 293T cells transiently expressing the proteins of interest were lysed in lysis buffer containing 1% trichloroacetic acid. MCF-7 cells either stably expressing short hairpin RNA of MLK3 or inducibly expressing MLK3 upon addition of AP21967 for 24 h were also lysed in the same lysis buffer as described previously. The total cellular ATP level from clarified cellular lysates was determined using the ENLITEN bioluminescence ATP detection kit (Promega, Inc.), according to the manufacturer's instructions. Beta-galactosidase activity, measured using a luminescent beta-galactosidase detection kit (BD Biosciences), was used as a transfection control. Protein concentration was determined using the Bradford method and equal amounts of proteins were used for the assays involving the stable cell lines.

4 Results

4.1 ANT was identified in MLK3 complexes

The MCF-7/iFlag-MLK3 cell line, engineered to inducibly express Flag-tagged MLK3, was previously established in our laboratory to study the role of MLK3 in breast cancer through the identification of its interacting proteins [31]. Inducibly expressed Flag-MLK3 and its associated proteins were isolated by affinity purification with the Flag antibody. MLK3-associated proteins were visualized by Coomassie Blue staining. In addition to Flag-MLK3, a Coomassie blue-stained 32 kDa protein band was consistently present only in the induced sample in several independent experiments, one of which is shown in Figure 2.3. Tryptic digestion followed by mass spectrometry analysis identified this 32 kDa band as adenine nucleotide translocase (ANT). All of the identified peptides from the ANT protein sequence from different experiments are listed in Table 2.1. In human cells, there are four isoforms of ANT encoded by four different genes. All of the ANT peptides identified by LC/MS/MS can be found in the protein sequence of ANT2, although a subset of them is present in the protein sequences of ANT1, ANT3 or ANT4. Therefore, we can reasonably conclude that ANT2 is present in the MLK3 complex. However, we cannot exclude the possibility that ANT1, ANT3 and/or ANT4 may interact with MLK3 as well.

4.2 Ectopically expressed ANT1 and ANT2 are targeted to the mitochondria

ANT is a six trans-membrane protein located in the inner membrane of the mitochondria. The function of ANT is to export ATP from the mitochondria to the cytoplasm, in exchange for ADP. The sequences of ANT1, ANT2 and ANT3 share 90%

identity; ANT4 is ~70% identical to ANT1. As a result, no antibody commercially available is known to discriminate between the different ANT isoforms. Furthermore, no commercially available antibodies reliably recognize ANT2. Indeed, it has been proven difficult to generate antibodies that recognize ANT2 (Dr. Catherine Brenner at Universite de Versailles/St. Quentin, France, personal communication). ANT1 is the best characterized of the ANT isoforms and the most abundant in many tissue types. To study the isoform selectivity of the MLK3-ANT interaction, ANT1 and ANT2 were cloned with an expressed HA epitope tag. ANT1 cDNA was amplified from total RNA of HeLa cells and ANT2 cDNA was amplified from total RNA of MCF-7 cells. The ANT cDNAs were cloned into expression vectors with the coding sequence for the HA epitope-tag at their carboxyl termini. The localization of HA-ANT1 and HA-ANT2 was assessed by biochemical fractionation and confocal microscopy. To generate a mitochondria-enriched fraction, post-nuclear lysates were centrifuged at 6,800g to generate a soluble fraction (S6.8) and a pellet fraction (P6.8). As shown in Figure 2.4, the S6.8 fraction contains cytosolic proteins like Cdc37 as well as light membrane proteins such as early endosome antigen 1 (EEA1). The P6.8 fraction contains the mitochondrial protein, COX IV, but is devoid of cytosolic and other light membrane proteins. Ectopically expressed HA-ANT1 and HA-ANT2 were found in the mitochondria-enriched fraction (Figure 2.4). Moreover, as shown in Figure 2.5, ANT2 transiently expressed in HeLa cells colocalized with MitoTracker Red, a mitochondrial dye that stains intact mitochondria. Taken together, these data indicate that the ectopically expressed ANT proteins are correctly targeted to the mitochondria, suggesting that they are properly folded and functional.

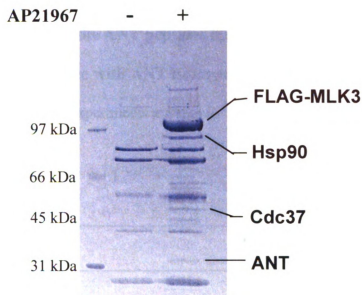


Figure 2.3. ANT was identified in affinity-isolated MLK3 complexes. MCF-7/iFlag-MLK3 cells were incubated in the presence or absence of AP21967 for 20 h. Flag-MLK3 and its associated protein complexes were immunopurified as described previously [31], resolved by SDS-PAGE on a 4–12% acrylamide gradient gel and stained with Coomassie Blue. Molecular weight markers are indicated on the *left* in kDa. Selected proteins identified by LC/MS/MS are indicated (experiment performed by Hua Zhang).

Table 2.1. Sequences of the ANT peptides identified by mass spectrometry and their correspondence with ANT isoforms. The total numbers of ANT peptides obtained in 5 independent experiments are shown.

Peptide sequence	# of times observed	ANT isoforms
DFLAGGVAAAISK	4	2
DFLAGGVAAAISKTAVAPIER	1	2
TAVAPIER	1	1,2,3,4
LLLQVQHASK	1	1,2,3
EQGVLSFWR	1	2,3
YFPTQALNFAFK	5	1,2,3,4
QIFLGGVDKR	2	2
AAYFGIYDTAK	4	2
NTHIVISWMIAQTVTAVAGLTSYPFDTVR	1	2
MMMQSGR	1	1,2,3

4.3 MLK3 interacts with ANT2 through its kinase domain

The mass spectrometry data indicate the presence of ANT2 in the MLK3 complex. It is possible that MLK3 may complex specifically with the ANT2 isoform. Alternatively, ANT2 may be present in the MLK3 complex because it is the predominant isoform expressed in the MCF-7 breast cancer cell line. To confirm the MLK3-ANT interaction and to determine whether MLK3 exhibits selectivity for ANT isoforms, co-immunoprecipitation experiments were performed. HEK 293T cells were co-transfected with expression vectors for MLK3 and HA-ANT1 or HA-ANT2. MLK3 was immunopurified from total cellular lysates and the presence of ANT1/2 was detected by immunoblotting. As shown in Figure 2.6, HA-ANT2, but not HA-ANT1, can interact with MLK3. These data suggest that MLK3 is competent to complex with ANT2, but not ANT1. In agreement with published reports, overexpression of HA-ANT1, but not HA-ANT2, induced apoptosis as judged by the cleavage of poly ADP ribose polymerase (PARP), a substrate for activated caspase 3 and 7. These data suggest that the ANT1 and ANT2 constructs used here are functionally competent. Notably, coexpression of MLK3 with ANT2 in HEK 293T cells did not result in PARP cleavage, suggesting that neither MLK3 nor ANT2 is proapoptotic under these conditions.

To determine which region of MLK3 is required for its interaction with ANT2, the NH₂-terminal or COOH-terminal halves of MLK3 were used in co-immunoprecipitation experiments. MLK3 (1-399) encompasses the NH₂-terminal glycine-rich region, the SH3 domain and the kinase domain; MLK3 (400-847) includes the leucine zipper region, the CRIB motif and the carboxyl-terminal Pro/Ser/Thr-rich

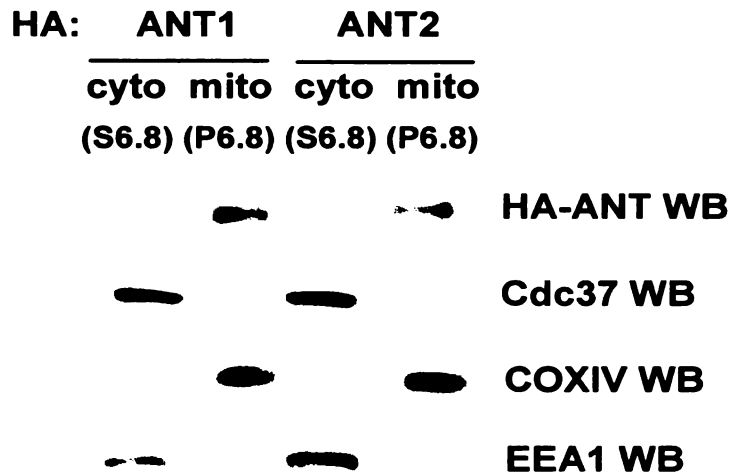


Figure 2.4. Ectopically expressed ANTs are mainly present in a mitochondria-enriched fraction. HEK 293T cells transiently expressing either HA-ANT1 or HA-ANT2 were biochemically fractionated as described in Materials and Methods. Proteins of interest from each fraction were analyzed by Western blotting with appropriate antibodies. Equal cellular equivalent proteins from each fraction were loaded. The efficiency of the fractionation was assessed by Western blotting with antibodies directed against the cytosolic Cdc37, the mitochondrial cytochrome c oxidase (COX) IV and early endosomal antigen 1 (EEA1). Data shown is representative of 3 independent experiments.

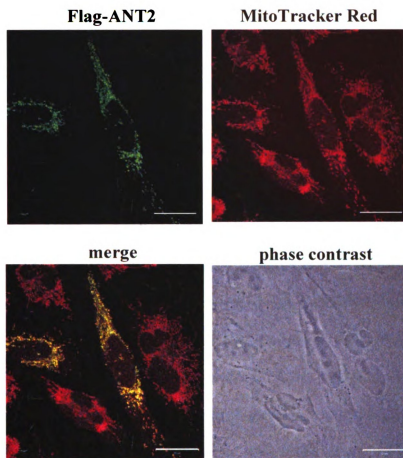


Figure 2.5. Ectopically expressed ANT2 localizes to the mitochondria. HeLa cells transiently expressing Flag-ANT2 were incubated with the mitochondrial probe, MitoTracker Red for 30 min, followed by formaldehyde fixation. The images of Flag-ANT2 (*green*) and mitochondria (*red*) were visualized with a Zeiss LSM Pascal confocal laser scanning microscope. A phase contrast image was taken as a control. Representative images shown here are from 3 independent experiments. Scale bar indicated is 10 μm .

region. MLK3 (1-399), but not MLK3 (400-847), associated with ANT2 (Figure 2.7A). Various Flag-tagged MLK3 truncations were used to confirm this result. MLK3 (1-598) lacks the Pro/Ser/Thr-rich region; MLK3 (1-485) terminates just after the zipper domain; and MLK3 (1-386) contains from the NH₂ terminus through the kinase domain. All of these MLK3 truncations associated with HA-ANT2 (Figure 2.7B), indicating that amino acids 1-386 of MLK3 are sufficient for its interaction with ANT2.

To further dissect which domain within MLK3 (1-386) is responsible for the interaction with ANT2, the binding ability of the individual regions or domains within this portion of MLK3 was evaluated by coimmunoprecipitation experiments. The isolated kinase domain, MLK3 (115-399) is able to associate with ANT2 whereas the region including the glycine-rich region and SH3 domain, MLK3 (1-114), fails to do so (Figure 2.7C). However, the expression level of MLK3 (1-114) is much lower than that of the kinase domain in transfected cells, which prevents a definitive conclusion. To rule out the possibility that MLK3 may also interact with ANT2 through its SH3 domain, a recombinant GST-SH3 fusion protein was used in a pull-down assay. ANT2 is incompetent to bind the SH3 domain of MLK3. MLK3 Y52A which previously shown to interact with the SH3 domain of MLK3 through the proline at 469, was used as a positive control and MLK3 P469A was used as a negative control (Figure 2.7D). Taken together, these data indicate that the kinase domain of MLK3 is necessary and sufficient for its interaction with ANT2.

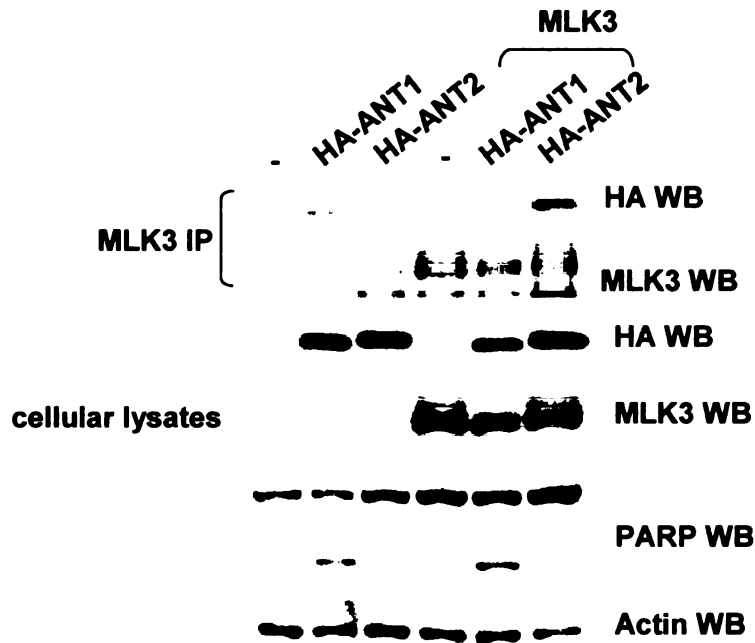


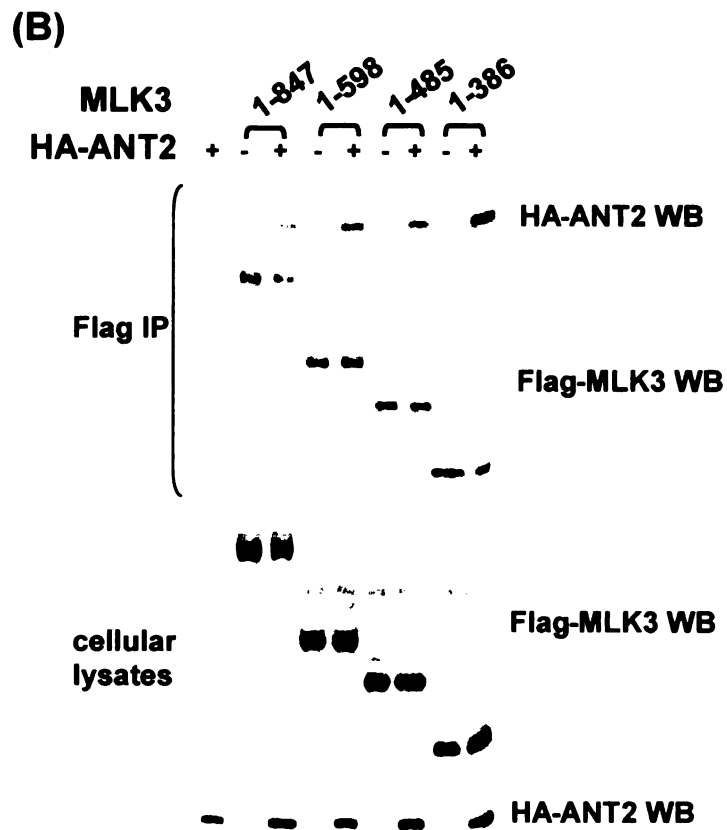
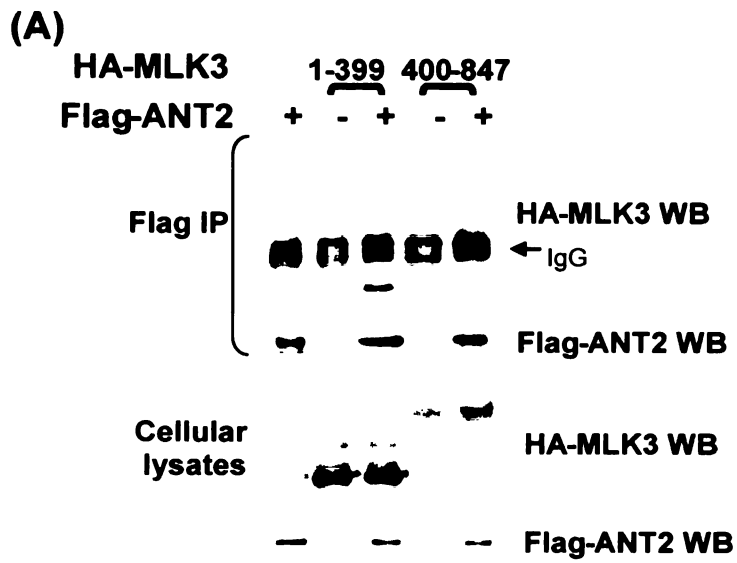
Figure 2.6. ANT2, not ANT1 specifically interacts with MLK3. HA-ANT1, HA-ANT2 with or without MLK3 were transiently expressed in HEK293T cells for 20-24 h. *Top panel*, MLK3 was immunoprecipitated using a MLK3 antibody from the clarified cellular lysates. The presence of ANT in the MLK3 immunoprecipitates was assessed by western blot with the HA antibody. *Bottom panel*, the protein level of MLK3, ANT in the total cellular lysates was assessed by western blot with appropriate antibodies. Actin was used as a loading control. Representative data shown is from 5 independent experiments.

4.4 The activation status of MLK3 regulates its association with ANT2

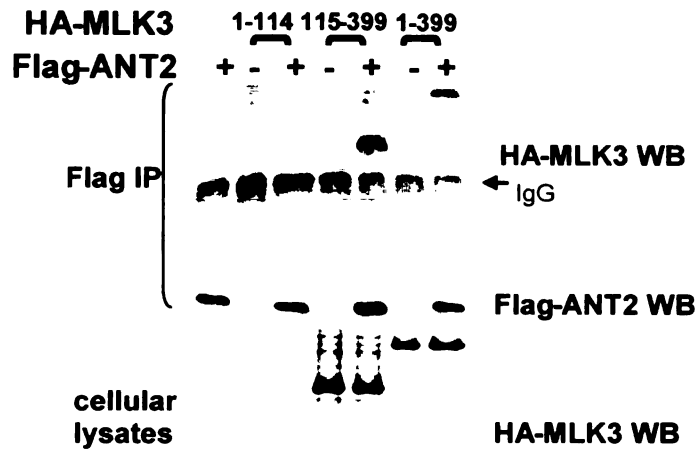
Since the kinase domain of MLK3 mediates its interaction with ANT2, it is conceivable that the activation state of MLK3 may influence this association. To investigate this possibility, a series of MLK3 mutants with various levels of catalytic activity were tested for their ability to associate with ANT2. A MLK3 leucine zipper mutant form, MLK3 L410P, has very low MLK3 kinase activity and fails to activate the JNK pathway ([29], Figure 2.8B). As shown in Figure 2.9A, MLK3 L410P fails to co-immunoprecipitate with ANT2. The association of a kinase-defective form of MLK3, MLK3 K144A (Figure 2.8B), with ANT2 was also dramatically decreased (Figure 2.9B). Conversely, MLK3 variants that have higher basal catalytic activity through disruption of MLK3 autoinhibition, MLK3 Y52A and MLK3 P469A ([30], Figure 2.8A and 2.8C), were more efficiently complexed with ANT2 than wild type MLK3. It has been postulated that relieving MLK3 autoinhibition results in a conformational change that opens and extends MLK3, exposing the kinase domain for catalysis. If the interaction of MLK3 with ANT2 depends on this conformational alternation, a MLK3 variant conformationally open but catalytically inactive would be expected to associate with ANT2. To test this hypothesis, MLK3 P469A and MLK3 K144A/P469A, a kinase dead/open conformer of MLK3, were tested for their catalytic activity first and then assessed for their ability to interact with ANT2 in the co-immunoprecipitation experiment. Since MLK3 activates JNK through activation and phosphorylation of MKK4/7, the JNK activity was used as a readout for MLK3 activity of MLK3 P469A and MLK3 K144R/P469A. MLK3 P469A strongly activates JNK whereas MLK3 K144A/P469A did not (Figure 2.9C), suggesting that, as expected, MLK3 P469A but not

Figure 2.7. The kinase domain of MLK3 is sufficient for the ANT2

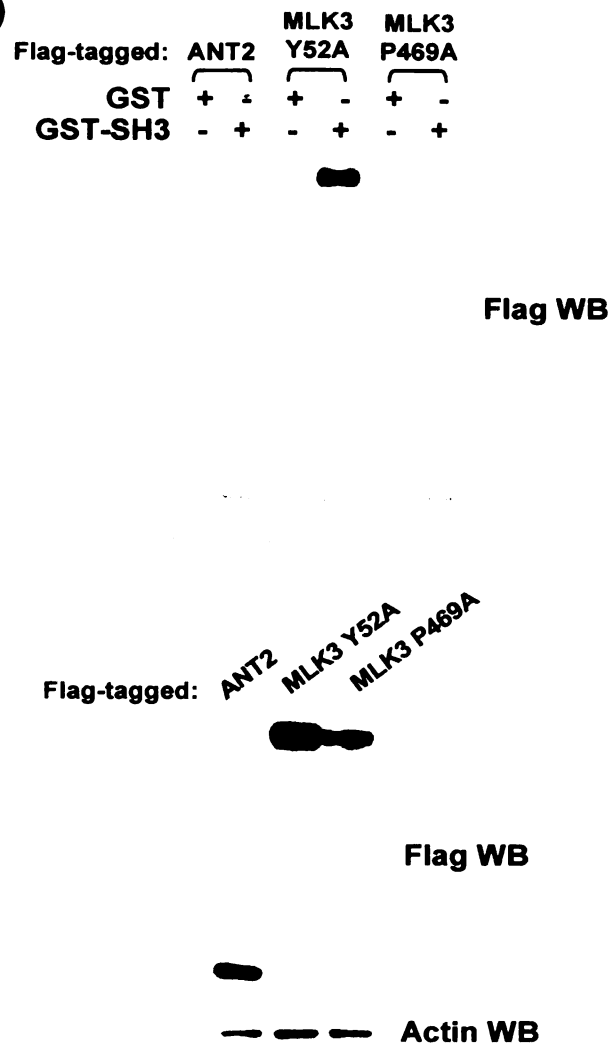
interaction. Different MLK3 truncation proteins were transiently coexpressed with or without ANT2 in HEK293T cells for 20-24 h. The interaction of ANT2 with different MLK3 truncation variants including (A) the N- and C-terminal halves, (B) the C-terminal truncations, (C) the glycine-rich sequence and SH3 domain (1-114) as well as the kinase domain (115-399) of MLK3 was assessed by co-immunoprecipitation assay. (D) *Top panel*, cellular lysates containing Flag-ANT2, Flag-MLK3 Y52A or Flag-MLK3 P469A from HEK 293T cells were used in the GST pull-down experiments as described in Materials and Methods. The presence of Flag-ANT2, Flag-MLK3 Y52A or Flag-MLK3 P469A in the pulldown was assessed by western blotting. Equal amounts of GST and GST-SH3 in the assays was confirmed by Coomassie staining. *Bottom panel*, levels of expressed proteins and of endogenous actin as a loading control, were detected by western blotting with the indicated antibodies. The numbers in the figure represent amino acid numbers in MLK3. IP, immunoprecipitation. Data shown is representative of 3 independent experiments.



(C)



(D)



MLK3 K144A/P469A is catalytically active. Moreover, MLK3 K144R/P469A associated very poorly with ANT2 as compared to MLK3 P469A, suggesting that the MLK3 catalytic activity rather than its open conformation regulates MLK3 interaction with ANT2. Taken together, these data suggest that MLK3 activity is crucial for formation of the MLK3-ANT2 complex.

4.5 A portion of MLK3 is present in mitochondria

Several groups have analyzed the subcellular localization of both endogenous and overexpressed MLK3. Expressed MLK3 is primarily found in the perinuclear region and partial colocalization has been demonstrated with Golgi marker, GM130 [32, 33] and in the centrosomal regions during G2/M cell cycle stage [34]. In addition, upon coexpression with activated Cdc42, MLK3 translocates to the plasma membrane [35]. To test whether MLK3 can localize to mitochondria, confocal microscopy experiments were performed using HeLa cells transiently expressing Flag-MLK3. Flag-MLK3 partially colocalized with cytochrome oxidase IV (COXIV), a mitochondrial inner membrane protein that participates in the oxidative phosphorylation process (Figure 2.10A), suggesting that a portion of MLK3 localized to mitochondria. To corroborate these results, crude biochemical fractionation experiments were performed. The presence of different organellar protein markers including lactate dehydrogenase (LDH) and COXIV in each fraction was assessed by immunoblotting of equal cellular equivalent of proteins from each fraction. LDH and COXIV proteins were found almost exclusively in the S6.8 and P6.8 fractions, respectively (Figure 2.10B), indicating that mitochondria has been

Figure 2.8. The regulation of MLK3 model and the diagram of the kinase activity of different MLK3 mutations. (A) The proposed regulation model of MLK3. *Top*, MLK3 is autoinhibited through a protein interaction mediated by the SH3 domain and a proline between the zipper region and Cdc42/Rac interactive binding (CRIB) motif. *Bottom*, GTP-bound Cdc42/Rac binds to the CRIB motif of MLK3 and disrupts the MLK3 autoinhibition, allowing the dimerization of MLK3 through the zipper region. Dimerization of MLK3 brings two kinase domains of MLK3 close to each other, resulting in the transphosphorylation of the activation loop of MLK3 and fully activation of MLK3. (B) The kinase defective mutant of MLK3 (K144A) and the leucine zipper mutant of MLK3 (L410P) that fails to mediate MLK3 dimerization have lower MLK3 catalytic activity. (C) *Top*, MLK3 is auto-inhibited through its SH3 domain and a single proline containing sequence. *Bottom*, amino acid substitution of Tyr52 in the SH3 domain with Ala or of Pro469 with Ala disrupts MLK3 autoinhibitory conformation resulting in a higher MLK3 catalytic activity.

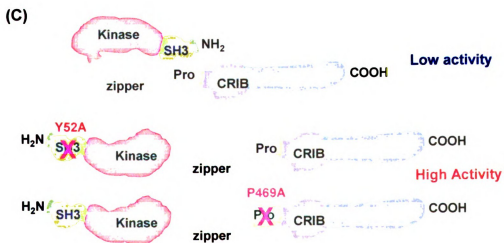
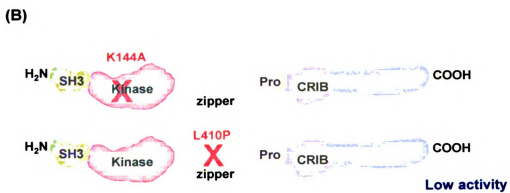
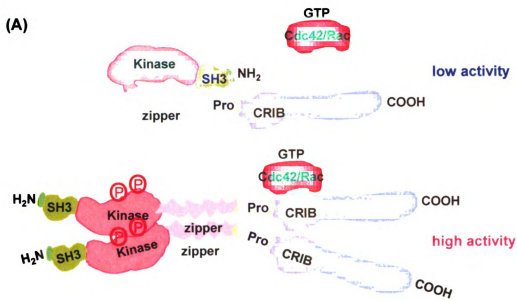
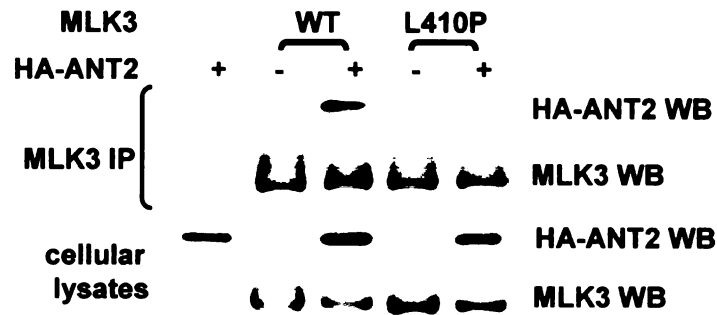


Figure 2.9. ANT2 preferentially associates with activated forms of MLK3.

Different MLK3 mutants, (A) zipper mutant (L410P), (B) kinase dead (K144A), mutants that disrupt autoinhibition of MLK3 (Y52A, P469A) and (C) kinase dead with disrupted autoinhibition (K144R/P469A) were transiently coexpressed with or without HA-ANT2 in HEK 293T cells. Co-immunoprecipitation assays were performed using total cellular lysates with the MLK3 antibody. The immunoprecipitates were subjected to SDS-PAGE electrophoresis followed by immunoblotting using the antibodies indicated. Levels of expressed proteins and of proteins of interest were accessed by immunoblotting with the indicated antibodies. Actin level was used as loading control. Data shown is representative of independent experiments.

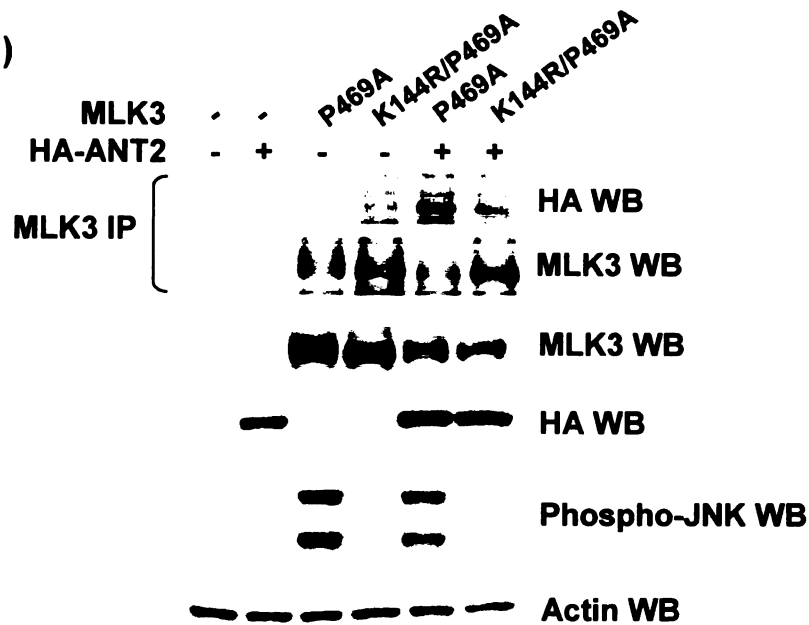
(A)



(B)



(C)



efficiently isolated. The biochemical fractionation further demonstrated that a portion of expressed MLK3 is distributed to a mitochondria-enriched fraction (Figure 2.10B). A portion of the MLK3 mutant forms including MLK3 L410P, MLK3 K144A and MLK3 P469A also partitioned to mitochondria-enriched fractions, suggesting that the localization of MLK3 to mitochondria is independent of its activation status.

The subcellular localization of endogenous MLK3 in HEK 293T cells and MCF-7 human breast cancer cells was also evaluated by biochemical fractionation. A portion of endogenous MLK3 was observed in the mitochondria-enriched fraction (Figure 2.11A) in both HEK 293T and MCF-7 cells. The same result was obtained in HeLa human cervical carcinoma cells and SH-SY5Y human neuroblastoma cells (Figure 2.11B). Since the previous fractionation generates the crude mitochondrial-enriched fraction which also contains other heavy membrane organelles including Golgi and endoplasmic reticulum (ER) (data not shown), MCF-7 cells were biochemically fractionated using the sucrose gradient to obtain a pure mitochondria-enriched fraction. As shown in Figure 2.11C, a portion of endogenous MLK3 from MCF-7 cells was also present in the pure mitochondria-enriched fraction. Taken together, the data suggest that a portion of MLK3 is associated with the mitochondria in multiple cell lines.

4.6 Mitochondrial MLK3 interacts with ANT2

Based on these results, one would predict that MLK3 interacts with ANT2 in the mitochondria. To determine if this is indeed the case, HEK 293T expressing MLK3 and/or ANT2 were subjected to biochemical fractionation. As previously shown, nearly

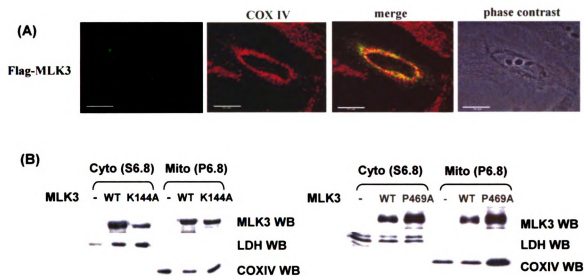
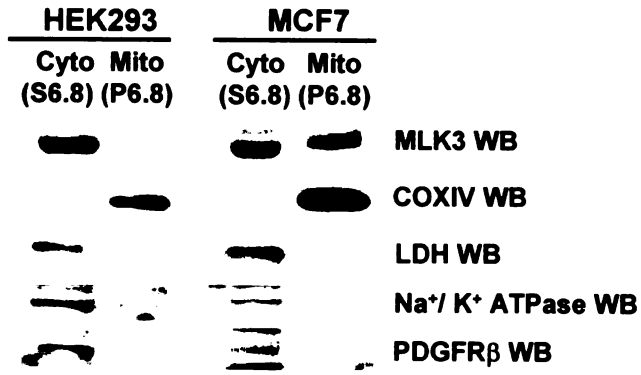


Figure 2.10. A portion of expressed MLK3 is present in mitochondria. (A)

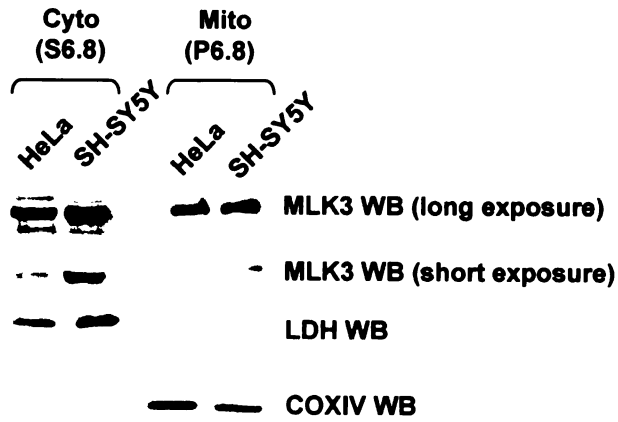
Flag-MLK3 was transiently expressed in HeLa cells. Cells were directly fixed and permeabilized with cold methanol. The subcellular localization of MLK3 was detected using a Flag-FITC-conjugated antibody (*green*). Mitochondria were detected using a cytochrome c oxidase IV (COXIV) antibody and an Alexa Fluor 546-conjugated secondary antibody (*red*). The images were obtained using a confocal laser scanning microscope. A phase contrast image was taken as a control. Scale bar is 10 μm . (B) Post-nuclear HEK 293T cell lysates expressing different MLK3 mutants were fractionated by centrifugation at 6800g. Proteins of interest from the soluble (S6.8) and pellet (P6.8) fractions were analyzed by western blotting with appropriate antibodies. Equal cellular equivalents from each fraction were loaded. The efficiency of the fractionation was assessed by western blotting with antibodies directed against cytosolic lactate dehydrogenase (LDH) and mitochondrial cytochrome c oxidase (COX) IV.

Figure 2.11. A portion of endogenous MLK3 is present in a mitochondria-enriched fraction. Fractionation by differential centrifugation was performed on various cell lines (A, HEK 293T and MCF-7; B, HeLa and SH-SY5Y), as described previously. Equal cellular equivalents from each fraction were analyzed by immunoblotting using the indicated antibodies. Potential contamination with other organelles in each fraction was assessed by western blotting using antibodies against different organelle markers. LDH was used as cytosol protein marker. COXIV is a mitochondrial protein marker. Both sodium potassium ATPase and platelet derived growth factor receptor (PDGFR) were used as the markers of plasma membrane. The presence of MLK3 in each fraction was assessed by western blotting using the MLK3 antibody. (C) Mitochondria from MCF-7 cells were fractionated through a sucrose gradient as described in “Materials and Methods”, and fractions were analyzed as for A and B. Cdc37 was the cytosolic protein marker. In addition to COXIV, AIF was also used as another mitochondrial protein marker.

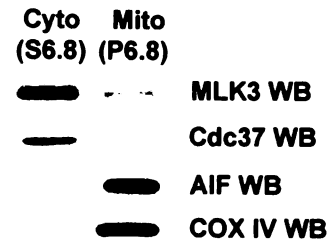
(A)



(B)



(C)



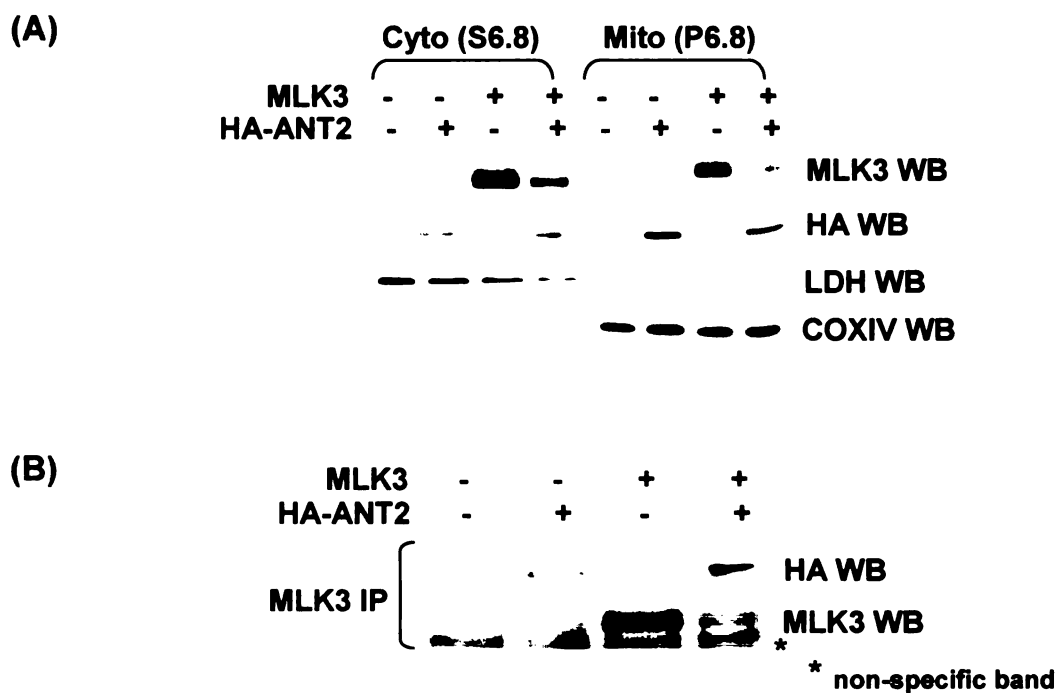


Figure 2.12. Expressed MLK3 present in the mitochondria-enriched fraction interacts with ANT2. HEK 293T cells expressing MLK3 with or without HA-ANT2 were subjected to a biochemical fractionation as previously described. (A) The presence of MLK3 and HA-ANT2 proteins in each fraction was assessed by western blotting using the MLK3 and HA antibodies. Equal cellular equivalent from each fraction were loaded. The efficacy of the fractionation was assessed by western blotting with LDH and COXIV antibodies. (B) MLK3 from the mitochondrial fraction was immunoprecipitated using the MLK3 antibody. The presence of ANT2 in the MLK3 immunoprecipitates was assessed by western blotting with the HA antibody. Data shown is representative from 5 independent experiments.

all LDH was found in the S6.8 cytosolic fraction and mitochondrial COXIV was in the P6.8 fraction, suggesting that P6.8 mitochondria-enriched fraction is devoid of cytosol (Figure 2.12A). The majority of ANT2 and a portion of MLK3 were present in the mitochondria-enriched fraction. MLK3 was then immunopurified from the mitochondria-enriched fraction and the presence of associated ANT2 was analyzed by western blotting. As expected, the MLK3 present in the mitochondria-enriched fraction was capable of complexing with ANT2 (Figure 2.12B).

4.7 Effect of the MLK3-ANT2 interaction on total cellular ATP level

The mitochondrion is a major site of ATP production. Knockdown of ANT2 in HeLa cells was recently shown to decrease the cellular ATP content [19]. To test whether the interaction of MLK3 with ANT2 might influence cellular ATP, levels of ATP were measured in cells expressing MLK3 and/or ANT2. The expression vectors encoding MLK3 and/or ANT2 were transfected into HEK 293T cells. A beta-galactosidase construct was used as a transfection control. The cellular ATP level was determined using a luciferin-based assay. The total cellular ATP level, normalized for beta-galactosidase transfection efficiency, in cells coexpressing MLK3 and ANT2 is 4-fold higher than in cells transfected with empty vector (Figure 2.13A). The normalized total cellular ATP level in ANT2 expressing cells increased 1.5 fold and in MLK3 expressed cells increased 2.5 fold over control. Notably, the total cellular ATP level was synergistically enhanced by coexpression of MLK3 and ANT2, suggesting that the interaction of MLK3 with ANT2 may contribute to cellular ATP increasement.

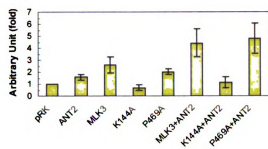
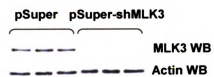
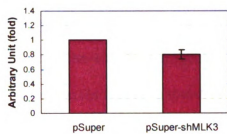
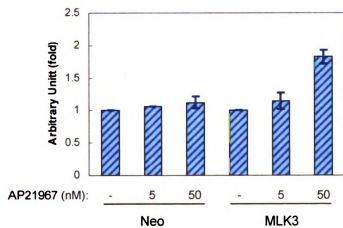
To address whether catalytic activity is required for MLK3's ability to enhance total cellular ATP, the kinase inactive MLK3 K144A and hyperactive MLK3 P469A variants were used. Cellular ATP content was diminished upon the expression of the catalytically inactive MLK3 alone or with ANT2 (Figure 2.13A), suggesting that this effect was dependent on MLK3 kinase activity because the catalytically inactive MLK3 K144A decreased cellular ATP level. The cellular ATP level was synergistically increased 5 fold in cells coexpressing MLK3 P469A and ANT2 as compared to MLK3 P469A or ANT2 alone.

Kinase inactive MLK3 can also localize to mitochondria (Figure 2.10B) but binds ANT2 only weakly (Figure 2.9B). Therefore it is possible that either MLK3 activity or its interaction with ANT2 is required for modulation of total cellular ATP cellular levels. As an alternative approach, the impact of silencing of endogenous MLK3 on ATP levels was determined. A stable population of MCF-7 cells in which MLK3 expression has been largely reduced showed decreased total cellular ATP content compared with a control vector population (Figure 2.13B).

We previously engineered MCF-7 cells to inducibly express Flag-MLK3 [31]. Addition of the small molecular inducer, AP21967, to the parental inducible cells containing an empty expression vector had no effect on cellular ATP levels (Figure 2.13C). However, induction of Flag-MLK3 increased total cellular ATP level about 2 fold. Taken altogether, these data suggest that catalytically active MLK3 modulates cellular ATP, possibly through its interaction with ANT2.

Figure 2.13. Effect of MLK3 and ANT2 on total cellular ATP level. (A)

Expression vectors encoding MLK3 variants, ANT2 and beta-galactosidase were transfected using Lipofectamine 2000 into HEK 293T cells for 20-24 h. Cells were lysed in a lysis buffer containing 1% trichloroacetic acid. The total cellular ATP level from the clarified cellular lysates was measured as described in Material and Methods. Beta-galactosidase was used as an internal control; activity was measured using a luminescent beta-galactosidase detection kit. The cellular ATP levels were normalized to beta-galactosidase activity and plotted in arbitrary units with empty vector control (pRK) set as one. Error bars represent standard deviation. (B) MCF-7 cells stably expressing a MLK3 short hairpin RNA interference vector were lysed, and total cellular ATP levels were measured as described in A. MLK3 levels after knockdown were assessed by immunoblotting. The total cellular ATP content was determined from cellular lysates containing equal amounts of proteins and plotted as arbitrary units with control cells (pSuper) set as one. (C) MCF-7/iFlag-MLK3 cells were incubated with various concentrations of AP21967 for 20 h to induce Flag-MLK3 expression. The total cellular ATP content was determined from cellular lysates containing equal amounts of proteins as described in A. Data from 3 independent experiments is plotted in arbitrary units with control cells set as one. Error bars represent standard deviation.

(A)**(B)****(C)**

5 Discussion

In this chapter, a novel interaction between the protein kinase MLK3 and the mitochondrial translocase ANT2 is characterized. Interestingly, despite the high amino acid identity that is shared among ANT isoforms, the interaction with MLK3 appears to be isoform specific. One possible explanation for this unexpected finding is that different isoforms of ANT may have distinct submitochondrial localization patterns. The well characterized ANT1 isoform is localized in the peripheral inner membrane, near the outer membrane, where it can interact with VDAC and cyclophilin D [36, 37]. The localization of ANT2 is less well defined. The highly folded regions of the inner membrane of the mitochondria are known as the cristae. Based on isolation of cristae-enriched membranes and a multiwell detergent screening assay, ANT2 has been shown to physically interact with the Pi carrier and F₀F₁-ATP synthase [38] forming the ATP synthasome that is confined to the cristae [36, 37]. Thus, ANT isoform selectivity of MLK3 may be explained by the distinct submitochondrial localization of ANT2 and by inference of MLK3.

Characterization of the MLK3-ANT2 interaction revealed that the kinase domain is sufficient for its association with ANT2 and that MLK3 mutants with high catalytic activity preferentially bound ANT2. Given the association of active MLK3 with ANT2, one might predict that MLK3 could phosphorylate ANT2 or another protein involved in the MLK3-ANT2 interaction. No well-defined consensus phosphorylation sequence within MLK3 substrates exists. MLK3 is known to phosphorylate MKK4 and MKK7 in their activation loops (Figure 2.14). Intriguingly, examination of the sequences of the ANT isoforms revealed that a sequence similar to the known MLK3 substrate

phosphorylation sites is present in ANT2. Preliminary metabolic labeling did not conclusively show ANT2 phosphorylation in HEK 293T cells coexpressing ANT2 and active MLK3. However, this intriguing but speculative hypothesis can be further examined using potential phosphorylation site mutants of ANT2 in conjunction with *in vitro* metabolic labeling and co-immunoprecipitation assays.

Consistent with previous reports, overexpressed ANT1, but not ANT2, induced apoptosis, as judged by PARP cleavage. Overexpression of ANT2 with MLK3 neither induced apoptosis nor impaired MLK3 signaling integrity, suggesting that this interaction primarily affected ANT2 function. It is tempting to speculate that interaction with MLK3 or phosphorylation by MLK3 might enhance ANT2 activity to accelerate ADP/ATP exchange. To test this hypothesis, an ANT2 activity assay using isolated intact mitochondria or ANT2-reconstituted liposomes will be required.

Most mitochondrial proteins are translated in the cytoplasm and their translocation to mitochondria is mediated through a mitochondrial targeting sequence at their NH₂ termini. MLK3 contains no predicted mitochondrial targeting sequence based upon analysis using the Predotar computer program (ExPASy proteomics server). N-terminal epitope tags have been shown to mask mitochondrial targeting sequences, abolishing protein translocation to mitochondria [39]. Furthermore, a portion of MLK3 was present in a mitochondria-enriched fraction even though it contains a Flag epitope at its NH₂ terminus (Figure 2.15), consistent with the idea that MLK3 lacks a classical mitochondrial targeting sequence.

Several studies have demonstrated that, in response to particular cellular stimuli, certain protein kinases that are generally found in the cytosol and/or nucleus, such as the

tyrosine kinase Src [40, 41][27], JNK [26] and B-Raf [42] are targeted to mitochondria through interaction with proteins which contain canonical mitochondrial targeting sequences. For instance, cotransfection experiments have shown that the scaffold protein AKAP121 promotes Src translocation to mitochondria where Src phosphorylates unknown mitochondrial proteins and increases oxidative phosphorylation, causing an elevation of mitochondrial membrane potential and increased ATP production [27]. Intriguingly, cytochrome c has been demonstrated to be tyrosine-phosphorylated in bovine heart [43]. Upon TNF- α stimulation, Src is targeted to mitochondria through interaction with the mitochondrial adaptor protein, Dok4, leading to decreased levels of complex I through an as yet undefined mechanism [41]. Expressed kinase inactive MLK3 variants bind only poorly to ANT2, yet they are present in the mitochondria-enriched fraction. It is unclear how MLK3 mitochondrial localization is controlled. It is possible that in addition to ANT2, there are other mitochondrial (adaptor) proteins target a portion of MLK3 to mitochondria and this interaction is kinase activity independent. It is also unclear whether the interaction between MLK3 and ANT2 is direct or mediated through an intervening protein.

In most normal cells, the majority of cellular ATP is derived through oxidative phosphorylation rather than through glycolysis. Under hypoxic conditions, tumor cells rely primarily on glycolysis for energy production. This idea has re-emerged in cancer research but whether this is a universal property of all cancer cells remains under debate. Our data indicate that coexpression of MLK3 and ANT2 dramatically increases the total cellular ATP levels and that cellular ATP levels correlate with MLK3 activity and protein levels. It is quite possible that MLK3 modulates mitochondrial proteins of oxidative

phosphorylation and Krebs cycle which is known as TCA cycle, resulting in higher level of total ATP. Indeed, peptides corresponding to these mitochondrial proteins crucial for ATP production, especially ATP synthase, were detected in the mass spectrometry experiments (Table 2.2) Recent studies combining knockdown of individual ANT isoforms and treatment with oligomycin, the ATP synthase inhibitor, in HeLa cancer cells suggest that ANT2 cooperates with ATP synthase [19] to increase cellular ATP levels. It will be interesting to determine the impact of MLK3 and ANT2 on ATP synthase activity in tumor cell lines grown under different conditions including normoxia and hypoxia.

Given that phosphorylation is a reversible modification, the effect of mitochondrial phosphatases on cellular energy regulation is postulated being opposite to that of mitochondrial kinases. Depletion of PTPMT1, a mitochondrial PTEN-like phosphatase, by short hairpin RNA has been demonstrated to promote mitochondrial ATP production [25].

Unpublished work from our lab demonstrated that transient knockdown of MLK3 by siRNA in MCF-7 breast cancer cells decreased DNA synthesis in response to the stimulation of growth factors and the steroid hormones, estrogen and progesterone. A previous study showed that depletion of MLK3 by siRNA in human immortalized colon fibroblasts, colon adenocarcinoma cells with the oncogenic Ras and neurofibromatosis 1 (NF-1) schwannoma cells reduced serum-induced cell proliferation as judged by counting of cell numbers [44]. It has been suggested that MLK3 scaffolds the Ras-Raf-MEK-ERK pathway upon growth factor stimulation [45] to contribute to cell proliferation. The experiments presented in this Chapter show a correlation between reduced total cellular ATP levels and decreased cell proliferation upon knockdown of MLK3 in breast cancer

cells. Notably, coexpression of MLK3 and ANT2 synergistically enhances cellular ATP levels, suggesting that the MLK3-ANT2 interaction contributes the increased ATP levels. It will be important to evaluate the biological function of the MLK3-ANT2 interaction by directly testing whether depletion of ANT2 by siRNA blocks the MLK3-induced increase in cellular ATP levels and affects cellular proliferation. Taken altogether, these data suggest a novel function for MLK3 and open up the possibility that, in addition to its role in the MAPK pathway, MLK3 may promote cancer cell proliferation and/or survival by facilitating the energetic metabolism through regulation of a MLK3-ANT2 containing synthasome (Figure 2.16).

MKK4	257	[Ⓟ] S	IAKT	[Ⓟ] T	261
MKK7	271	SKAKT			275
ANT1	41	SKQIS			45
ANT2	41	SKQIT			45
ANT3	41	SKQIA			45
ANT4	54	SKQIS			58

Figure 2.14. Alignment of the sequences containing the phosphorylation sites of MLK3 in human MKK4 and MKK7 with human ANT isoforms. The Ser and Thr of human MKK4 and MKK7 phosphorylated by MLK3 are labeled with phosphate symbols. The phospho-Ser and phospho-Thr within MKK4 and MKK7 are separated by 3 amino acids, giving the phosphorylation consensus motif as SXAKT. The phosphorylation consensus motif of MLK3 is not clearly defined. The potential phosphorylation motif of MLK3 in human ANT isoforms is listed. The numbers shown correspond to the amino acids in each protein. X: any amino acid residues.

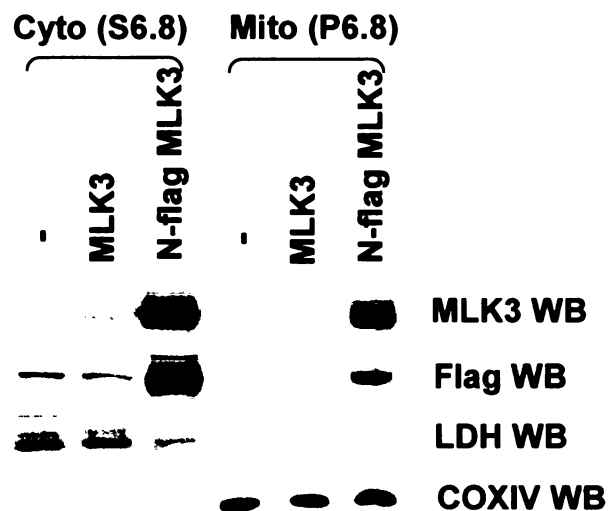


Figure 2.15. N-Flag tagged MLK3 partially fractionates with mitochondria. MLK3 or N-Flag MLK3 expression vector was transfected in HEK 293T cells. Twenty four hours after transfection, cells were subjected to a biochemical fractionation as described in Figure 2.2.10. Equal cellular equivalents of each fraction were loaded. Ectopically expressed MLK3 in each fraction was detected by immunoblotting with the MLK3 and Flag antibodies, respectively. The efficacy of the fractionation was assessed by immunoblotting with LDH (cytosolic marker) and COXIV (mitochondrial marker) antibodies. Data shown is representative of 3 independent experiments.

Table 2.2. Peptide sequences of the oxidative phosphorylation proteins and the voltage dependent anion channel 3 (VDAC 3) identified by mass spectrometry.

protein	complex subunit of oxidative phosphorylation	identified peptide sequence
NADH dehydrogenase	Complex I α , subunit 4	FYSVNVDYSK
NADH dehydrogenase	Complex I α , subunit 9	SSVSGIVATVFGATGFLGR
NADH dehydrogenase	Complex I α , subunit 13	IALLPLLQAETDR
NADH dehydrogenase	Complex I β , subunit 4	TLPETLDPAEYNISPETR
Ubiquinol-cytochrome c reductase	Complex III, subunit 7	HVISYSLSPFEQR
Ubiquinol-cytochrome c reductase	Complex III, subunit 10	AFDQGADAIYDHINEGK
Cytochrome c oxidase	Complex IV, subunit 7a2	LFQEDDEIPLYLK
ATP synthase	Complex V, F chain	DFSPSGIFGAFQR
VDAC 3		LTLDTIFVPNTGK LTLALIDGK

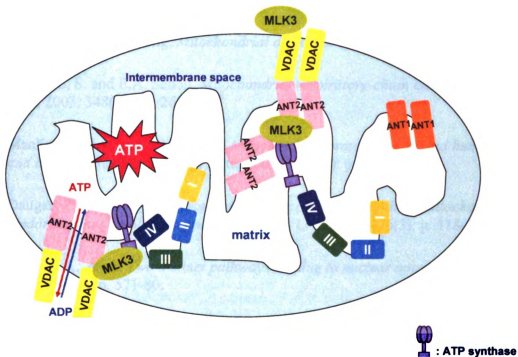


Figure 2.16. The proposed model of how the interaction of MLK3 with ANT2 in elevation of the total cellular ATP level. The model is proposed based on the data shown in this Chapter, the findings from other labs and the preliminary data from mass spectrometry. It has been demonstrated that ANT2 interacts and cooperates with ATP synthase for ATP production. The identified peptides of VDAC3 and the electron transport chain complexes from mass spectrometry (listed in Table 2.2) were present in the MLK3 protein complex. MLK3 could interact with the VDAC3-ANT2-ATP synthase-the complexes of the electron transport chain from the mitochondrial surface or/and the intermembrane space of mitochondria or/and the matrix through the direct or indirect interaction. The interaction of MLK3 with this protein complex leads to an elevation of the total cellular ATP level. Abbreviation, VDAC: voltage dependent anion channel.

6 References

1. Carew, J.S. and P. Huang, *Mitochondrial defects in cancer*. Mol Cancer, 2002. 1: p. 9.
2. DiMauro, S. and E.A. Schon, *Mitochondrial respiratory-chain diseases*. N Engl J Med, 2003. 348(26): p. 2656-68.
3. MacKenzie, J.A. and R.M. Payne, *Mitochondrial protein import and human health and disease*. Biochim Biophys Acta, 2007. 1772(5): p. 509-23.
4. Daugas, E., et al., *Apoptosis-inducing factor (AIF): a ubiquitous mitochondrial oxidoreductase involved in apoptosis*. FEBS Lett, 2000. 476(3): p. 118-23.
5. Susin, S.A., et al., *Two distinct pathways leading to nuclear apoptosis*. J Exp Med, 2000. 192(4): p. 571-80.
6. Saelens, X., et al., *Toxic proteins released from mitochondria in cell death*. Oncogene, 2004. 23(16): p. 2861-74.
7. Jacotot, E., et al., *Control of mitochondrial membrane permeabilization by adenine nucleotide translocator interacting with HIV-1 viral protein rR and Bcl-2*. J Exp Med, 2001. 193(4): p. 509-19.
8. Vieira, H.L., et al., *Cell permeable BH3-peptides overcome the cytoprotective effect of Bcl-2 and Bcl-X(L)*. Oncogene, 2002. 21(13): p. 1963-77.
9. Zamzami, N., et al., *Bid acts on the permeability transition pore complex to induce apoptosis*. Oncogene, 2000. 19(54): p. 6342-50.
10. Verrier, F., et al., *Study of PTPC composition during apoptosis for identification of viral protein target*. Ann N Y Acad Sci, 2003. 1010: p. 126-42.
11. Dahout-Gonzalez, C., et al., *Molecular, functional, and pathological aspects of the mitochondrial ADP/ATP carrier*. Physiology (Bethesda), 2006. 21: p. 242-9.
12. Sokolikova, B., et al., *A carbon-source-responsive element is required for regulation of the hypoxic ADP/ATP carrier (AAC3) isoform in Saccharomyces cerevisiae*. Biochem J, 2000. 352 Pt 3: p. 893-8.
13. Doerner, A., et al., *Tissue-specific transcription pattern of the adenine nucleotide translocase isoforms in humans*. FEBS Lett, 1997. 414(2): p. 258-62.

14. Dolce, V., et al., *A fourth ADP/ATP carrier isoform in man: identification, bacterial expression, functional characterization and tissue distribution*. FEBS Lett, 2005. 579(3): p. 633-7.
15. Barath, P., et al., *The growth-dependent expression of the adenine nucleotide translocase-2 (ANT2) gene is regulated at the level of transcription and is a marker of cell proliferation*. Exp Cell Res, 1999. 248(2): p. 583-8.
16. Stepien, G., et al., *Differential expression of adenine nucleotide translocator isoforms in mammalian tissues and during muscle cell differentiation*. J Biol Chem, 1992. 267(21): p. 14592-7.
17. Zamora, M., et al., *Adenine nucleotide translocase 3 (ANT3) overexpression induces apoptosis in cultured cells*. FEBS Lett, 2004. 563(1-3): p. 155-60.
18. Jacotot, E., et al., *Mitochondrial membrane permeabilization during the apoptotic process*. Ann N Y Acad Sci, 1999. 887: p. 18-30.
19. Le Bras, M., et al., *Chemosensitization by knockdown of adenine nucleotide translocase-2*. Cancer Res, 2006. 66(18): p. 9143-52.
20. Graham, B.H., et al., *A mouse model for mitochondrial myopathy and cardiomyopathy resulting from a deficiency in the heart/muscle isoform of the adenine nucleotide translocator*. Nat Genet, 1997. 16(3): p. 226-34.
21. Berwick, D.C. and J.M. Tavaré, *Identifying protein kinase substrates: hunting for the organ-grinder's monkeys*. Trends Biochem Sci, 2004. 29(5): p. 227-32.
22. Schulenberg, B., et al., *Analysis of steady-state protein phosphorylation in mitochondria using a novel fluorescent phosphosensor dye*. J Biol Chem, 2003. 278(29): p. 27251-5.
23. Pagliarini, D.J. and J.E. Dixon, *Mitochondrial modulation: reversible phosphorylation takes center stage?* Trends Biochem Sci, 2006. 31(1): p. 26-34.
24. Valente, E.M., et al., *Hereditary early-onset Parkinson's disease caused by mutations in PINK1*. Science, 2004. 304(5674): p. 1158-60.
25. Pagliarini, D.J., et al., *Involvement of a mitochondrial phosphatase in the regulation of ATP production and insulin secretion in pancreatic beta cells*. Mol Cell, 2005. 19(2): p. 197-207.

26. Kharbanda, S., et al., *Translocation of SAPK/JNK to mitochondria and interaction with Bcl-x(L) in response to DNA damage*. J Biol Chem, 2000. 275(1): p. 322-7.
27. Livigni, A., et al., *Mitochondrial AKAP121 links cAMP and src signaling to oxidative metabolism*. Mol Biol Cell, 2006. 17(1): p. 263-71.
28. Bock, B.C., et al., *Cdc42-induced activation of the mixed-lineage kinase SPRK in vivo. Requirement of the Cdc42/Rac interactive binding motif and changes in phosphorylation*. J Biol Chem, 2000. 275(19): p. 14231-41.
29. Vacratsis, P.O. and K.A. Gallo, *Zipper-mediated oligomerization of the mixed lineage kinase SPRK/MLK-3 is not required for its activation by the GTPase cdc 42 but is necessary for its activation of the JNK pathway. Monomeric SPRK L410P does not catalyze the activating phosphorylation of Thr258 of murine MITOGEN-ACTIVATED protein kinase kinase 4*. J Biol Chem, 2000. 275(36): p. 27893-900.
30. Zhang, H. and K.A. Gallo, *Autoinhibition of mixed lineage kinase 3 through its Src homology 3 domain*. J Biol Chem, 2001. 276(49): p. 45598-603.
31. Zhang, H., et al., *Hsp90/p50cdc37 is required for mixed-lineage kinase (MLK) 3 signaling*. J Biol Chem, 2004. 279(19): p. 19457-63.
32. Cha, H., et al., *Inhibition of mixed-lineage kinase (MLK) activity during G2-phase disrupts microtubule formation and mitotic progression in HeLa cells*. Cell Signal, 2006. 18(1): p. 93-104.
33. Cha, H., et al., *Phosphorylation of golgin-160 by mixed lineage kinase 3*. J Cell Sci, 2004. 117(Pt 5): p. 751-60.
34. Swenson, K.I., K.E. Winkler, and A.R. Means, *A new identity for MLK3 as an NIMA-related, cell cycle-regulated kinase that is localized near centrosomes and influences microtubule organization*. Mol Biol Cell, 2003. 14(1): p. 156-72.
35. Du, Y., et al., *Cdc42 induces activation loop phosphorylation and membrane targeting of mixed lineage kinase 3*. J Biol Chem, 2005. 280(52): p. 42984-93.
36. Faustin, B., et al., *Mobilization of adenine nucleotide translocators as molecular bases of the biochemical threshold effect observed in mitochondrial diseases*. J Biol Chem, 2004. 279(19): p. 20411-21.
37. Vyssokikh, M.Y., et al., *Adenine nucleotide translocator isoforms 1 and 2 are differently distributed in the mitochondrial inner membrane and have distinct affinities to cyclophilin D*. Biochem J, 2001. 358(Pt 2): p. 349-58.

38. Ko, Y.H., et al., *Mitochondrial ATP synthasome. Cristae-enriched membranes and a multiwell detergent screening assay yield dispersed single complexes containing the ATP synthase and carriers for Pi and ADP/ATP.* J Biol Chem, 2003. 278(14): p. 12305-9.
39. Ventura, A., et al., *A cryptic targeting signal induces isoform-specific localization of p46Shc to mitochondria.* J Biol Chem, 2004. 279(3): p. 2299-306.
40. Cardone, L., et al., *Mitochondrial AKAP121 binds and targets protein tyrosine phosphatase D1, a novel positive regulator of src signaling.* Mol Cell Biol, 2004. 24(11): p. 4613-26.
41. Itoh, S., et al., *Mitochondrial Dok-4 recruits Src kinase and regulates NF-kappaB activation in endothelial cells.* J Biol Chem, 2005. 280(28): p. 26383-96.
42. Wang, H.G., U.R. Rapp, and J.C. Reed, *Bcl-2 targets the protein kinase Raf-1 to mitochondria.* Cell, 1996. 87(4): p. 629-38.
43. Lee, I., et al., *New prospects for an old enzyme: mammalian cytochrome c is tyrosine-phosphorylated in vivo.* Biochemistry, 2006. 45(30): p. 9121-8.
44. Chadee, D.N. and J.M. Kyriakis, *MLK3 is required for mitogen activation of B-Raf, ERK and cell proliferation.* Nat Cell Biol, 2004. 6(8): p. 770-6.
45. Chadee, D.N., et al., *Mixed-lineage kinase 3 regulates B-Raf through maintenance of the B-Raf/Raf-1 complex and inhibition by the NF2 tumor suppressor protein.* Proc Natl Acad Sci U S A, 2006. 103(12): p. 4463-8.

III. A Novel GTPase Domain of the Parkinson's Disease-Associated Kinase LRRK2

1. Abstract

Parkinson's disease (PD) is the most common neurodegenerative movement disorder in western countries. Emerging evidence from genetic studies has demonstrated that mutations in *PARK8*, which encodes the leucine-rich repeat kinase (LRRK) 2, causes late-onset familial PD. LRRK2 contains multiple predicted catalytic and protein-interaction domains; and pathogenic amino acid substitutions are located throughout LRRK2.

Roc, a distinct, putative GTPase of the Ras superfamily, always exists in tandem with so-called COR domain of unknown function. No representative structures of either Roc or COR domains have been solved to date. Of solved GTPase structures, Roc is most similar to the Rab7 GTPase; therefore a molecular homology model of Roc was created using the murine GTP-bound Rab7 crystal structure as a template. This model was used in conjunction with the GTPase literature to predict the functional consequence of PD mutation in the Roc.

To investigate the GTPase activity of the Roc and Roc-COR domains, recombinant bacterial expression of Glutathione S-Transferase (GST) fusion proteins of Roc and Roc-COR, as well as their mutants that are predicted to be conformationally active and inactive, has been studied. Most GST-Roc variant proteins were optimally soluble under autoinducible conditions and can be further purified by glutathione affinity

agarose. However, GST-Roc-COR remained in inclusion bodies under all conditions, including co-expression with chaperone proteins.

Roc and its predicted constitutively/conformationally active mutants, Roc A1396T as well as R1398L, specifically bound GTP, whereas Roc T1348N, the predicted inactive form of Roc GTPase, failed to do so. Consistent with the prediction from the Roc homology model, no apparent deficiency of GTP binding was observed in the PD-associated variant, Roc R1441C. Using an enzymatic coupling assay, a weak GTPase activity of a recombinant Roc fusion protein was detected.

The idea that LRRK2 might adopt a conformation that involves interactions among its domain was tested by coimmunoprecipitation experiments of expressed fragments of LRRK2. A Roc-COR fragment complexed with the carboxyl terminal region consisting of Roc, COR, kinase domains and WD 40 repeats of LRRK2, but not the N-terminal region containing the ankyrin domain. Introduction of the PD-associated COR mutation, Y1699C, in the Roc-COR domain enhanced its association with carboxyl terminal region of LRRK2. However, the R1441C/G mutation in the context of Roc or Roc-COR resulted in reduction of protein complex formation with the carboxyl terminal region of LRRK2. Taken altogether, the data presented in this chapter suggest that Roc domain of LRRK2 is a *bona fide* GTPase, and provide evidence that LRRK2 domains interact with one other in ways that are altered by the introduction of PD-associated mutations.

2. Introduction

Parkinson's disease (PD) is the most common neurodegenerative movement disorder in western countries. The clinical symptoms of PD include resting tremor, bradykinesia, muscle rigidity and impaired balance. The loss of the dopaminergic neurons in the *substantia nigra pars compacta* and the presence of protein aggregations named Lewy bodies in the surviving neurons of the brainstem are the pathological hallmarks of PD [1]. To date, all available treatments aim to ameliorate the clinical symptoms but do not cure the disease.

The etiology of PD remains ambiguous so far. At the cellular level, PD has been generally thought to correlate with the mitochondrial dysfunction, abnormality of protein aggregation/degradation and/or defects in vesicular trafficking [2]. Many environmental or genetic factors have been demonstrated to increase the risk of PD such as rotenone which is a commonly used pesticide and inhibits complex I of the oxidative phosphorylation [3].

Over the past several years, mutations in several genes including *alpha-synuclein*, *parkin*, *UCH-L1*, *PINK1*, and *DJ-1* have been tightly linked to Parkinsonism [4]. More recently, evidence from genetic studies has indicated that mutations of leucine-rich repeat kinase (LRRK) 2 gene cause autosomal dominant, late-onset familial Parkinsonism [5, 6]. LRRK2 is an extraordinarily large protein which contains 2,527 amino acids, giving an estimated molecular weight of around 286 kDa. LRRK2 contains multiple predicted catalytic and protein-interaction domains (Figure 3.1). The Roc domain of LRRK2 is a putative GTPase and, like all other Roc containing proteins, is found in tandem with the

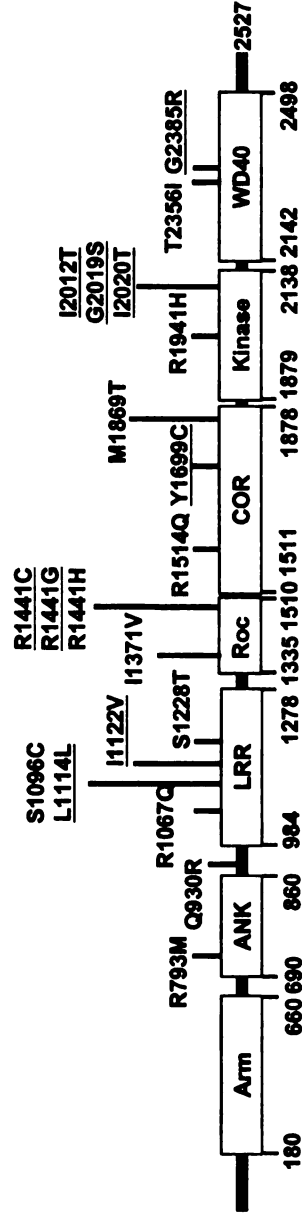


Figure 3.1. Diagram of LRRK2 domains with mutations found in Parkinson's disease patients. LRRK2 contains

multiple domains based on the prediction from its amino acid sequences. Mutations that have been demonstrated to segregate with

Parkinson's disease are underlined. Numbers below the diagram correspond to amino acid numbers. Abbreviations: Arm: armadillo,

ANK: ankyrin, LRR: leucine-rich repeat, COR: C-terminus of Roc.

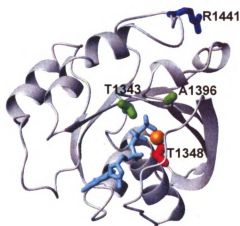
so called C-terminal of Roc (COR) region. The armadillo, ankyrin, leucine rich repeat (LRR) found in the N-terminal half of LRRK2 and the C-terminal WD-40 domains are likely to be involved in protein-protein interactions. PD associated mutations resulted in amino acid substitutions scattered throughout the LRRK2 protein [7-9], suggesting alterations in each structural domain contribute in some way to PD.

Several recent biochemical studies have demonstrated a weak *in vitro* protein kinase activity of LRRK2 [10-18]. The most prevalent PD associated mutation has a Ser substituted for Gly at 2019 near the predicted activation loop in the kinase domain. LRRK2 G2019S exhibits slightly enhanced LRRK2 catalytic activity *in vitro* [10, 11, 13, 16-18]. Transiently expressed LRRK2 G2019S increased neuronal apoptosis as judged by caspase 3 activation in primary rat nigral dopamine neurons [19] and positive TUNEL staining in SH-SY5Y human neuroblastoma cells and mouse primary cortical neurons [16]. Modulation of LRRK2 catalytic activity *in vitro* by other PD mutations has not been conclusive so far.

The Ras superfamily consists of the Ras, Rho/Rac, Ran/Rab, and Arf subfamilies. Bosgraaf et al. have constructed a dendrogram comparing the relatedness of Roc domains to GTPases of the Ras superfamily. According to a dendrogram of GTPase domains, Roc is distantly related to the other 4 subgroups [20]. LRRK2 belongs to the ROCO family of proteins since it contains both Roc and COR domains. Notably, Roc-COR tandem domains are found in a variety of organisms including prokaryotes, *Dictyostelium*, plants and metazoa, but are absent in yeast and *Plasmodium*. Roc domains are always found in tandem with COR regions, suggesting that their functions may be interdependent. However, no function has been assigned to any COR domain in the ROCO proteins. Nor

has any representative structure of a COR domains been solved to date. Like COR, no Roc structures have been solved but, based on its amino acid sequence similarity with GTPases of determined structures, the Roc domain is most similar to Rab7, a GTPase involved mainly in vesicular trafficking. Based on the known structure of murine Rab7, the Roc domain of LRRK2 has been modeled by Dr. William Wedemeyer (BMB, Michigan State University) (Figure 3.2).

GTPases play crucial roles in signal transduction through regulation of protein kinases and numerous other effector proteins [21][22, 23]. Based on the sequence of the kinase domain, LRRK2 and MLK3 are closely related and both reside in the tyrosine kinase like (TKL) subfamily. Members of the TKL subfamily, though they share sequence similarity with tyrosine kinases, appear to function as either serine/threonine kinases or, in some cases, as catalytically inactive scaffold proteins [24]. Our lab has suggested that LRRK2 may be regulated in manner [25] somewhat similar to that which we have described for MLK3 [26, 27]. In our model for MLK3 activation, binding of GTP-bound Cdc42 or Rac1 through the CRIB motif disrupts an autoinhibitory interaction, resulting in elevation of MLK3 kinase activity and subsequent activation of its downstream pathways [26-28]. LRRK2 is interesting in that it contains both a putative GTPase and kinase in the same polypeptide chain. It is conceivable that Roc domain might activate LRRK2 protein kinase activity as Cdc42/Rac activates MLK3 as we suggested [25]. Therefore, determining whether the Roc domain of LRRK2 functions as a *bona fide* GTPase is a key to understanding LRRK2 regulation and this knowledge may contribute to the development of therapeutic drugs for treating Parkinson's disease.



LRRK2 Roc	1336	KLMIVGN	T	GSGK	T	TL	VWDF	A	G	R	E	E	F	1401	
RAB7	10	KVIILGD	S	GVGK	T	SL	IWD	T	A	G	Q	E	R	F 70	
CDC42	5	KCVVVD	G	AVGK	T	CL	LFD	T	A	G	Q	E	D	Y 64	
RAS	5	KLVVVGA	G	GVGK	S	AL	I	L	D	T	A	G	Q	E	EY 64

Figure 3.2. Molecular model of GTPase domain of LRRK2 A homology model of Roc domain of LRRK2 was generated by Dr. William Wedemeyer based on the murine Rab7 structure (1VG8). *TOP*, residues mutated to generate the predicted active forms of LRRK2 GTPase and dominant negative form of LRRK2 GTPase are shown in *green* stick side chains and *red* stick side chain, respectively. R1441 is shown as a *blue* stick side chain. GTP analog and Mg^{2+} are labeled as a *sky blue* side chain and an *orange* sphere, respectively. *BOTTOM*, alignment of human Roc domain of LRRK2 with other small GTPases. Identical residues are highlighted in solid *yellow* boxes and similar residues are highlighted in the *sky blue* boxes. Residues usually mutated to generate a conformationally active or a dominant negative GTPase are labeled with *green* and *red*.

Three LRRK2 R1441C/G/H mutations, two of which (R1441C/G) are known to segregate with disease, result in amino acid substitutions of Arg 1441 within the Roc domain. Based on the model of Roc, Arg 1441 is found on the surface of Roc, distant from the predicted site of catalysis (Figure 3.2). Thus we have hypothesized that PD associated substitutions, R1441C/G/H, disrupt a protein-protein interaction leading to pathology associated with disease [25]. Tremendous effort from many labs has been focused on LRRK2 since its recent association with PD was discovered. Work from some labs, as well as the data presented in this Chapter, indicates that LRRK2 can bind GTP through its Roc domain [12, 14-16, 18, 29]. Two studies have demonstrated that LRRK2 *in vitro* kinase activity was slightly increased in the presence of non-hydrolysable GTP [14, 16, 18, 29]. Under different experimental conditions and contexts, different labs have reported different effects upon introduction of R1441C or R1441G in the Roc domain on GTP hydrolysis [14, 15, 29]. In addition, whether PD mutations within the Roc-COR tandem domains affect LRRK2 *in vitro* catalytic activity remains controversial.

In the first part of Chapter 3, I present optimization of conditions for production of recombinant GST-Roc in *E. Coli*. In addition, the recombinant GST-Roc is shown to function as a *bona fide* GTPase, albeit with the low intrinsic GTPase activity, consistent with other recent reports [14-16, 29]. The GTP-binding ability of Roc variants, expressed in both mammalian and bacterial systems, was examined. Notably, I found that the PD-associated mutation, R1441C, had no effect on GTP binding, consistent with our molecular model which shows this residue is distant from the GTP binding site. This finding led me to test the idea that the Roc-COR tandem domains might be involved in

intra- or inter-molecular interactions within LRRK2. The Roc-COR region was found to mediate the intra or inter molecular protein interactions of LRRK2 through interaction with the carboxyl terminal region of LRRK2 containing Roc, COR, kinase and WD40 domains. Introduction of R1441C/G reduced the interaction of Roc-COR with the C-terminal domains of LRRK2, whereas Y1699C enhanced it. The results shown herein support the idea that LRRK2 domains interact with one another and that PD associated mutations impact these protein-protein interactions.

3. Materials and Methods

3.1 Reagents and antibodies

The actin monoclonal antibody, V5 monoclonal antibody, hemagglutinin (HA) rabbit polyclonal antibody, GTP conjugated agarose resin, GTP, ATP, CTP and Protein A resin were from Sigma-Aldrich. Protein G resin and isopropyl- β -D-thiogalactopyranoside (IPTG) were from Roche. Glutathione sepharose 4B affinity agarose beads were purchased from GE Healthcare. Other antibodies used were the MLK3 antibody, HA mouse monoclonal antibody (BAbCO), glutathione *S*-transferase (GST) mouse monoclonal antibody (Santa Cruz), c-myc monoclonal antibody (Santa Cruz) and horseradish peroxidase-conjugated secondary antibodies (Bio-Rad). Autoinduction media was from Novagen.

3.2 Construction of expression vectors and mutagenesis

For bacterial expression vectors, the Roc (amino acid 1331-1521 of LRRK2), Roc-COR (amino acid 1331-1862 of LRRK2) regions were amplified by PCR with following primers and the pCDNA3.1-LRRK2-V5/His as the template.

Roc: 5'-GCTGGATCCTACCTTATAACCGAATGAAAC-3',

5'-CTCCTCGAGTCACTGTCCAACAACAAGCTG-3'.

Roc-COR: 5'-GCTGGATCCTACCTTATAACCGAATGAAAC-3',

5'-CCGCTCGAGTCAGTCAGCCAAAATCAAGTA-3'. The amplified Roc and Roc-COR cDNAs were each inserted into the pGEX-5X vector (GE healthcare, NJ) using the BamHI and XhoI restriction sites.

Mammalian expression constructs, for Roc (amino acid 1327-1521 of LRRK2), Roc-COR (amino acid 1327-1836 of LRRK2), N-terminal half of LRRK2 (amino acid 1-984), C-terminal half of LRRK2 containing Roc-COR-kinase-WD 40 through the end (amino acid 1335-2527), LRR-Roc-COR-kinase (amino acid 984-2160), and kinase domain of LRRK2 (amino acid 1879-2160) were similarly generated with the following primers.

Roc: 5'-CGCTCGAGAAAAGGCTGTGCCTTATAACC-3',
5'-ATAAGAAATGCGGCCGCTCACTGTCCAACAACAAGCTGATC-3'.

Roc-COR: 5'-CGCTCGAGAAAAGGCTGTGCCTTATAACC-3',
5'-ATAAGAAATGCGGCCGCTCATTCTCTGCTTTCTTCATCAA-3'.

N-terminal half of LRRK2: 5'-GGGGCTCGAGGTATGGCTAGTGGCAGCTGTC-3',
5'-ATAAGAATGCGGCCGCTCTTACTCAACAGATGTTCG-3'.

Roc-COR-kinase-WD 40 through the end of LRRK2:
5'-CGCTCGAGAAAAGGCTGTGCCTTATAACC-3',
5'-ATAAGAATGCGGCCGCTCTTACTCAACAGATGTTCG-3'

LRR-Roc-COR-kinase: 5'-GTTCTCGAGCAATTACATCACTAGACCTTTCAG-3',
5'-ATAAGAAATGCGGCCGCTCAGTGATGTGTAGCAACCATGC-3'.

Kinase: 5'-GTTCTCGAGGTCAAGCTCCAGAGTTTCTCCTAG-3',
5'-ATAAGAAATGCGGCCGCTCAGTGATGTGTAGCAACCATGC-3'.

The amplified cDNAs were individually inserted into pCMV-HA vector and pCMV-myc vector (Clontech Laboratories, CA) using XhoI and NotI restriction sites.

The COR (amino acid 1522-1857 of LRRK2), Roc-COR (amino acid 1331-1857 of LRRK2) and WD40-end (amino acid 2197-2527 of LRRK2) cDNAs were amplified by PCR and individually inserted into the pCDNA3.1/V5-His TOPO expression vector (a gift from Dr. Julie Taylor, Michigan State University).

Variants of Roc and Roc-COR constructs were generated by the QuickChange site-directed mutagenesis (Stratagene) using the following oligonucleotides and their reverse complements. For Roc A1396T: 5'-TGGGATTTTACCGGTCGTGAG-3'; Roc R1398L: 5'-TTTGCAGGTCTGGAGGAATTC-3'; Roc T1348N: 5'-AGTGGTAAAAACACCTTATTG-3'; Roc R1441G: 5'-TAAAGGCTGGCGCTTCTTC-3'; Roc R1441C: 5'-TAAAGGCTTGCGCTTCTTC-3'; Roc-COR Y1699C: 5'-AAATGCCTTGTTTTCCAATG-3'. All constructs were subsequently verified by DNA sequencing (MSU-GTSF facility).

3.3 Bacterial expression and purification of GST fusion proteins

GST-fusion proteins were expressed in Rostta (DE3) pLysS bacteria using either the auto-induction method or IPTG induction. For chaperone coexpression, GST-fusion proteins were induced in BL21 (DE3) bacteria containing pGTf2 or pGJKE8 plasmids (a gift from Dr. Jennifer Ekstrom, Michigan State University) by IPTG induction. For auto-induction, Rosetta (DE3) pLysS derivatives of *E. coli* containing the various recombinant plasmids were grown at 37 °C in LB medium supplemented with ampicillin (100 µg/ml) and chloramphenicol (37 µg/ml). Proteins were expressed in overnight express instant TB auto-induction media (Novagen, CA) at 30°C for 16-18 h according to the

manufacturer's instructions. For IPTG induction, Rosetta (DE3) pLysS bacteria containing the pGEX-5X-1-Roc variant plasmids and pGEX-5X-1-Roc-COR plasmid were cultured at 37 °C in the LB media supplemented with ampicillin (100 µg/ml) and chloramphenicol (37 µg/ml) overnight. The BL21 (DE3) bacteria containing the pGEX-5X-1-Roc-COR recombinant plasmid and pGTf-2 or pGJKE8 plasmids were cultured at 37°C overnight in LB media supplemented with ampicillin (100 µg/ml) and chloramphenicol (37 µg/ml) and inducers including 10 ng/ml tetracycline and/or 2 mM L-arabinose for chaperone expression. When OD₆₀₀ reached 0.6, protein expression was induced by addition of 1 mM IPTG for 2 h. Cells were harvested by centrifugation at 4000 × g for 20 min, resuspended in 30 mL cold Tris buffer (50 mM Tris, pH 8) containing the protease inhibitor cocktail and lysed by three passes through a French pressure cell. GST fusion proteins were purified by affinity chromatography using Glutathione sepharose 4B affinity agarose beads and eluted with the elution buffer (50 mM Tris-HCl, pH 8, 250 mM NaCl, 0.5 mM DTT, 10% glycerol, 20 mM reduced glutathione). The concentration of eluted protein was determined by the Bradford method using Bio-Rad protein assay kit with BSA as standard according to manufacturer's protocol.

3.4 Cell culture, transfection and cell lysis

Human embryonic kidney (HEK) 293T cells were transfected using Lipofectamine 2000 (Invitrogen) following the manufacturer's instructions. Cells were maintained at 37 °C in a humidified incubator containing 5% CO₂ in air. Cells were harvested 20-24 h after transfection and lysed either in lysis buffer G (100 mM Tris-HCl

pH 7.5, 50 mM KCl, 0.1 mM EDTA, 0.1 mM DTT, 5 mM MgCl₂, 1% Triton X-100) for GTP binding assay or in the lysis buffer (50 mM HEPES (pH 7.5), 150 mM NaCl, 1.5 mM MgCl₂, 2 mM EGTA, 1% Triton X-100, 10% glycerol, 1 mM Na₄PPi, 100 μM β-glycerophosphate, 1 mM Na₃VO₄ and 1X protease inhibitor cocktail (Sigma Aldrich)) and kept on ice for immunoprecipitation .

3.5 Immunoprecipitation, gel electrophoresis and western blot analysis

Antibodies were prebound to protein A or G agarose beads for 30 min at room temperature: HA rabbit polyclonal antibody (0.15 μg/μl slurry), c-myc monoclonal antibody (0.04 μg/μl slurry). Clarified cellular lysates from an xmm plate were incubated with 20 μl antibody-bound protein A or G agarose resin for 90 min at 4°C.

Immunoprecipitates were washed twice with HNTG buffer (20 mM HEPES (pH 7.5), 150 mM NaCl, 0.1% Triton X-100, and 10% glycerol). Cellular lysates and immunoprecipitates were resolved by SDS-PAGE. Proteins were transferred to nitrocellulose membranes and immunoblotted using appropriate antibodies. Immunoblots were developed by the chemiluminescence method.

3.6 GTP-binding assay

Aliquots (5 μg) of affinity isolated GST-Roc variants, except GST-Roc T1348N, were incubated with 60 μl GTP-conjugated agarose beads in the GTP-binding buffer (50 mM Tris-HCl pH 7.6, 50 mM KCl, 0.1 mM DTT, 5 mM MgCl₂, 1% Triton X-100) at 4°C for 1 h. Since GST-Roc T1348N was likely contaminated with dnaK (see Results, Figure 3.7A)), 50 μg of total protein was used to ensure that each sample contained the same

amount of. The supernatant was removed and GTP-conjugated beads were washed 3 times with ice-cold HNTG buffer. Proteins were eluted from GTP-conjugated beads by boiling in SDS loading buffer and resolved by SDS-PAGE followed by immunoblotting using a GST antibody.

In mammalian cells, the GTP-binding experiment was performed according to Korr et al. [30]. Briefly, HEK 293T cells transiently expressing HA-Roc or HA-Roc-COR variant proteins were lysed in lysis buffer G containing protease inhibitor cocktail and clarified. Clarified total cellular lysates were incubated with GTP-conjugated agarose beads in the lysis buffer G and bound HA-Roc variants were detected by Western blot as described above.

After binding of Roc variants to GTP-conjugated resins, nucleotide competition experiments were performed by adding the indicated concentration of GTP, ATP or CTP for additional 1 h incubation at 4°C. GTP beads were then washed 3 times with ice-cold HNTG buffer followed by Western blot analysis as described above.

3.7 GTPase activity assay

The GTPase assays were performed using the EnzChek phosphate assay kit (Molecular Probes) according to the manufacturer's instructions. This assay measures phosphate released from GTP hydrolysis by using purine nucleoside phosphorylase (PNP) as coupling enzyme and 2-amino-6-mercapto-7-methylpurine riboside (MESG) as a co-substrate. Typically, purified GST or GST-Roc variant proteins were incubated in 50 mM Tris, pH 7.5 buffer including 5 mM MgCl₂, 0.2 mM MESG substrate and 1 U/ml PNP at

room temperature for 10 min. GTP hydrolysis was initiated by addition of 0.5 mM GTP at 30°C and the reaction was followed by monitoring the absorbance at 360 nm in every 10 seconds using a 96-well plate spectrophotometer (SpectraMax plus, Molecular Devices).

4. Results

4.1 Recombinant GST-Roc variants, but not GST-Roc-COR are expressed as soluble proteins under condition of auto-induction

Studies of Ras family GTPases have demonstrated that a single amino acid substitution within the catalytic site renders the GTPase either GTP-bound (conformationally active) or GDP-bound (conformationally inactive). These GTPase variants are commonly used to study their physiological roles in various cellular processes and to identify their regulators, guanine exchange factors (GEFs) and GTPase activating proteins (GAPs) (see Chapter 1). A single amino acid substitution of Gly at codon 12 with Val [31-34], Ala at codon 59 with Thr [31] or Gln at codon 61 [35, 36] with Leu in Ras reduces the rate of GTP hydrolysis by the activated Ras GTPase and constitutively activates Raf-MEK-ERK pathway. In contrast, substituting Asn for Ser at codon 17 in Ras displaces the Mg^{2+} that is required for GTP nucleotide binding, resulting in a higher affinity of binding GDP [37, 38].

To evaluate whether Roc is a *bona fide* GTPase and to test the proposed hypothesis that the R1441C PD-associated LRRK2 mutation impacts protein interactions rather than GTPase activity, mutations predicted to generate conformationally active and inactive forms of Roc were introduced to the Roc cDNA in bacterial expression constructs. For creation of a conformationally active form of Roc (GTPase defective), the sequence of the LRRK2 Roc domain was compared with representative members of the Ras superfamily: Rab7, Cdc42 and Ras. Notably, substitution of Gly 12 with Val renders both Ras and Cdc42 conformationally active and competent to bind effector proteins including protein kinases. Unfortunately, this critical Gly residue is not

conserved in LRRK2 or in Rab7, a closer relative of the Roc domain of LRRK2. In Rab7, Cdc42 and Ras, mutation of the conserved Gln residue to Leu, Q67L, Q60L and Q60L, respectively, renders each of these GTPases conformationally active. Instead of Gln at this position, the Roc domain has an Arg residue, R1398. However, a less well-known Ras variant, A59T, renders Ras conformationally active. This Ala residue, A1396, is conserved within Roc as well as the other representative GTPases (Figure 3.2).

In order to create conformationally active variants of Roc, two different mutations, A1396T and R1398L, were introduced into the Roc domain. Conformationally inactive forms of Ras, Cdc42 and Rab7 have been created by substituting the conserved Ser/Thr residue, corresponding to Ser17 in Ras to Asn. Therefore the corresponding conserved Thr at 1348 in LRRK2 was substituted with Asn in order to create a predicted conformationally inactive variant.

GST-Roc variants, GST-Roc A1396T and R1398L, predicted to be conformationally active and the predicted inactive variant, GST-Roc T1348N, were overexpressed in *E. Coli* upon IPTG induction. All GST-Roc variants expressed well but were found mainly in the insoluble fraction (Figure 3.3). Wild type GST-Roc-COR exhibited similar insolubility. Massive expression of protein in a short time as takes place during IPTG induction may result in protein aggregation. Gradual expression of proteins often renders them more soluble, allowing time for proper folding, resulting in a higher enzymatic activity. In the autoinduction system, the growth media contain a mixture of carbon source including lactose. After glucose is consumed by *E. Coli*, lactose will be used, thus automatically inducing protein expression but at a much slower rate than occurring upon acute addition of IPTG.

The solubility of expressed GST-Roc variants and GST-Roc-COR was determined under autoinduction conditions. As shown in Figure 3.4A and 3.4C, all GST-Roc variants as well as GST-Roc-COR expressed well under autoinduction conditions. Wild type and predicted constitutively active GST-Roc R1398L were highly soluble (Figure 3.4B), whereas the predicted inactive GST-Roc T1348N had limited solubility and GST-Roc-COR was still completely insoluble. The PD associated variant R1441G was introduced into wild type GST-Roc and GST-Roc R1398L. Both variants expressed well upon autoinduction as shown in Figure 3.4C (two different clones shown for each construct). A portion of the expressed variants was insoluble, but over 50% remained in the soluble portion.

In a final effort to facilitate the solubility of Roc-COR, the expression vectors encoding bacterial chaperones, pGTf2 and pGJKE8, were coexpressed with GST-Roc-COR. The pGTf2 expression vector encodes three chaperones including groES, groEL and tig and these chaperones are expressed upon tetracyclin induction [39]. The pGJKE8 plasmid encodes five chaperones including dnaK, dnaJ, grpE, groES and groEL and the expression of these five chaperones is induced by addition of L-Arabinose and tetracycline [39]. In the presence of chaperones, the protein expression and solubility of GST-Roc-COR were assessed by SDS-PAGE followed by Coomassie blue staining. As shown in Figure 3.5, GST-Roc-COR was expressed in the presence of different chaperones upon IPTG induction. However, almost all of GST-Roc-COR coexpressed with several chaperones still remained in the insoluble fraction. A summary of the protein solubility

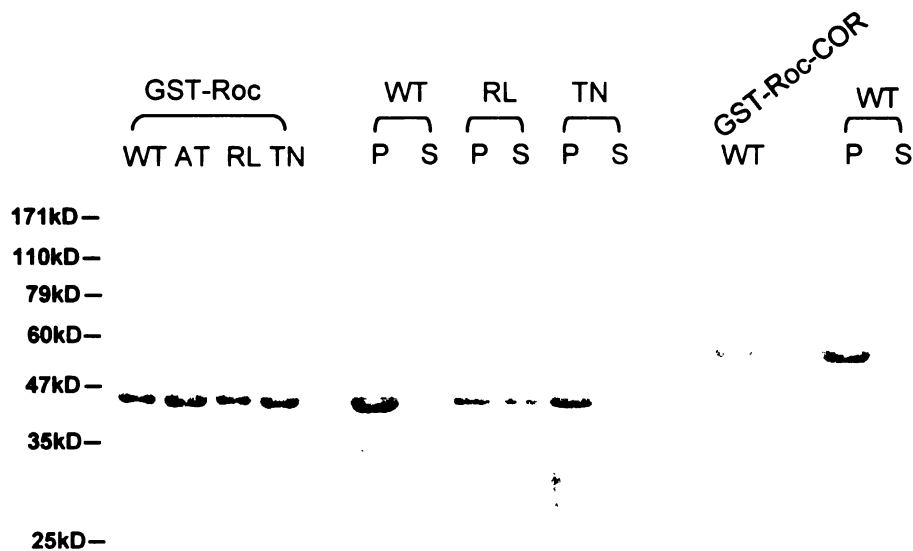
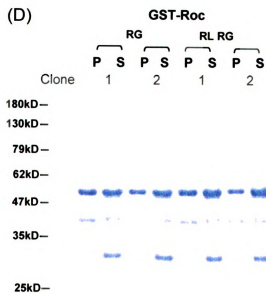
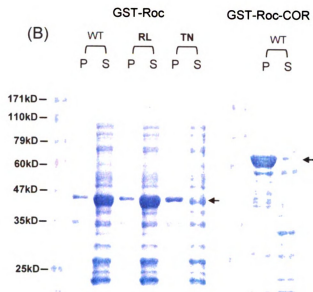
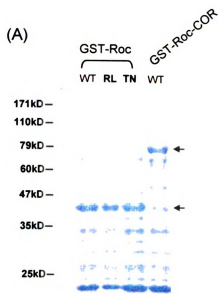


Figure 3.3. Expression and solubility of GST-Roc variants and GST-Roc-COR upon IPTG induction. *Left panel*, GST-Roc variant proteins and *right panel*, GST-Roc-COR were individually expressed in Rosetta (DE3) pLysS cells upon IPTG induction for 2 h at 37°C. The expression level and solubility of GST-Roc and GST-Roc-COR were evaluated as described previously by Coomassie staining. WT: wild type, RL: R1398L, TN: T1348N, P: pellet fraction (insoluble), S: supernatant fraction (soluble). Equal cellular equivalents from each fraction were loaded.

Figure 3.4. Expressed GST-Roc variant proteins but not GST-Roc-COR are soluble under the auto-induction condition. pGEX-5X-1-Roc and pGEX-5X-1-Roc-COR variant plasmids were individually transformed into Rosetta (DE3) pLysS cells. GST-Roc and GST-Roc-COR variant proteins were induced by auto-induction media at 30°C for 16-18 h. A, bacteria were spun down and lysed in SDS-sample loading buffer. Levels of expressed GST-Roc variants and GST-Roc-COR were evaluated by Coomassie staining. B, bacteria were collected followed by sonication on ice as described in Materials and Methods. Equal cellular equivalents of protein in supernatant (S) and pellet (P) fractions were subjected to SDS-PAGE followed by Coomassie staining for solubility assessment. Arrows indicated the GST-Roc variants and GST-Roc-COR, respectively. C, Level of expressed GST-Roc harboring PD mutation was assessed as A. D, as described in B, equal cellular equivalents of protein in each fraction was loaded and the presence of GST-Roc with PD mutation in each fraction was checked by SDS-PAGE with a Coomassie staining. WT: wild type, RL: R1398L, TN: T1348N, RG: R1441G.



of bacterially expressed GST-Roc variants and GST-Roc-COR under various conditions is presented in Table 3.1.

Soluble GST-Roc variant proteins were purified from cellular lysates by glutathione affinity chromatography and checked for their purity by SDS-PAGE followed by Coomassie blue staining. The control proteins, GST and GST-Cdc42 G12V, were efficiently eluted from glutathione agarose beads. About half of the GST-Roc variants were obtained from an eluted fraction (Figure 3.6).

4.2 Roc domain of LRRK2 binds GTP

Purified GST-Roc variant proteins were tested for their ability to bind GTP-conjugated resin. Wild type as well as predicted conformationally active variants, A1396T and R1398L of, GST-Roc bound GTP-conjugated agarose, suggesting that bacterially expressed Roc is a GTP-binding protein. As predicted, GST-Roc T1348N failed to bind GTP (Figure 3.7A). However, it is unclear whether the bacterially expressed GST-Roc T1348N was correctly folded since a massive 60 kD protein band, likely the bacterial dnaK heat shock protein which often copurifies with unfolded GST fusion proteins in bacteria (Figure 3.7A). To confirm these results, HA-tagged Roc variants were also transiently expressed in mammalian HEK 293T cells and tested for their ability to bind GTP conjugated agarose. In HEK 293T cells, the HA-Roc proteins were all expressed at similar levels (Figure 3.7B). Consistent with the bacterially expressed GST-Roc variants, both wild type and its predicted conformationally active variant, R1398L bound GTP-conjugated beads. Intriguingly, one of the predicted

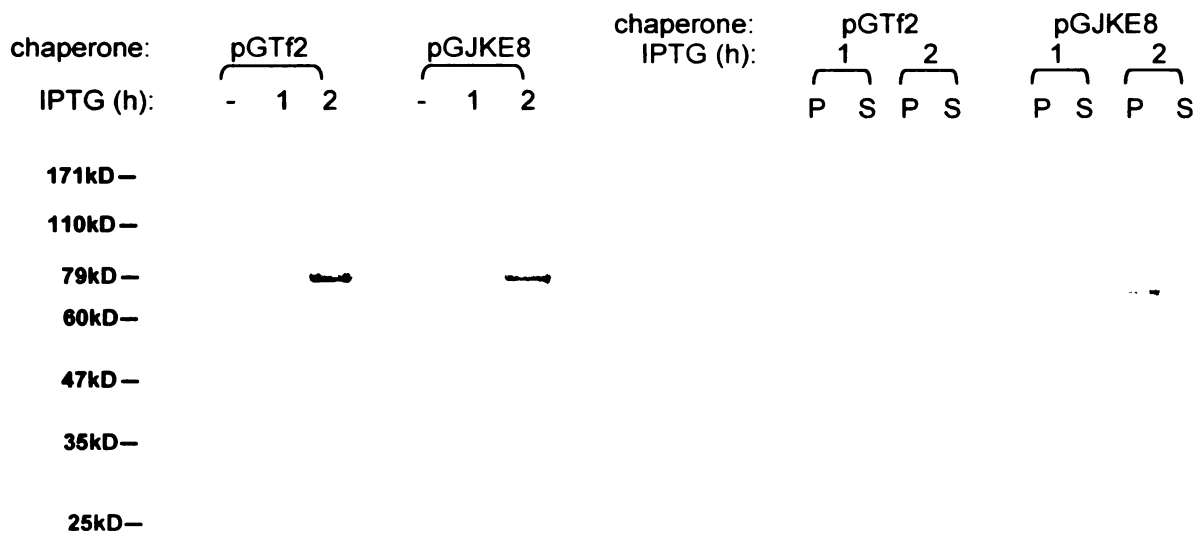


Figure 3.5. Expression and solubility of GST-Roc-COR by IPTG induction

with coexpressed chaperones. GST-Roc-COR was coexpressed with either pGTf2 or pGJKE8 chaperones in BL21 (DE3) cells by IPTG induction for the indicated times at 30°C. pGTf2 encodes 3 bacterial chaperones, groES, groEL and tig. pGKJE8 encodes 5 bacterial chaperones, dnaK, dnaJ, dnaE, groES and groEL. *Left panel*, the induced level of GST-Roc-COR with different chaperones at different induction time points was assessed by Coomassie staining. *Right panel*, the solubility of GST-Roc-COR with expressed chaperones was determined as described in Materials and Methods. P: pellet fraction (insoluble), S: supernatant fraction (soluble). Equal cellular equivalents of protein from each fraction were loaded

Table 3.1. Summary of the protein solubility of bacterial GST-Roc and GST-Roc-COR variant proteins under various induced conditions.

construct	mutation	bacterial strain	induction	chaperones	protein solubility
pGEX-5x-1-Roc	no	Rosetta (DE3) pLysS	auto	no	soluble
	A1396T	Rosetta (DE3) pLysS	auto	no	soluble
	R1398L	Rosetta (DE3) pLysS	auto	no	soluble
	T1348N	Rosetta (DE3) pLysS	auto	no	soluble
	R1441G	Rosetta (DE3) pLysS	auto	no	soluble
	R1398L, R1441G	Rosetta (DE3) pLysS	auto	no	soluble
pGEX-5x-1-Roc-COR	no	Rosetta (DE3) pLysS	auto	no	insoluble
		Rosetta (DE3) pLysS	IPTG	pGro	insoluble
		BL21 (DE3)	IPTG	pG-JKE8 or pG-Tf2	insoluble

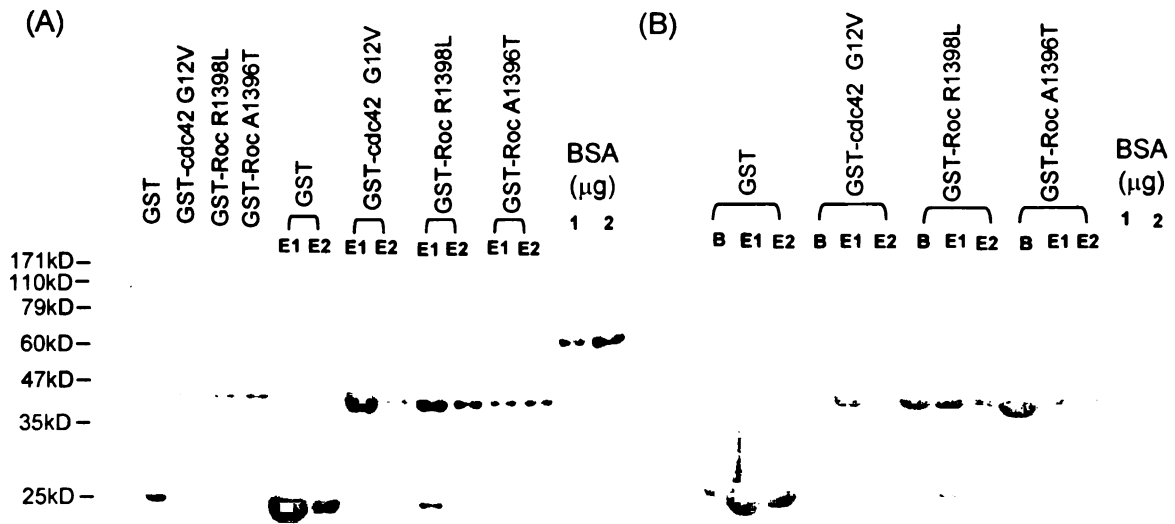
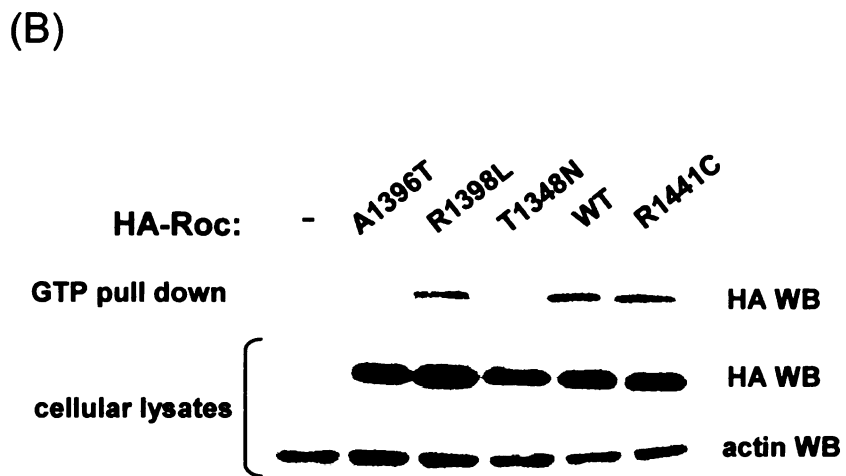
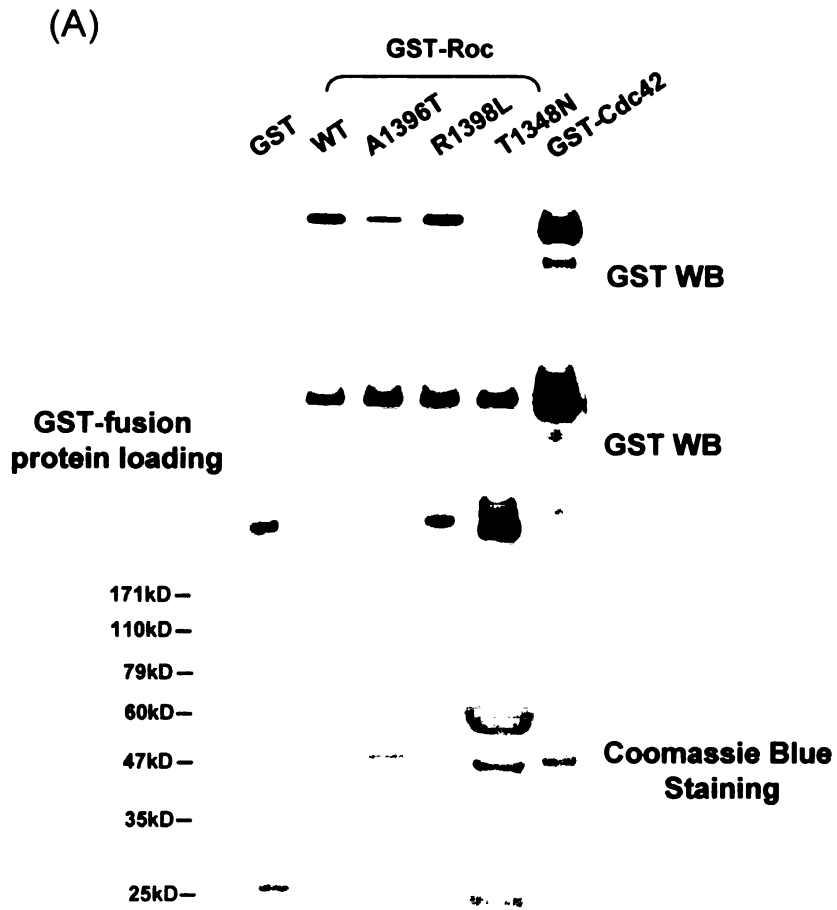


Figure 3.6. Purification of recombinant GST-Roc variant proteins induced by auto-induction condition. GST, GST-Cdc42 G12V and GST-Roc variant proteins were induced by auto-induction media at 30°C for 16-18 h, and bacteria were lysed using a French pressure cell. GST and GST-fusion proteins were incubated with glutathione sepharose 4B beads at 4°C for 1.5 h followed by washing. Proteins attached to the glutathione beads were eluted with appropriate buffer containing 0.5 mM DTT and 20 mM reduced glutathione. Proteins from beads (B) and each elution (E1, E2) were assessed by Coomassie blue staining. GST and GST-Cdc42 G12V proteins were used as controls. Equal cellular equivalents from each fraction were loaded. Protein concentration was determined using a Biorad protein assay kit and re-confirmed with Coomassie blue staining as compared to the known amount of BSA.

Figure 3.7. The GTP-binding ability of Roc variant proteins. *A, top*, 5 μ g purified GST, GST-Roc variant proteins and GST-Cdc42 from *E. Coli* was incubated with GTP-conjugated agarose beads. The level of GST-fusion proteins bound to GTP agarose beads was assessed by Western blotting using the GST antibody. GST-Cdc42 protein was used as a positive control. *Bottom*, the total amount of each GST-fusion protein used in the GTP-binding experiments was examined by Western blotting with the GST antibody. *B.* GTP-binding experiment was performed using total cellular lysates from HEK 293T cells expressing various HA-Roc proteins. The level of HA-Roc variant proteins bound to the GTP-conjugated agarose beads was accessed by Western blotting using a HA antibody. The expression levels of various HA-Roc constructs and the loading control were examined by immunoblotting using the antibodies against HA and actin, respectively. WT: wild type.



conformationally active Roc variants, A1396T, bound to GTP resin inefficiently when isolated from bacteria and cultured cells, suggesting that this mutation may not render Roc conformationally active. These data suggest that Roc domain of LRRK2 is a GTP-binding protein. Consistent with predictions, Arg at 1398 to Leu of Roc is able to bind GTP, whereas replacement of Thr at 1348 to Asn fails to bind GTP.

Furthermore, the Roc domain containing the PD-associated substitution, R1441C, bound GTP resin similarly to wild type Roc. This finding is consistent with our model which shows that Arg1441 is located far from the GTP binding site [25].

4.3 COR region affects the GTP binding of Roc

Because the Roc domain always exists in tandem with the COR region in proteins of the ROCO family, they may be functionally interdependent. To date, the function of COR regions in the ROCO proteins is a mystery. To decipher whether the presence of the COR region regulates the ability of Roc to bind GTP, cellular lysates from HEK 293T cells transiently expressing HA-tagged Roc-COR proteins with different mutations were assessed in the GTP-binding assay. As shown in Figure 3.8, HA-Roc-COR R1398L, predicted to be conformationally active, bound GTP conjugated resin slightly better than the wild type HA-Roc-COR and its mutants including A1396T and T1348N. Surprisingly, HA-Roc-COR T1348N, the predicted conformationally inactive variant which failed to bind GTP-agarose in the context of HA-Roc, binds GTP-conjugated agarose as efficiently as wild type HA-Roc-COR. This may indicate that within the Roc-COR context, the T1348N variant either nonspecifically associates with GTP resin or the presence of the

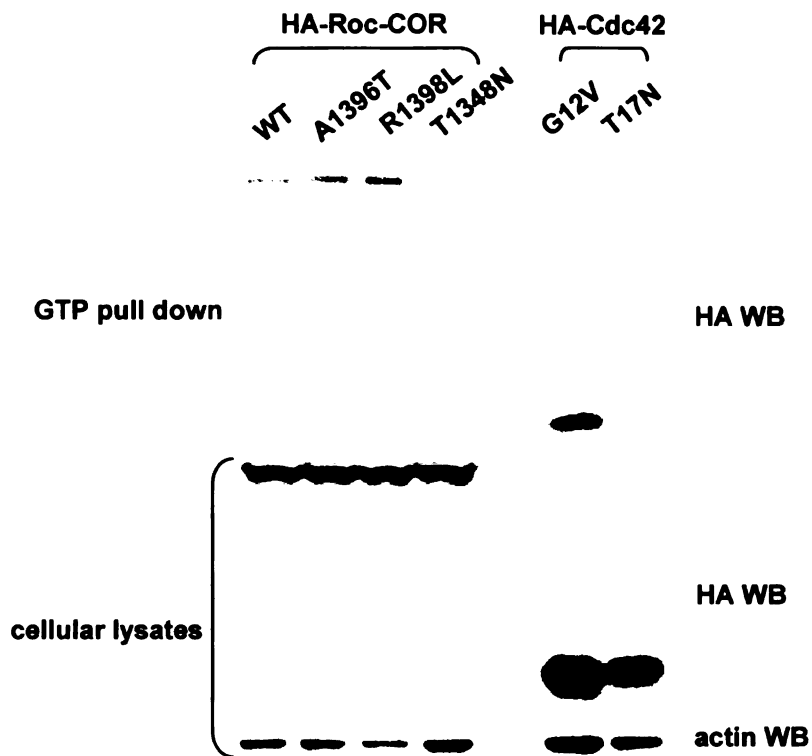


Figure 3.8. The GTP-binding ability of Roc-COR variant proteins. Total cellular lysates from HEK 293T cells expressing various HA-Roc-COR proteins and HA-Cdc42 variants were used in GTP-binding experiments as described in Materials and Methods. HA-Roc-COR variant proteins bound to the GTP-conjugated agarose beads were detected by western blotting using a HA antibody. The expression levels of various HA-Roc-COR constructs and the loading control were examined by immunoblotting using the antibodies against HA and actin respectively. HA-Cdc42 G12V and HA-Cdc42 T17N were used as the positive and negative controls, respectively. WT: wild type.

COR region somehow alters the conformation of the Roc domain to facilitate GTP binding despite the presence of the T1348N mutation. Direct comparison of the GTP binding ability of HA-Roc and HA-Roc-COR proteins in parallel will be necessary to further address whether COR regulates the GTP binding of Roc.

4.4 The GTP-binding specificity of Roc

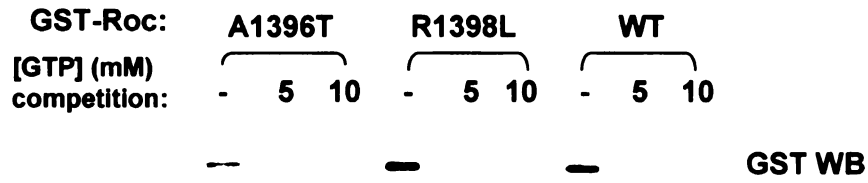
The nucleotide specificity of Roc variants was tested in a competition assay. The interaction of Roc variants with GTP resin was abolished upon addition of increasing amount of free GTP (Figure 3.9A). Moreover, addition of GTP, but not other nucleotides including ATP or CTP led to release of Roc from GTP resin (Figure 3.9B and 9C), suggesting that Roc preferentially binds GTP, but not other nucleotide triphosphates.

4.5 Hydrolysis of GTP by the Roc domain of LRRK2

To assess whether the Roc domain of LRRK2 possesses GTPase activity, an enzymatic coupling method to detect free phosphate generated from GTP hydrolysis was employed. Enzymatic conversion of free phosphate and 2-amino-6-mercapto-7-methylpurine ribose (MESG) by purine nucleoside phosphorylase (PNP) produces 2-amino-6-mercapto-7-methylpurine which absorbs at 360 nm. As shown in Figure 3.10, readings of absorbance at 360 nm over time increased in the presence of purified GST-Roc, suggesting that GST-Roc hydrolyzed GTP. Notably, no increase in absorbance was observed using GST.

4.6 Interaction of Roc-COR region with the carboxyl terminal region of LRRK2

(A)



(B)

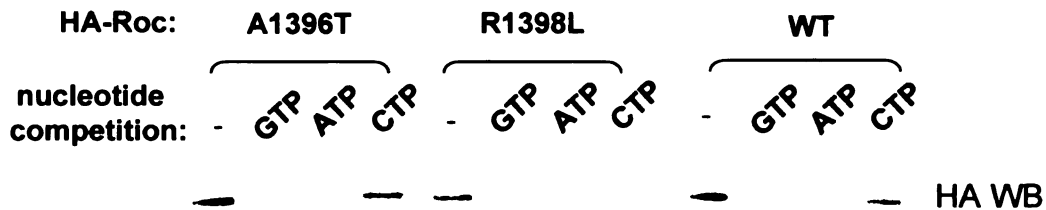


Figure 3.9. GTP-binding specificity of Roc variant proteins. One microgram purified GST-Roc variant proteins was incubated with GTP conjugated agarose beads for 90 min at 4°C followed by nucleotide competition with A, different concentrations of exogenous GTP as indicated or B, 5 mM indicated nucleotides for 1 h. Levels of GST-Roc variants retained in the GTP resin after competition were evaluated by western blotting using the GST antibody. C, cellular lysates from HEK 293T cells transiently expressing HA-Roc variant proteins were used in the nucleotide competition assay and analyzed as described above. Data shown is representative of three independent experiments.

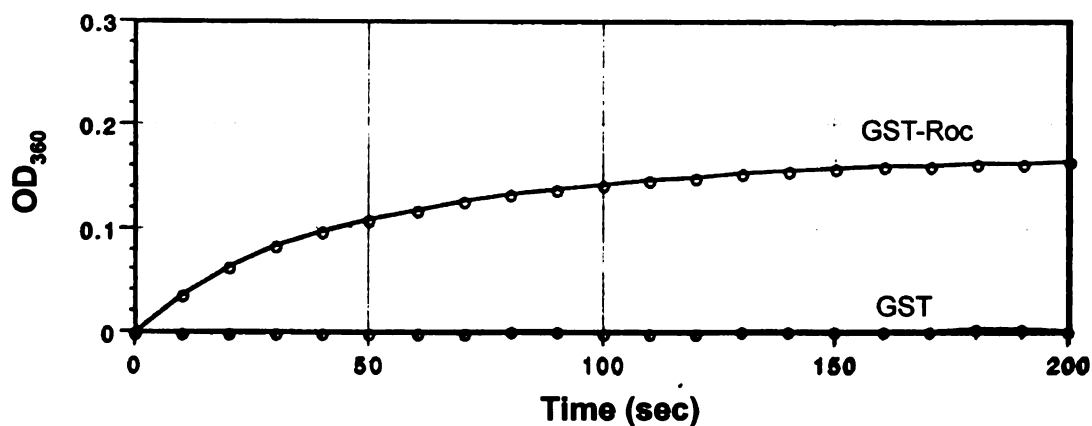


Figure 3.10. The GTP hydrolysis ability of Roc. The GTPase activity of Roc was assessed using an Enzchek phosphate assay kit. One microgram purified GST-Roc was used in the reaction as described in Materials and Methods. 0.5 mM GTP was added to initiate GTP hydrolysis reaction at 30°C. Readings of absorbance at 360 nm in every 10 seconds were plotted. Purified GST was used as a negative control.

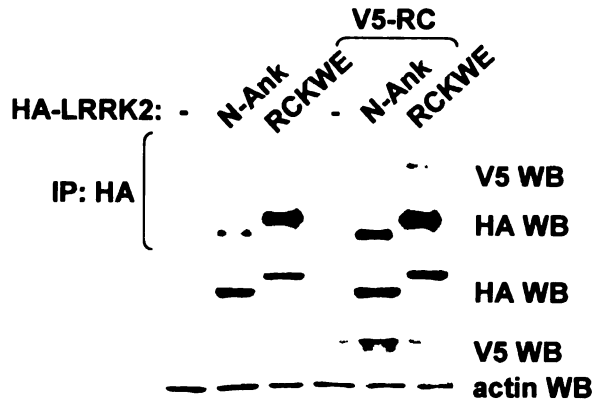
In addition to the protein kinase domain, LRRK2 also possesses several predicted protein-protein interaction domains. Emerging genetic studies have indicated that mutations in these potential protein interacting regions result in familial Parkinson's disease, suggesting a pivotal role for LRRK2 protein interactions in the pathogenesis of PD. In familial PD, three different mutations impact Arg 1441 resulting in substitutions with Cys, Gly or His. Since three distinct amino acid substitutions at Arg 1441 result in pathogenesis, we have hypothesized that, rather than altering some catalytic protein of LRRK2, they might disrupt protein interactions to cause Parkinson's disease. This idea is supported by molecular modeling of Roc which predicts that Arg 1441 resides on the Roc surface distant from the catalytic site where protein interactions might occur. It is conceivable that PD mutations in the Roc-COR region might affect its interaction with other parts of LRRK2, impacting LRRK2 kinase activity and mediating pathogenesis.

Many multi-domain protein kinases adopt conformations that involve domain-domain interactions within the same protein kinase. To test whether the Roc-COR domain interacts with other regions of LRRK2, expression vectors for the NH₂-terminal or COOH-terminal halves of LRRK2 were cotransfected with Roc-COR in HEK 293T cells and co-immunoprecipitation experiments were performed. The N-terminal half of LRRK2 includes the NH₂-terminal through the ankyrin repeat domain (N-Ankyrin), and the C-terminal half of LRRK2 encompasses the Roc domain, COR region, kinase domain and WD 40 repeats through the end (RCKWE). RCKWE, but not N-Ankyrin, interacted with the Roc-COR domain (Figure 3.11A). The central region of LRRK2 containing the LRR, Roc, COR and kinase domains (LRCK), but lacking the C-terminal WD40 domain,

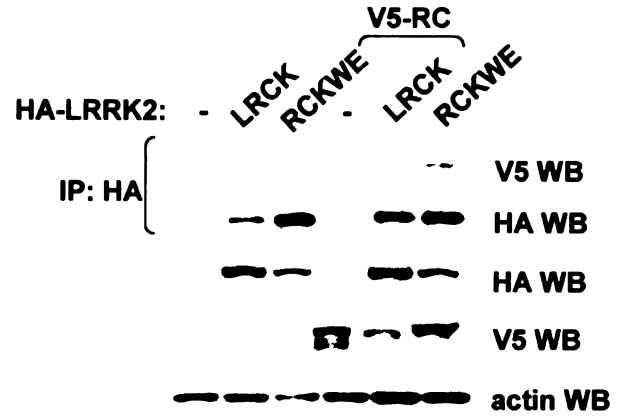
Figure 3.11. Interaction of Roc-COR with different regions of LRRK2.

Different LRRK2 truncation proteins were transiently coexpressed with or without Roc-COR in HEK293T cells for 20-24 h. The interaction of different LRRK2 truncation variants including (A) the N- and C-terminal halves as N-Ank and RCKWE respectively, (B) the region consist of LRR-Roc-COR-Kinase, (C) WD 40 repeats of LRRK2 with Roc-COR was assessed by co-immunoprecipitation assay. Levels of expressed proteins and of endogenous actin as a loading control, were detected by Western blotting with the indicated antibodies. N-Ank: N-terminal half of LRRK2 up to Ankyrin, RCKWE: Roc-COR-kinase-WD40 to the end of LRRK2, LRCK: LRR-Roc-COR-kinase, WD: WD 40 repeats, R-C: Roc-COR. Data shown is representative of three independent experiments.

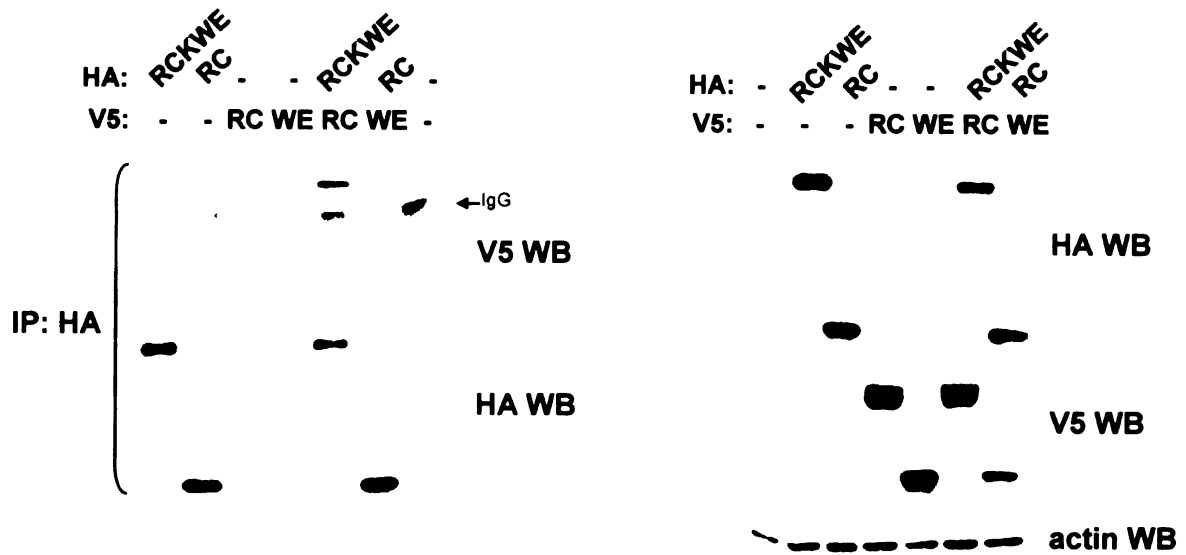
(A)



(B)



(C)



failed to interact with Roc-COR in the co-immunoprecipitation assay (Figure 3.11B), suggesting that the region containing WD-40 domain through the end (WE) of LRRK2 is required for interaction with Roc-COR. To test whether the WE region is sufficient to interact with Roc-COR, HEK 293T cells transiently expressing WE and Roc-COR of LRRK2 were used in the co-immunoprecipitation assays. No WE region was detected in the Roc-COR immunoprecipitates (Figure 3.11C). Taken together, these data suggest that the RCKWE interacts with Roc-COR and the WE region is necessary, but not sufficient, for this interaction.

4.7 Effect of PD mutations of Roc-COR on the protein interaction of Roc-COR with RCKWE of LRRK2

To dissect which region within Roc-COR is responsible for its interaction with RCKWE of LRRK2 and how PD mutations within the Roc-COR region affect this association, Roc and Roc-COR domains with or without PD mutations were assessed in the co-immunoprecipitation experiments. As shown in Figure 3.12, more RCKWE is detected in the Roc-COR immunoprecipitates than in the Roc immunoprecipitates, suggesting the association of RCKWE with Roc is weaker than its association with Roc-COR.

The impact of PD-associated mutations on interactions among LRRK domains was assessed in co-immunoprecipitation experiments. Introduction of the PD-associated mutations in Roc, Roc R1441C and Roc R1441G, dramatically reduced the association with RCKWE (Figure 3.13A). Consistently, substitution of Arg 1441 to Cys and/or Gly in the Roc-COR region also diminished the association of Roc-COR with RCKWE

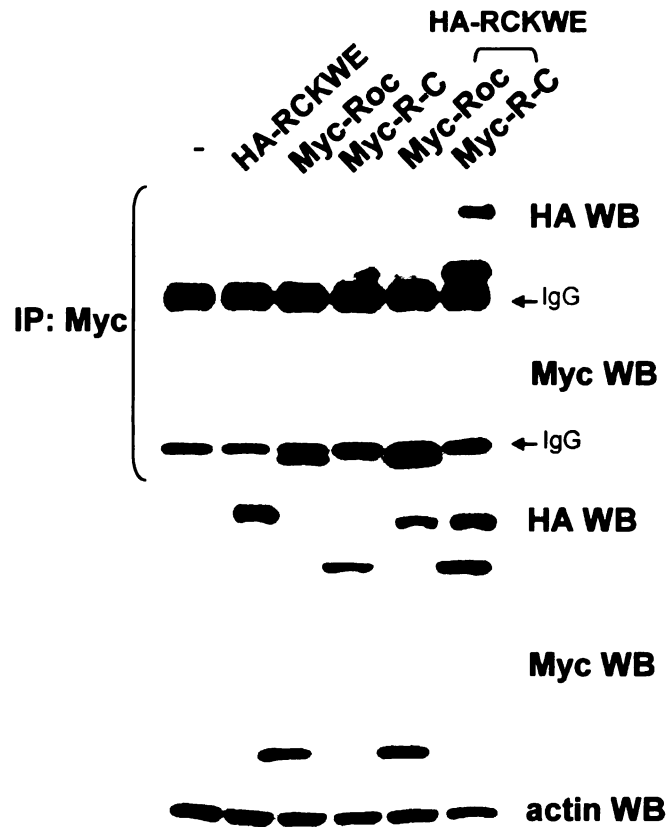
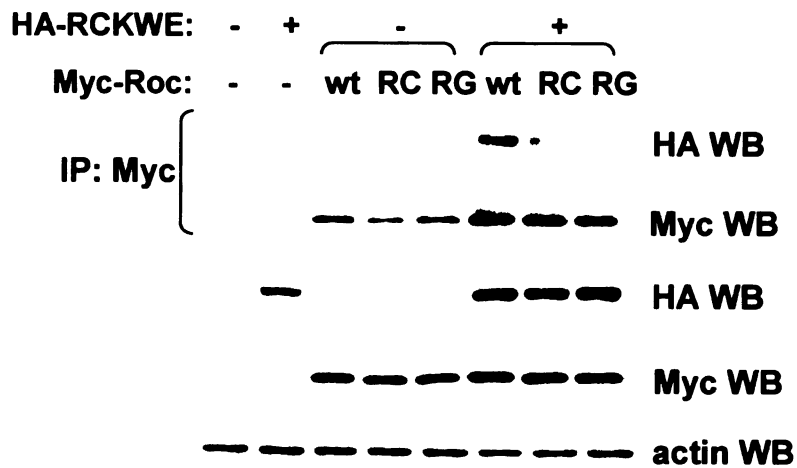


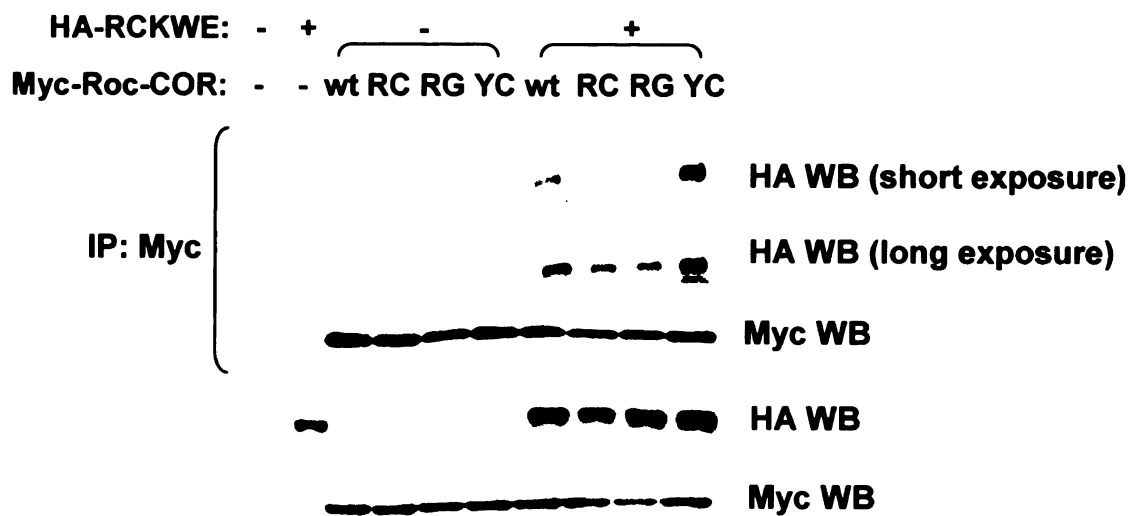
Figure 3.12. Association of Roc with Roc-COR-kinase-WD 40 through the end of LRRK2. Expression vector consists of either Roc or Roc-COR was cotransfected with Roc-COR-kinase-WD 40 to the end of LRRK2 construct in HEK 293T cells for 24 h. The presence of RCKWE in the Roc or Roc-COR immunoprecipitates was evaluated by Western blotting using the HA antibody. Levels of expressed proteins and of endogenous actin as a loading control, were detected by Western blotting with the indicated antibodies.

Figure 3.13. Effect of PD mutations found in the Roc and COR domains on their interaction with the region of Roc-COR-kinase-WD 40 through the end of LRRK2. Roc or Roc-COR variant proteins harboring PD mutations were coexpressed with HA-RCKWE in HEK 293T cells. The presence of RCKWE in the Roc or Roc-COR immunoprecipitates was assessed by immunoblotting using the HA antibody. Clarified lysates were analyzed by Western blotting with appropriate antibodies for the levels of expressed proteins and of endogenous actin as a loading control. WT: wild type, RC: R1441C, RG: R1441G, YC: Y1699C.

(A)



(B)



(Figure 13B) although the effect was less dramatic than for Roc. Interestingly, Roc-COR Y1699C which harbors a PD-associated mutation within the COR region more efficiently complexed with RCKWE of LRRK2 than did its wild type counterpart.

5 Discussion

Small GTPases are key signal transducing proteins regulating diverse cellular processes through interactions with key effector proteins, including protein kinases. Dysregulation of GTPases, or their regulators, is commonly associated with human disease, especially cancer. LRRK2 is a large protein containing a putative protein kinase and GTPase which, when mutated, can cause Parkinson's disease. In the present study, we provide evidence that the Roc domain of LRRK2, expressed as a GST fusion in bacteria, functions as a *bona fide* GTPase. However, solubility issues and variability of some preparations of some LRRK2 domains and variants produced in *E. coli* suggest that alternative expression systems, such as insect cells, may prove useful for kinetic and structural analyses.

In order to determine whether the GTPase activity and/or nucleotide binding properties of the Roc domain might influence LRRK2 activity and/or pathogenesis, we sought to generate Roc variants with different GTP binding/hydrolysis properties, based on known properties of variants of small GTPases of the Ras superfamily. As expected, the predicted conformationally inactive variant, T1348N, failed to bind GTP. Two predicted conformationally active variants, R1398L and A1396T, were also generated. The R1398L variant bound GTP as predicted whereas the A1396T exhibited variable GTP binding properties depending on its context. These data are consistent with the notion that the R1398L mutation renders Roc conformationally active. GTPase assays will be needed to fully characterize this Roc variant.

Introduction of the PD-associated mutation, R1441C, had no effect on the GTP binding of Roc, consistent with our hypothesis that this PD mutation disrupts protein interactions rather than influences the Roc GTP binding and/or GTPase activity. It is thus conceivable that the Roc domain of LRRK2 interacts with other cellular proteins and that, in Parkinson's disease, these Roc-mediated interactions are disrupted leading to pathogenesis. Since LRRK2 is such a large multidomain protein, it seemed plausible that the Roc domain might interact with another domain(s) within LRRK2 and that PD-associated mutations might impact these domain-domain interactions. Indeed coimmunoprecipitation experiments indicate that the tandem Roc-COR domains are able to interact with a carboxyl terminal region of LRRK2 encompassing Roc-COR, kinase domain and WD 40 repeats through the end. Thus LRRK2 may be regulated through intra- or inter-molecular protein interactions involving its Roc-COR region. Furthermore, pathogenic mutations within the Roc-COR region impacted these interactions. R1441C/G of Roc domain slightly attenuated Roc-COR interaction with the RCKWE of LRRK2, whereas Y1699C located in COR region dramatically enhanced this interaction.

LRRK2 is a member of the ROCO family of proteins. ROCO proteins, which contain both Roc and COR domains, are found in prokaryotes, plants and metazoa. Considerable domain diversity exist outside of the Roc and COR regions of ROCO proteins. Very few ROCO proteins have been studied in any detail, and their biological functions are largely unknown. In particular, no biochemical function has been described for any COR domain. Results from our GTP-binding study have demonstrated that the efficiency of GTP binding of Roc variants was influenced when it was in conjunction with COR, giving a possibility that COR may regulate the GTP binding ability of Roc. A

direct comparison of the GTP binding ability of Roc and Roc-COR will be crucial for addressing this hypothesis. In addition, the studies presented here mapping the region within Roc-COR responsible for its interaction with RCKWE, indicate that Roc interacts with RCKWE much weakly than Roc-COR. These results may suggest that this interaction may primarily mediated by COR. Future experiments assessing the ability of COR to interact with RCKWE in the co-immunoprecipitation assay will provide key clues for understanding the role of COR in LRRK2 regulation.

Recently, the GTPase activity of Roc has also been demonstrated by other research groups using different experimental contexts. It has been demonstrated that expressed full length human LRRK2 hydrolyzed GTP in a slow rate as judged by the thin layer chromatography assay [14][29]. Disruption of the nucleotide binding site in the Roc domain of full length LRRK2 by substitution of Lys 1347 to Ala failed to hydrolyze GTP [14]. These data suggest that the Roc domain in the full length LRRK2 construct is a GTPase. Introduction of the PD-associated mutation, R1441C, in full length LRRK2 reduced the GTP hydrolysis rate [14, 29]. In these studies, the low expression level of full length LRRK2 may be the cause of the low GTPase activity. In addition, unequal amount of the full length LRRK2 containing Roc mutations used in GTPase assay makes quantitation more difficult. Li et al. has reported that the purified Roc domain of murine LRRK2 from bacteria possessed a GTPase activity [15], consistent with my finding presented in this Chapter. The Roc T1348N of murine LRRK2 which failed to bind GTP did not hydrolyze GTP [15]. The GTPase activity was moderately reduced in Roc R1441C and R1441G of murine LRRK2 [15] which is consistent with the result in the full length LRRK2 study. However, a recent study from other lab has demonstrated that

bacterially expressed GST-Roc R1441C has same GTP hydrolysis rate as wild type Roc [29]. Altogether, these data suggest the Roc domain is able to hydrolyze GTP. However, the effect of PD-associated mutation, R1441C/G, on GTPase activity of Roc remains inconclusive. In this Chapter, I also demonstrated that the Roc domain of human LRRK2 functions as a *bona fide* GTPase. The intrinsic GTPase activity of Roc is relatively low *in vitro* which is consistent with previous studies of Ras and Rho subfamily GTPases as well as Roc. An insect cell expression system and the mammalian expression system stimulated by stresses are commonly used to evaluate the ability of GTP hydrolysis of Ras and Rho subfamily GTPases since these activated GTPases usually undergo post-translational modifications including prenylation [40] with a farnesyl [41] or geranylgeranyl [42] group which renders them hydrophobic and be targeted to cellular membranes. Loss of appropriate cellular structure(s) such as lipids during purification procedure may result in the low GTPase activity of Roc. Based on this, the insect cell expression vectors of His-tagged Roc variants and Roc-COR are under construction in the lab. Moreover, the GTP hydrolysis ability of purified Roc variants as well as Roc-COR from insect cells will be tested and compared in parallel with that from bacteria. Roc is very distinct from Ras and Rho subfamilies and no potential prenylation sites are predicted in the Roc-COR region. However, previously, we also proposed that the LRR and WD40 domains have high net positive charge located on the surface, allowing LRRK2 possibly bind phospholipids [25]. It suggests that the LRR and/or WD40 domain might be required for higher Roc GTPase activity.

Emerging biochemical studies from last couple years have mainly focused on several particular pathogenic mutations of LRRK2 elevated its catalytic activity *in vitro*

resulted in morphological degeneration of neurons. However, whether mutations within Roc-COR region of LRRK2 directly impact LRRK2 kinase activity *in vitro* responsible for neuronal cell death remains obscure. In our study, the Roc domain of LRRK2 not only functioned as a real GTPase but also competently interacted with the RCKWE region of LRRK2, suggesting that the Roc domain involved in regulation of LRRK2 itself through an intra or inter molecular interaction. Interestingly, this interaction was attenuated by the PD mutations of Roc, R1441C/G, whereas it was increased by the PD mutation of COR, Y1699C, suggesting that the alteration of the LRRK2 itself domain-domain interactions may contribute to the pathogenesis of PD. These data presented here provide important information to obtain a novel mechanism of LRRK2 regulation and open a possibility that the dysregulation of LRRK2 protein itself interaction mediated by Roc-COR domain may lead to Parkinson's disease.

6 References

1. Fahn, S., *Description of Parkinson's disease as a clinical syndrome*. Ann N Y Acad Sci, 2003. 991: p. 1-14.
2. Cookson, M.R., *The biochemistry of Parkinson's disease*. Annu Rev Biochem, 2005. 74: p. 29-52.
3. Sherer, T.B., et al., *An in vitro model of Parkinson's disease: linking mitochondrial impairment to altered alpha-synuclein metabolism and oxidative damage*. J Neurosci, 2002. 22(16): p. 7006-15.
4. Moore, D.J., et al., *Molecular pathophysiology of Parkinson's disease*. Annu Rev Neurosci, 2005. 28: p. 57-87.
5. Paisan-Ruiz, C., et al., *Cloning of the gene containing mutations that cause PARK8-linked Parkinson's disease*. Neuron, 2004. 44(4): p. 595-600.
6. Zimprich, A., et al., *Mutations in LRRK2 cause autosomal-dominant parkinsonism with pleomorphic pathology*. Neuron, 2004. 44(4): p. 601-7.
7. Berg, D., et al., *Type and frequency of mutations in the LRRK2 gene in familial and sporadic Parkinson's disease**. Brain, 2005. 128(Pt 12): p. 3000-11.
8. Khan, N.L., et al., *Mutations in the gene LRRK2 encoding dardarin (PARK8) cause familial Parkinson's disease: clinical, pathological, olfactory and functional imaging and genetic data*. Brain, 2005. 128(Pt 12): p. 2786-96.
9. Mata, I.F., et al., *Lrrk2 pathogenic substitutions in Parkinson's disease*. Neurogenetics, 2005. 6(4): p. 171-7.
10. Gloeckner, C.J., et al., *The Parkinson disease causing LRRK2 mutation I2020T is associated with increased kinase activity*. Hum Mol Genet, 2006. 15(2): p. 223-32.
11. Greggio, E., et al., *Kinase activity is required for the toxic effects of mutant LRRK2/dardarin*. Neurobiol Dis, 2006. 23(2): p. 329-41.
12. Ito, G., et al., *GTP binding is essential to the protein kinase activity of LRRK2, a causative gene product for familial Parkinson's disease*. Biochemistry, 2007. 46(5): p. 1380-8.

13. Jaleel, M., et al., *LRRK2 phosphorylates moesin at threonine-558: characterization of how Parkinson's disease mutants affect kinase activity*. *Biochem J*, 2007. 405(2): p. 307-17.
14. Lewis, P.A., et al., *The R1441C mutation of LRRK2 disrupts GTP hydrolysis*. *Biochem Biophys Res Commun*, 2007. 357(3): p. 668-71.
15. Li, X., et al., *Leucine-rich repeat kinase 2 (LRRK2)/PARK8 possesses GTPase activity that is altered in familial Parkinson's disease R1441C/G mutants*. *J Neurochem*, 2007. 103(1): p. 238-47.
16. Smith, W.W., et al., *Kinase activity of mutant LRRK2 mediates neuronal toxicity*. *Nat Neurosci*, 2006. 9(10): p. 1231-3.
17. West, A.B., et al., *Parkinson's disease-associated mutations in leucine-rich repeat kinase 2 augment kinase activity*. *Proc Natl Acad Sci U S A*, 2005. 102(46): p. 16842-7.
18. West, A.B., et al., *Parkinson's disease-associated mutations in LRRK2 link enhanced GTP-binding and kinase activities to neuronal toxicity*. *Hum Mol Genet*, 2007. 16(2): p. 223-32.
19. MacLeod, D., et al., *The familial Parkinsonism gene LRRK2 regulates neurite process morphology*. *Neuron*, 2006. 52(4): p. 587-93.
20. Bosgraaf, L. and P.J. Van Haastert, *Roc, a Ras/GTPase domain in complex proteins*. *Biochim Biophys Acta*, 2003. 1643(1-3): p. 5-10.
21. Marshall, C.J., et al., *Signal transduction by p21ras*. *Int J Cancer Suppl*, 1989. 4: p. 29-31.
22. Lim, L., et al., *Regulation of phosphorylation pathways by p21 GTPases. The p21 Ras-related Rho subfamily and its role in phosphorylation signalling pathways*. *Eur J Biochem*, 1996. 242(2): p. 171-85.
23. Schiller, M.R., *Coupling receptor tyrosine kinases to Rho GTPases--GEFs what's the link*. *Cell Signal*, 2006. 18(11): p. 1834-43.
24. Manning, G., et al., *The protein kinase complement of the human genome*. *Science*, 2002. 298(5600): p. 1912-34.
25. Mata, I.F., et al., *LRRK2 in Parkinson's disease: protein domains and functional insights*. *Trends Neurosci*, 2006. 29(5): p. 286-93.

26. Bock, B.C., et al., *Cdc42-induced activation of the mixed-lineage kinase SPRK in vivo. Requirement of the Cdc42/Rac interactive binding motif and changes in phosphorylation.* J Biol Chem, 2000. 275(19): p. 14231-41.
27. Du, Y., et al., *Cdc42 induces activation loop phosphorylation and membrane targeting of mixed lineage kinase 3.* J Biol Chem, 2005. 280(52): p. 42984-93.
28. Xu, Z., et al., *The MLK family mediates c-Jun N-terminal kinase activation in neuronal apoptosis.* Mol Cell Biol, 2001. 21(14): p. 4713-24.
29. Guo, L., et al., *The Parkinson's disease-associated protein, leucine-rich repeat kinase 2 (LRRK2), is an authentic GTPase that stimulates kinase activity.* Exp Cell Res, 2007. 313(16): p. 3658-70.
30. Korr, D., et al., *LRRK1 protein kinase activity is stimulated upon binding of GTP to its Roc domain.* Cell Signal, 2006. 18(6): p. 910-20.
31. Gibbs, J.B., et al., *Intrinsic GTPase activity distinguishes normal and oncogenic ras p21 molecules.* Proc Natl Acad Sci U S A, 1984. 81(18): p. 5704-8.
32. Manne, V., E. Bekesi, and H.F. Kung, *Ha-ras proteins exhibit GTPase activity: point mutations that activate Ha-ras gene products result in decreased GTPase activity.* Proc Natl Acad Sci U S A, 1985. 82(2): p. 376-80.
33. McGrath, J.P., et al., *Comparative biochemical properties of normal and activated human ras p21 protein.* Nature, 1984. 310(5979): p. 644-9.
34. Sweet, R.W., et al., *The product of ras is a GTPase and the T24 oncogenic mutant is deficient in this activity.* Nature, 1984. 311(5983): p. 273-5.
35. Der, C.J., T. Finkel, and G.M. Cooper, *Biological and biochemical properties of human rasH genes mutated at codon 61.* Cell, 1986. 44(1): p. 167-76.
36. Temeles, G.L., et al., *Yeast and mammalian ras proteins have conserved biochemical properties.* Nature, 1985. 313(6004): p. 700-3.
37. Farnsworth, C.L. and L.A. Feig, *Dominant inhibitory mutations in the Mg(2+)-binding site of RasH prevent its activation by GTP.* Mol Cell Biol, 1991. 11(10): p. 4822-9.
38. Feig, L.A. and G.M. Cooper, *Inhibition of NIH 3T3 cell proliferation by a mutant ras protein with preferential affinity for GDP.* Mol Cell Biol, 1988. 8(8): p. 3235-43.

39. Nishihara, K., et al., *Chaperone coexpression plasmids: differential and synergistic roles of DnaK-DnaJ-GrpE and GroEL-GroES in assisting folding of an allergen of Japanese cedar pollen, Cryj2, in Escherichia coli*. Appl Environ Microbiol, 1998. 64(5): p. 1694-9.
40. Silvius, J.R., *Mechanisms of Ras protein targeting in mammalian cells*. J Membr Biol, 2002. 190(2): p. 83-92.
41. Seabra, M.C., *Membrane association and targeting of prenylated Ras-like GTPases*. Cell Signal, 1998. 10(3): p. 167-72.
42. Leung, K.F., R. Baron, and M.C. Seabra, *Thematic review series: lipid posttranslational modifications. geranylgeranylation of Rab GTPases*. J Lipid Res, 2006. 47(3): p. 467-75.

IV Concluding Remarks

This work presented in this thesis is comprised of two major parts. The first part describes work evaluating the interaction of the protein kinase MLK3 with the mitochondrial ATP/ADP translocase ANT2 and the investigation of how this interaction is regulated. The second part of this thesis is focused on a Parkinson's associated protein kinase, LRRK2. Specifically the Roc domain of LRRK2 has been shown to function as a *bona fide* GTPase. Previously we proposed that the Roc domain of LRRK2 may activate its own protein kinase domain. Furthermore we predicted that PD-associated mutations of Arg 1441 within the Roc domain should interfere with protein interactions rather than influence the GTPase activity of Roc since the mutated residue is far from the GTPase catalytic site and multiple, diverse amino acid substitutions (Cys, His, and Gly) found in PD patients result in the same disease phenotype. In addition, an intra- or inter-molecular interaction of LRRK2 mediated by the Roc-COR tandem domains is also demonstrated.

Our lab has focused on understanding MLK3 function and regulation by identifying its interacting proteins in human breast cancer MCF-7 cell line. MLK3 is expressed at a high level in MCF-7 cells. Using the immunoaffinity purification coupled with mass spectrometry, numerous potential MLK3 interacting proteins have been identified in the lab and ANT is one of them. Data in Chapter II demonstrates that expressed MLK3 interacts with ANT2 using the co-immunoprecipitation technique. Furthermore, the interaction of expressed MLK3 with ANT is specific for the ANT2 isoform. The kinase domain of MLK3 is sufficient for the MLK3-ANT2 interaction. The activation status of MLK3 regulates its interaction with ANT2, with higher activity

forms of MLK3 complexing more efficiently with ANT2. A portion of expressed MLK3 present in or associated with the mitochondria is capable of coimmunoprecipitating with ANT2, implicating that the MLK3-ANT2 interaction occurs at the mitochondria. Coexpression of MLK3 with ANT2 synergistically increases total cellular ATP levels, suggesting that the elevation of ATP levels is primarily a consequence of the MLK3-ANT2 interaction.

The biological function of the elevated cellular ATP levels from the MLK3-ANT2 interaction requires further investigation. Based on unpublished work in our lab, transient knockdown of MLK3 reduces cell proliferation induced by growth factors and steroid hormones, estrogen and progesterone, in MCF-7 cells. It is conceivable that the elevated cellular ATP levels from the MLK3-ANT2 coexpression may contribute to MCF-7 cell proliferation. Knockdown of ANT2 with or without MLK3 in MCF-7 cells under estrogen and/or progesterone stimulation will be necessary to further test whether the MLK3-ANT2 interaction contributes to cancer cell proliferation. Total cellular ATP levels are increased upon the coexpression of MLK3 and ANT2, important questions remain. The source of the increased ATP, whether glycolysis or oxidative phosphorylation, is as yet unknown. The detailed mechanism by which cellular ATP levels increase upon MLK3/ANT2 coexpression remains to be determined. Based on ANT's classical function in ATP/ADP exchange, one would not necessarily predict that ANT2 should affect total level of ATP. Intriguingly, we obtain the peptides corresponding to the mitochondrial proteins of oxidative phosphorylation including ATP synthase in our mass spectrometry data. It will be important to determine whether these proteins of the oxidative phosphorylation are also present in the MLK3-ANT2 complex.

Such future studies, in conjunction with this work, may provide a novel mechanism for the regulation of cellular energetics in cancer cells.

Chapter III has described the investigation and characterization of the novel Roc GTPase domain of LRRK2. Conditions for expression and purification of soluble GST-Roc variant proteins were optimized. Unfortunately, GST-Roc-COR largely remained insoluble under numerous conditions that were tested. The purified GST-Roc from bacterial expression system possesses a weak intrinsic GTPase activity, consistent with the concurrent published reports. Activated GTPases are commonly post-translationally modified by prenylation. These modifications render the activated GTPases hydrophobic and allow the activated GTPases to be targeted to cellular membranes. LRRK2 lacks a classical motif for posttranslational prenylation, but it is conceivable that the absence of appropriate cellular structure(s) such as lipids during expression or purification processes may result in low GTPase activity. For instance, Cdc42 and Rac, display much higher catalytic activities when expressed and purified from insect cells as compared with bacterially expressed proteins. Therefore insect cell expression vectors encoding His-tagged Roc variants are under construction in the lab. The assessment of the GTPase activity of the purified Roc from insect cells in parallel with the purified Roc from bacteria will give insight into the cause of the low GTPase activity of GST-Roc.

The second portion of Chapter III reveals that Roc-COR can interact *in trans* with a region of LRRK2 containing Roc, COR, kinase, WD40 through the end (RCKWE). Roc weakly interacts with RCKWE, suggesting that COR contributes to the interaction of Roc-COR with RCKWE. Notably, R1441C/G, the PD associated mutation in the Roc domain, slightly reduces the Roc-COR mediated domain interaction whereas Y1699C,

the PD associated mutation in the COR domain, enhances this interaction. It is possible that, in the context of full length LRRK2, the Roc-COR domain is captured in an inhibitory conformation. Introduction of the PD associated mutation, Y1699C, in this domain disrupts its inhibition, allowing Roc-COR Y1699C efficiently interacts with the RCKWE region. The interaction between Roc and COR will be a key to the proposed hypothesis and future experiments will test this interaction using co-immunoprecipitation assays. These findings provide knowledge to establish a new mechanism for explaining how these amino acid substitutions result in PD.

In conclusion, the research findings in this thesis contribute to the understanding of the new role of MLK3 in regulation of cellular energetics through its mitochondrial interacting protein, ANT2. These studies shown herein also support our previous hypothesis of the LRRK2 regulation and provide knowledge to develop a novel mechanism of Roc-COR regulates LRRK2 molecular interaction that might be involved in PD pathogenesis.

MICHIGAN STATE UNIVERSITY LIBRARIES



3 1293 02956 3396